ANALYSIS OF THE INFLAMMATORY AND DEGENERATIVE STATE OF OSTEOARTHRITIC JOINTS

A Dissertation

Submitted to

the Temple University Graduate Board

---

in Partial Fulfillment

of the Requirements for the Degree

DOCTOR OF PHILOSOPHY

---

by

Jeffrey B. Driban

August, 2008

ABSTRACT

ANALYSIS OF THE INFLAMMATORY AND DEGENERATIVE STATE OF OSTEOARTHRITIC JOINTS

By Jeffrey B. Driban

Doctor of Philosophy

Temple University, August, 2008

Major Advisor: Dr. Michael Sitler

Development of disease modifying osteoarthritis drugs has been hindered by an inability to diagnose osteoarthritis prior to structural changes and by animal models that cannot predict human responses to disease modifying interventions. The first part of this dissertation evaluated if a novel nonsurgical-voluntary animal model was capable of producing joint inflammation and degeneration as well as if ibuprofen could attenuate these outcomes. Spraque-Dawley rats were divided among 7 groups. The four experimental groups consisted of two trained to perform a high-repetition, high-force (HRHF) task without ibuprofen for 6 (N = 5) and 12 weeks (n = 16) and two trained to perform a HRHF task for 6 (N = 5) and 12 weeks (N = 16) with ibuprofen initiated at week 4 of the 12

week training protocol. Three groups served as controls: trained controls (N = 8), trained controls plus ibuprofen (N = 9), and normal controls that were not trained or provided ibuprofen (N = 13). Twelve weeks of the HRHF task produced joint inflammation and degeneration. Ibuprofen attenuated these outcomes.

The second part of this dissertation evaluated if skin potentials were a noninvasive diagnostic marker for osteoarthritis. Skin and intra-articular potentials as well as synovial protein concentrations were measured in osteoarthritic (N = 4) and normal knees (N = 4). Skin potentials were not different between the groups but correlated to 7 synovial protein concentrations. Six synovial protein concentrations were significantly different between the groups.

The HRHF task animal model induced joint inflammation and degeneration, and may be useful for assessing therapeutic and disease modifying responses to interventions. Future research needs to assess if this model is predictive of human responses to interventions. Although skin potentials may not differentiate between osteoarthritic and normal knees, they do relate to biochemical conditions within the knee. Future research needs to determine the mechanism that produces this

relationship with the goal of improving measurement techniques to develop an early diagnostic marker for osteoarthritis. Development of new diagnostic markers for osteoarthritis and animal models for studying early osteoarthritis and disease modifying drugs represents the key to advancing disease modifying osteoarthritis drugs.

ACKNOWLEDGEMENTS

Over the past few years, I've been fortunate to meet people who were willing to contribute a lot of time, work, and patience into helping me develop as a researcher and a person. I'd like to thank Drs. Sitler, Barbe and Swanik. Without the three of you this dissertation and experience would not exist. Dr. Sitler, your mentorship over the past few years has helped me grow as a teacher, researcher, critical thinker, person, and a writer (see, I remembered the comma before "and"). Dr. Barbe, I can't thank you enough for all of the time you have committed to helping me learn and grow. It's hard to believe it was only a few years ago that we started doing independent studies together and I didn't even know that the word "interleukin" existed (now I can't seem to go a day without seeing it somewhere). Dr. Swanik, thank you for offering me the opportunity to begin pursuing this area of research. Each of you provided me with great opportunities, conversations that inspired and challenged me, and role models for the type of person I would like to be as I pursue a career.

I would also like to thank Drs. Barr, Kendrick, and Ziskin for assisting in the dissertation process and providing your insights. Dr. Ziskin, after every meeting I have left with a better understanding of the topic at hand. I would like to thank Dr. Bala as well, not only for the time you have committed to the research but also for our weekly discussions (whether it was about osteoarthritis or the Phillies). My understanding of osteoarthritis was greatly enhanced through our discussions.

I would also like to thank Dani, Kellie, Ryan, Sarah and Jamie for their friendship, advice, and for always being there to talk. To Phil, Neil, and Christina thanks for always being there, even if I wasn't. My parents and brother also deserve a lot of credit for their patience and support. Without these last eleven people the past few years would have been a lot less fun.

Finally, I would like to thank the Crystal Leopanto, Jeanette Butkiewicz, Linda Muraresku, Sean Conran, Mamta Amin, Jeff Martoff, and all of the staff members of the Department of Orthopaedics. Without your help and patience this study would have never been completed.

I consider all of you great friends and role models and I look forward to a continued friendship.

TABLE OF CONTENTS

LIST OF TABLES

LIST OF FIGURES

CHAPTER 1

REVIEW OF LITERATURE

Human Osteoarthritis

Osteoarthritis is the most common form of arthritis and affects more than 20 million Americans (National Institute of Arthritis and Musculoskeletal and Skin Diseases, 2002; Swagerty & Hellinger, 2001). By 2030, over 20% of the United States population will be over the age of 65 and more than half of these people will have at least one joint which demonstrates osteoarthritis on x-rays (National Institute of Arthritis and Musculoskeletal and Skin Diseases). The World Health Organization estimates that 10% of the world population over 60 years of age has symptomatic osteoarthritis (70.85 million osteoarthritic patients; Symmons, Mathers, & Pfleger, 2006; US Census Bureau, 2007). In 2007, the United Nations announced that the world population would increase by 2.5 billion between 2005 and 2050. Half of the increase is attributed to the population over 60 years of age. This increase alone represents 125 million new osteoarthritis patients, and

this may be an underestimate as developing nations progress, life styles change, and the prevalence of obesity increases.

Osteoarthritis is a progressive degeneration of the cartilage further characterized by changes in synovium, subchondral bone, and the periarticular muscles and ligaments (Baddour & Bradley 1999). As the degenerative changes progress, the subchondral bone thickens and new bone forms at the joint margins. Osteoarthritis has historically been characterized as a noninflammatory arthritis, but recent research has demonstrated that inflammatory cytokines (protein messengers), catabolic proteins, and cells play a critical role in the development of osteoarthritis.

Biochemical Changes

The onset and progression of osteoarthritis is characterized by several features, dominated by three important changes: (a) disappearance of a balanced cytokine network, including pro-inflammatory/catabolic (e.g., interleukin [IL]-1β, IL-1α, IL-6, IL-8, tumor necrosis factor [TNF]-α, soluble tumor necrosis factor receptor [sTNFr], receptor activator of nuclear factor-κB ligand [RANKL]) and anti-inflammatory/anabolic/protective (e.g., IL-4, IL-10, IL-1 receptor antagonist [IL-1Ra],

osteoprotegerin [OPG]) soluble factors expressed in the articular tissue; (b) changes in the expression of chemokine receptors in chondrocytes; and (c) disturbed protein transport and sugar synthesis in chondrocytes due to a deficiency in the Golgi apparatus (Yamamoto, Shishido, Masaoka, & Imakiire, 2005).

Chemokines have been described as important mediators at the articular level because they attract and activate T cells, monocytes, and granulocytes (Honorati, Bovara, Cattini, Piacentini, & Facchini, 2002). Chemokines (e.g., regulated upon activation of normal T cell expression and secretion [RANTES], eotaxin-1, macrophage chemoattractant protein-1 [MCP-1], growth related gene product [GRO-α]) induced by IL-1β and TNF-α in chondrocytes can stimulate the release of soluble factors, such as inducible nitric oxide synthase and proteolytic enzymes (e.g., metalloproteinases, aggrecanase, and TNF-α converting enzyme), which are responsible for cartilage degeneration (Alaaeddine, Olee, Hashimoto, Creighton-Achermann, & Lotz, 2001; Borzi et al., 2000; David, Farley, Huang, Lavoie, & Laverty, 2007; Honorati et al.; Hsu et al., 2004; Pulsatelli et al., 1999; Punzi et al., 2003).

IL-1β and TNF-α inhibit the synthesis of aggrecan and collagen type II (key components of the extracellular matrix of cartilage; Punzi et al., 2003). These two cytokines are considered key proteins regulating the progression of osteoarthritis (Fernandes, Martel-Pelletier, & Pelletier, 2002; Haynes, Hume & Smith, 2002). Both are capable of promoting bone resorption; inhibiting the synthesis of anti-inflammatory and anabolic proteins; as well as stimulating the production of proteolytic enzymes, pro-inflammatory cytokines, and prostaglandin E_2 (PGE_2; Fernandes et al.).

IL-6 has been proposed as a contributor to the osteoarthritis pathological process by increasing the number of inflammatory cells in the synovial tissue, stimulating the proliferation of chondrocytes, inducing an amplification of the effects of IL-1 on the increased synthesis of matrix metalloproteinase (MMP), and inhibiting proteoglycan production. IL-6, however, can induce the production of tissue inhibitory matrix metalloproteinases (TIMP) and not MMP. This cytokine is believed to be involved in a feedback mechanism that limits proteolytic damage (cartilage matrix degeneration; Fernandes et al., 2002).

IL-8 has been reported to be a potent chemotactic cytokine for polymorphonuclear neutrophils, stimulating their chemotaxis and generating reactive oxygen metabolites. IL-8 enhances the release of IL-1β, IL-6, and TNF-α (Fernandes et al., 2002).

Leukemia inhibitory factor (LIF) has also been implicated in osteoarthritis because it induces the synthesis of acute phase proteins and the inhibition of lipoprotein lipase activity (removal of fatty acids from triglycerides). LIF enhances the expression of IL-1β and IL-8 in chondrocytes and IL-1β and TNF-α in synovial fibroblasts. IL-1β and TNF-α both help up regulate the production of LIF. LIF also up regulates the metabolism of connective tissue such as cartilage and bone, inducing the expression of collagenase and stromelysin (Fernandes et al., 2002).

IL-11 may have a similar role as LIF and IL-6 since they share the same receptor domain (gp130). It has been found to decrease the release of PGE_2 from synovial fibroblasts and can prevent excessive extracellular matrix degradation induced by the synovial inflammation (Fernandes et al., 2002).

IL-17 up regulates a number of gene products involved in cell activation, including the production of pro-inflammatory cytokines and MMPs in target cells such as macrophages. It also increases the production of nitric oxide in chondrocytes in vitro (Fernandes et al., 2002). IL-17 can stimulate chemokines (e.g., IL-8 and GRO-α) in both synovial fibroblasts and chondrocytes and MCP-1 in chondrocytes (Honorati et al., 2002). While IL-17 appears to have a similar function to IL-1β and TNF-α, only low concentrations have been detected in osteoarthritic synovial fluid (Kotake et al., 1999; unpublished data).

There are three key anti-inflammatory cytokines (IL-4, IL-10, and IL-13) that are increased in the synovial fluid of osteoarthritic joints. They decrease the production of IL-1β, TNF-α, and MMPs, and up regulate IL-1ra, TIMP-1 and inhibit PGE_2 release (Fernandes et al., 2002). Due to a loss in homeostasis in osteoarthritis these cytokines are not capable of inhibiting the stimulation of proteolytic enzymes.

Proteolytic enzymes (i.e., MMPs, a disintegrin and metalloproteinase [ADAMs], a disintegrin-like and metalloprotease domain [reprolysin-type] with thrombospondin type I motifs [ADAMTS]) are the primary enzymes responsible for the degenerative process seen in

osteoarthritis cartilage (Punzi et al., 2003; Roach, Aigner, Soder, Haag, & Welkerling, 2007). The central role of these enzymes is performed by the MMPs and ADAMTS (e.g., ADAMTS-4, ADAMTS-5), which in the joint may be produced by synoviocytes or chondrocytes and are involved in early structural changes. The most important MMPs in osteoarthritis are MMP-1 (collagenase 1), MMP-13 (collagenase 3) and MMP-3 (stromelysin, a cytokine driven MMP; Punzi et al.). MMP-1 and MMP-13 are associated with collagen breakdown while, MMP-3 has been linked to proteoglycan breakdown (Punzi et al.; Shi, Schmitt-Talbot, DiMattia, & Dullea, 2004). When the chondrocytes are stimulated by pro-inflammatory cytokines, they can produce inactive forms of the MMPs, which become subsequently activated by a number of substances locally produced in the joint, including enzymes from the serine- and cysteine-dependent protease family (which function similar to MMPs; Punzi et al.; Fernandes et al., 2002). Leptin, an adipokine (a cytokine-like protein produced by adipose tissue) can also stimulate the production of MMP-9 and MMP-13 (Simopoulou et al., 2007). Adipokines (e.g., leptin and adiponectin) are produced not only by adipose tissue but also by osteoarthritic chondrocytes (Presle et al., 2006; Simopoulou et al.). These proteins represent a biochemical

link between joint degeneration and obesity. Proteolytic enzymes lead to joint space narrowing, the most pronounced sign of osteoarthritis.

Physical Changes

The progression of osteoarthritis is instigated typically by an incident (macro-trauma) or series of small events (repetitive micro-trauma) which causes the release of proteolytic and collagenolytic enzymes from chondrocytes, leading to cartilage breakdown (Shikhman, Brinson, & Lotz, 2000). Following trauma, proteoglycan degradation is initiated as the cartilage water content increases and collagen fatigue and microfractures occur with the repetitive stress of weight bearing. The microfractures in the subchondral bone decrease the ability of the cartilage to efficiently absorb shock. Next, a breakdown of joint integrity overloads the capacity to repair, leading to structural breakdown of the cartilage that initially involves fissuring, pitting, and erosion. Erosion can become so extensive that the articular surface denudes the full thickness of the cartilage. Osteophyte-spur formation, sclerosis of subchondral bone, and cyst formation are all examples of structural changes present in progressive osteoarthritis. Osteophytes can eventually break off into the joint.

In addition to osteochondral changes, the synovium becomes inflamed and secretes an increased amount of synovial fluid, resulting in joint effusion. Over 50% of osteoarthritic synoviums have inflammatory infiltrates (e.g., T cells and macrophage/monocytes; Haynes et al., 2002; Lindblad & Hedfors, 1987; Myers et al., 1990; Revell, Mayston, Lalor, & Mapp, 1988). Adiponectin, a adipocytokine which is elevated in osteoarthritic synovial fluid, induces IL-6 production in osteoarthritic synovial fibroblasts (Tang, Chiu, Tan, Yang, & Fu, 2007). Furthermore, adiponectin stimulated NFκB which has been associated with production of numerous cytokines (e.g., TNF-α, IL-1β, IL-6, IL-8, IFN-γ; Roman-Blas & Jimenez, 2006; Tang et al.). Cultured osteoarthritic synovium spontaneously secrete proteins involved in the progression of osteoarthritis: pro-and anti-inflammatory cytokines (e.g., TNF-α, IL-1β, IL-6, IL-8, MCP-1), multiple MMPs (MMP-1, 3, 9, 13), and TIMP-1 (Bondeson, Wainwright, Lauder, Amos, & Hughes, 20006). The synovium and articular cartilage may directly influence the other tissue. The synovium produces Human High Temperature Requirement A1 (Human HTrA1), a serine protease, and MMPs which contribute to the destruction of articular cartilage (Grau et al., 2006). Because the fibronectin fragments from degenerating articular cartilage

can promote MMP synthesis in synovial fibroblasts, the degenerative cycle between the synovium and articular cartilage continues (Grau et al.). In addition to biochemical changes, a majority of osteoarthritic patients demonstrate synovitis, increased synovial surface, increased number of synoviocytes, as well as capsular thickening and fibrosis (Fernandez-Madrid et al., 1995; Roach et al., 2007). It remains unclear how synovium interacts with other tissues in an osteoarthritic joint; however, at least in a subset of patients it appears to be a significant element (Roach et al.). New diagnostic procedures (e.g., magnetic resonance imaging) include synovium changes as an important sign of osteoarthritis (Guermazi et al., 2003).

Diagnostics

Diagnosis of osteoarthritis is made with clinical assessment, radiographic imaging, synovial fluid analysis, and, occasionally, blood serum or urine analyses (Punzi et al., 2003). During the evaluation, it is important that osteoarthritis be differentiated from the other forms of arthritis (e.g., rheumatoid, infectious, gout, pseudogout) to determine the appropriate intervention. The differential diagnosis most commonly consists of a synovial fluid analysis.

Based upon a clinical examination, osteoarthritic patients commonly have enlarged joint(s), crepitus with movement, morning stiffness, and pain. The main diagnostic hallmarks of osteoarthritis are the degenerative changes, which are present on radiographs but only once the articular degeneration has already begun (Punzi et al., 2003). Magnetic resonance imaging has lead to earlier diagnoses of osteoarthritis but is unable to detect changes before osteochondral degradation (Guermazi et al., 2003; Phan et al., 2005). After a general diagnosis of an arthritic process has been made, a more confirmative differential diagnosis can be made by examining the synovial fluid. A crystal analysis can be performed to evaluate the presence of apatite and calcium pyrophosphate dehydrate in contrast to uric acid related crystals (associated with gout). Calcium pyrophosphate dehydrate is most commonly associated with pseudogout (Punzi et al.). In addition to a crystal analysis of the synovial fluid, a study of the inflammatory conditions within the synovial fluid can also be made to differentiate osteoarthritis from more inflammatory arthritic pathologies (e.g., rheumatoid, infectious; Punzi et al.). Valuable biochemical/ histological markers include white blood cell count, total proteins, various catabolic enzymes, and cytokines (IL-1β,

IL-6, TNF, sTNFr, sIL-2r; Punzi et al.). Many of these cells and proteins are driven into the synovial fluid after they reach a sufficient concentration in the synovial membrane or articular cartilage. The inflammatory cells that have migrated into the synovial fluid continue to produce cytokines and metalloproteinases, increasing the observed concentration.

Non-Operative Management

Though there are many surgical options for the management of osteoarthritis, including total joint arthroplasties, partial joint arthroplasties, and osteotomies, conservative care is commonly provided as long as possible to delay surgical treatments. In recent years, a greater appreciation of non-operative management has emerged throughout the orthopaedic community especially for lower extremity osteoarthritis (American College of Rheumatology, 2000; Zhang et al., 2008).

Therapeutic Exercise and Activity Modification

The most commonly performed non-operative strategies include patient education regarding activity modification, weight-loss, and low impact exercise. Although it may be important for the individual patient to modify his/her current activity, it is undesirable to decrease overall

activity level since it leads to a decrease in muscle strength and flexibility. Weaker muscles may increase joint loading, exacerbating the osteoarthritis (Buckwalter et al., 2001). Exercise can also increase the patient's sense of well being, mental function, and reduce their disability, anxiety, and depression (Buckwalter et al.; Fransen, McConnell, & Bell, 2003; Roddy, Zhang & Doherty, 2005). Proper nutrition and an active lifestyle can also promote weight loss, reducing the stress on weight-bearing joints (Focht, Rejeski, Ambrosius, Katula, & Messier, 2005; Messier, Gutekunst, Davis, & DeVita, 2005).

External Load Reduction Techniques

Another alternative to slow the progression of osteoarthritis in weight-bearing joints and relief of patient symptoms is to alter the load distribution through the involved joints (Krohn, 2005; Toda & Tsukimara, 2005). This may be accomplished through the use of canes, braces, or shoe modification. Well-designed running shoes have been found to decrease the impact transmitted through the skeleton. In contrast, high heels have been demonstrated to increase forces through the lower extremity (Buckwalter et al., 2001). Lateral heel wedges placed inside a patient's shoe can help alleviate symptoms if the

individual has unicompartmental osteoarthritis within the medial compartment of the knee (Buckwalter et al.; Toda & Tsukimura). Canes are another means of reducing the load transmitted through the joints and increase the patient's stability. Unloader braces have also been developed to redistribute ground reaction forces in the case of unicompartmental osteoarthritis of the knee (Buckwalter et al.; Krohn). While these unloader braces have been reported to reduce pain, many patients claim that simple elastic joint sleeves provide pain relief and improved stability (Buckwalter et al.; Krohn). Though these methods have been found to reduce the patients pain and may reduce the progression of osteoarthritis, they are commonly combined with some form of therapeutic intervention to include exercise, electromagnetic modalities, and pharmaceutical interventions.

Electromagnetic Energy

Pulsed electromagnetic fields (PEMF) have been demonstrated to decrease pain and improve functional performance (Trock et al., 1993; Trock, Bollet, & Markoll, 1994; Pipitone & Scott, 2001). Previous research has evaluated the electrical phenomenon in cartilage and demonstrated a mechanical-electrical transduction mechanism similar to that in bone. When cartilage is compressed (as

in weight-bearing conditions) fluid and electrolytes are forced to move, leaving negative charges in the proteoglycans and collagen in the cartilage matrix (Trock et al., 1994). PEMF have been demonstrated in vitro to enhance fibroblasts, chondrocyte, and osteoblast metabolism, as well as to modulate the effects of hormones and neurotransmitters on the receptors of different cells (Pipitone & Scott, 2001). In addition to PEMF, pulsed electrical stimulation reduces patient pain and increases their function (Zizic et al., 1995).

In 1996, researchers began finding that exposure to electromagnetic fields enhanced chondrogenic differentiation and the synthesis of cartilage extracellular matrix proteins (Ciombor, Aaron, Wang, & Simon, 2003; Wang, Wang, Zhang, Clark, & Brighton, 2004; Brighton, Wang, & Clark, 2008). Ciombor et al. reported that pulsed electromagnetic fields reduced the severity of osteoarthritis and preserve the cartilage. It has now been theorized that TGF-β, which has an increased concentration in treated joints' articular cartilage, may be one of the key mechanisms for the therapeutic benefits of PEMF in articular cartilage (Ciombor et al.). TGF-β helps up-regulate the gene expression for aggrecan, up-regulate inhibitors of proteolytic enzymes, and down-regulate

proteolytic enzymes and IL-1 activity (Ciombor et al.). Electromagnetic fields can increase matrix anabolism (e.g., promote collagen and aggrecan production) with a concomitant decrease in matrix catabolism (e.g., downregulate IL-1 induced mRNA expression of MMP-1, MMP-3, MMP-13 and ADAMTS4; Brighton et al.). While a great potential has been placed on the use of electromagnetic energy to slow if not reverse osteoarthritis there is still limited data to conclusively demonstrate that pulsed electromagnetic fields are the ideal means for non-operative management.

Pharmacological Options

Patients suffering from osteoarthritis have five major pharmaceutical/supplemental options: oral analgesics, oral nonsteroidal anti-inflammatory drugs (NSAIDs), intra-articular corticosteroid injection, intra-articular hyaluronan injections, and oral glucosamine with chondroitin sulfate. Intra-articular corticosteroid injections are a direct method for relieving symptoms and minimizing the occurrence of an acute inflammatory reaction (Buckwalter et al., 2001). Another injectable, intra-articular hyaluronan, has recently become available and has been found to provide improved joint lubrication and may help slow the degenerative process (Sezgin et al., 2005).

Oral glucosamine and chondroitin sulfate have become increasing popular in recent years (McAlindon, LaValley, Gulin, & Felson, 2000). Glucosamine is an amino sugar precursor to the glycosaminoglycans (a key protein found in articular cartilage) and chondroitin sulfate is one of the glycosaminoglycans (Buckwalter et al.). Though these supplements have been found to decrease patient symptoms there remain many questions regarding their mechanism of action and efficacy (McAlindon et al.; Poolsup, Suthisisang, Channark, & Kittikilsuth, 2005). Oral analgesics include acetaminophen, codeine, and are commonly used in conjunction with a low dose of NSAID (Buckwalter et al.). This combination avoids high doses of either drug from having to be used. A wide variety of NSAIDs have been marketed over the past 20 years (e.g., naproxen sodium, acetylsalicylic acid, ibuprofen, nabumetone).

Nonsteroidal Antiinflammatory Drugs/Ibuprofen

NSAIDs are commonly recommended to manage pain and inflammation associated with osteoarthritis (Zhang et al., 2008). NSAIDs may influence articular cartilage turnover. Dingle (1999) performed an ***in vitro*** assessment of thirteen NSAIDs on articular cartilage matrix synthesis and turnover. Three categories of NSAIDS were identified: (a)

stimulatory effect (e.g., aceclofenac, tenidap, and tolmetin), (b) negligible effect (e.g., piroxicam, tiaprofenic acid, and aspirin), and (c) inhibitory effect (e.g., naproxen, ibuprofen, indomethacin, nimezulide). The inhibitory effect of indomethacin and ibuprofen may be an individualized response (McKenzie, Horsburgh, Ghosh, & Taylor, 1976). *In vivo,* ibuprofen may prevent cartilage and synovial tissue degradation (Gineyts et al., 2004). Gineyts et al. conducted a randomized clinical trial with over 200 patients suffering a flare of osteoarthritis symptoms. Control subjects experienced an increase in urinary markers of type II collagen degradation (i.e., C-terminal crosslinking telopeptide of type two collagen) and synovial tissue degradation (i.e., glucosyl galactosyl pyridoline). The ibuprofen (2400 mg/day) group did not have a significant increase in cartilage turnover and the synovial tissue degradation marker increased by 4% compared to 10% in controls. It remains unclear what effect NSAIDs have on articular cartilage and what the optimal dose is for a disease modifying effect.

A common dosing issue experienced in the clinical setting is that many patients never achieve an anti-inflammatory concentration because of inconsistent use. A single dose of ibuprofen (400 mg or 800 mg) enters the

synovial fluid (Day et al., 1988; Glass & Swannell, 1978). Peak concentrations occur 80 to 360 min after a single oral administration (Day et al.; Glass & Swannell). A gradual decline then follows (Day et al.; Glass & Swannell). Ibuprofen has a longer time to max concentration, lower max concentration, and a higher elimination half life in osteoarthritis patients' synovial fluid compared to serum (Davies, 1998). A single dose of 400 mg of ibuprofen has a higher concentration in the serum for the first 150 min but then the synovial fluid concentration exceeds serum. After two days of ibuprofen (400 mg, three times per day) arthritis patient's total synovial fluid concentration was only 50% of the serum concentration (Davies). Ibuprofen only functions as an anti-inflammatory at sustained high doses (greater than 1200 mg/day; Godfrey & de la Cruz, 1975). Ibuprofen (2400 mg/day) for 3.25 days did not result in a significant accumulation in either serum or synovial fluid of arthritis patients (Cox, Gall, Forbes, Gresham, & Goris, 1991). In rheumatoid arthritis, ibuprofen (2400 mg/day) reduced joint swelling after four weeks but did not have a significant effect at one week (Godfrey & de la Cruz). Ibuprofen (1600 mg/day) may decrease acute skin inflammation but only after 36 hours of consistent consumption (Walker, Nguyen, & Day, 1994).

Interestingly, only half of the patients responded to ibuprofen after 36 hr and responsiveness at the first administration of ibuprofen did not predict a positive outcome at a second administration (Walker et al.). More research needs to explore patients' variable responses to NSAIDs and their potential role in cartilage metabolism. A better understanding of current medications in osteoarthritis may lead to the development of disease modifying osteoarthritic drugs (DMOADs).

Developing Class of Drug: Disease Modifying Osteoarthritic Drugs

DMOADs represent the ultimate goal for osteoarthritis research. Numerous pharmacological interventions are being explored but none have demonstrated efficacy in humans. Many researchers are focusing on substances currently available (e.g., chondroitin sulphate, curcumin, diacerein, forms of hyaluronan, glucosamine sulfate, green tea, ginger extract, methylprednisolone acetate, select NSAIDs) and are reassessing their structural modifying capabilities (Diaz-Gallego et al., 2005; Echigo, Mochizuki, Nishimura, & Sasaki, 2006; Fajardo & Di Cesare, 2005; Hulmes et al., 2004; Pasquali et al., 2001; Poolsup et al., 2005; Shakibaei, Schulze-Tanzil, John, & Mobasheri, 2005). Based on recent biochemical and genetic studies new chemical

candidates are being explored: (a) Doxycycline, a MMP inhibitor, (b) Licofelone, a cyclo-oxygenase/5-lipoxygenase (COX/5-LOX) inhibitor, (c) receptor blockades, (d) soluble receptors or monoclonal antibodies, (e) IL-1 receptor antagonist, (f) bisphosphonates, osteoclast inhibitors, and (g) growth factors (Fajardo & Di Cesare, 2005; Pelletier & Martel-Pelletier, 2007). Besides biochemical or genetic solutions, electrical stimulation and pulsed electromagnetic fields may have the potential to serve as a disease modifying osteoarthritic intervention (Brighton et al., 2008; Ciombor et al., 2003; Wang et al., 2004). While an array of options are being tested it is difficult to assess the true potential of these interventions in humans because early osteoarthritis in humans is difficult to evaluate and human trials typically occur in end-stage osteoarthritis. It has been theorized that a point of no return exists for restoring joint integrity (Aigner et al., 2006; Aigner, Soder, Gebhard, McAlinden, & Haag, 2007). New diagnostic tests need to be developed to diagnosis early osteoarthritis and assess small changes within joints. Animal models that closely resemble human osteoarthritis are also needed to explore the mechanisms of early osteoarthritis and to assess new therapeutic interventions.

Joint Degeneration in Rodents

The study of osteoarthritis in humans has been limited because most tissue samples are from end-stage osteoarthritis (Hayami et al., 2006). To explore the onset of early progression and potential for therapeutic interventions many models have been developed to explore the early stages of joint degeneration. Dogs, sheep, goats, and rabbits have multiple models for inducing joint degeneration (Glasson, Blanchet, & Morris, 2007; Hayami et al.). These animals are no longer preferred because of the lack of knowledge regarding their articular cartilage, the size of the animals, the cost of maintaining the animals, the time to develop joint degeneration, and the lack of biochemical reagents to evaluate them. Recently, the development of new joint degeneration models have focused on rodents.

Models for Inducing Degenerative Changes

Several animal models have been developed to explore the development of joint degeneration in animals. In rodents, these can be divided into four primary categories: (a) instability induced osteoarthritis (e.g., anterior cruciate ligament transection, destabilization of medial meniscus, bacterial collagenase; Blaney Davidson et al., 2006; Glasson et al., 2007; Hayami et al., 2006; Ma et al.,

2007), (b) meniscal resections (Fernihough et al., 2004; Meng et al., 2005), (c) spontaneous development (e.g., transgenic mice, knock out mice; Blaney Davidson et al.; Hu et al., 2006; Morko et al., 2004; Yamamoto et al., 2005), and (d) other models that include injections of sodium iodacetate (inhibits glycolysis and promotes chondrocyte death; Fernihough et al., 2004). Regardless of the adopted model, male rats are commonly used because of their greater prevalence and severity of degenerative joint changes (Glasson et al.; Ma et al.). Healthy females have less degeneration following surgical destabilization of the medial meniscus when compared to ovariectomized female mice and both healthy and orchiectomized male mice (Ma et al.). Healthy males also demonstrated greater joint degeneration than orchiectomized mice (Ma et al.). In addition to gender selection, the breed can also influence the susceptibility and severity of joint degeneration. 129/SvEv mice and C57B/10 mice exhibit the greatest severity when the medial meniscus is destabilized (Glasson et al.). The least severity is observed in DBA/1 and FVB/N mice (Glasson et al.)

Instability induced osteoarthritis models are the most common in laboratory animals and often require a surgical intervention to transect the anterior cruciate ligament or

destabilize the medial meniscus (Glasson et al., 2007). Several alternative methods have been proposed to replicate an instability induced osteoarthritis model. Bacterial collagenase has been previously used to rupture the cruciate ligaments and a closed needle transection of the cruciate ligaments has been reported (Blaney Davidson et al., 2006; Glasson et al.). Both of these models are used less often because of potential damage to other types of soft tissue besides the cruciate ligament (e.g., multiple ligaments; Glasson et al.). Closed needle cruciate transection is rarely performed because it may result in uncontrolled intra-articular bleeding. One benefit of bacterial collagenase is the rapid onset of degeneration. Focal proteoglycan depletion and early signs of osteophyte formation occur within 3 days of the injection (Blaney Davidson et al.).

Meniscal resections are another common model for promoting the development of osteoarthritis. Occasionally, meniscal resections are combined with other procedures (e.g., anterior cruciate ligament transection; Hayami et al., 2006). Together these two models produce a rapid onset and greater degenerative changes than either in isolation (Hayami et al.). The combination of the two models produce contralateral evidence of minor but non-

advancing osteoarthritis (e.g., proteoglycan depletion but no subchondral bone changes) indicative of a theoretical bilateral or systemic component to osteoarthritis in some humans (Appleton, McErlain, Henry, Holdsworth, & Beier, 2007; Appleton et al., 2007).

A new modification of the anterior cruciate transection with partial medial meniscectomy rodent model initiates forced weight-bearing mobilization after surgery (Appleton, McErlain, Henry, Holdsworth, & Beier, 2007; Appleton et al., 2007; Henry, 2004). This model allows the investigator to control the rate of progression and severity of degeneration by changing the intensity (e.g., forced weight-bearing mobilization [running], forced nonweight-bearing mobilization [swimming], voluntary weight-bearing) and duration of the activity (Henry). Forced mobilization or running without joint trauma does not induce gross degenerative joint changes in rats or dogs (Appleton et al.; Arokoski, Kiviranti, Jurvelin, Tammi, & Helminen, 1993; Kiviranta et al., 1992). In female beagles, only localized proteoglycan loss has been associated with prolong running (40 weeks; Arokoski et al.; Kiviranta et al.). Some research however has shown that strenuous exercise or life-long running may increase the incidence and severity of osteoarthritis (Lapvetelainen et

al., 1995; Pap et al., 1998). Intracranial self-stimulation has been used to motivate rats to strenuously run (often exceeding normal running loads by 100 fold; Pap et al., 1998). Under these extreme loads (500 m/day, 5 days/week, 646 m/hr) histological changes and MMP-3 immunoreactivity were strongly dependent on running distance (Pap et al.). The intracranial self-stimulation running model has not been replicated. Forced weight-bearing mobilization following injury is perceived as an excellent model because of the ability to adjust the rate of progression and severity of degeneration (Henry). This model however may represent primarily a unique subset of patients who suffer an injury and quickly return to high levels of physical activity (e.g., athletes).

Spontaneous models of osteoarthritis most closely mimic the perception for the natural progression of osteoarthritis in humans. Spontaneous models typically require special breeds of mice (e.g., SRT/ort male mice, C57 mice) and have a high incidence of osteoarthritis (Blaney Davidson et al., 2006; Yamamoto et al., 2005). The development of joint degeneration is gradual, similar to humans. By 6 months, over 80% of these male mice had signs of articular cartilage lesions. The mice typically experience end-stage joint degeneration between 6 to 12

months of age, characterized by significant erosion of the articular cartilage and mature osteophytes (Blaney Davidson et al.). Spontaneous models are sometimes produced by knocking out a gene so that a particular molecule is not produced. Hu et al. (2006) reported data from the spontaneous development of osteoarthritis in mice deficient in Collagen IX. By the 9th month, complete loss of articular cartilage was observed. A significant drawback of knock-out mice is that they may result in the production of no pups because a particular gene is critical to embryonic development (Glasson et al., 2007). Surgical instability models are typically preferred to the spontaneous models because of the time required to breed the mice, time required to develop degenerative changes, they exhibit less variability and have a decreased dependence on genetic background (Glasson et al.).

Sodium Iodacetate, an inhibitor of glycolysis, has also been reported to lead to the development of osteoarthritis in rodents (Fernihough et al., 2004). This model follows a similar progression as other models and often reaches an end-stage of joint degeneration within 3 weeks. While this model has been reported to lead to rapid joint degeneration and behavioral changes, it targets the entire joint (Fernihough et al.). Most of the other models

(e.g., anterior cruciate ligament transection, spontaneous development) result in articular cartilage degeneration beginning at weight-bearing regions (primarily the medial compartment of the knee), although iodacetate affects the entire articular cartilage surface (Fernihough et al.). New models are still being explored. An ideal model would mimic the interaction between inflammation and biomechanical changes observed in humans without surgical trauma, targeted genetic manipulation, or chemical induction.

Commonalities to Humans

The progression of degenerative joint changes in rodents is theorized to reflect the early changes in human osteoarthritis (Blaney Davidson et al., 2006; Hayami et al., 2006; Meng et al., 2005). The rate of progression and severity of each osteoarthritis model may differ; however, most rodent models initially develop focal cartilage damage, leading to increased bone resorption (Hayami et al.). The compromised cartilage and subchondral bone then leads to increased bone formation and increased cartilage damage (Hayami et al.). Prior to the increase in subchondral bone volume, the deep surface of articular cartilage becomes increasingly vascularized, leading to calcification of the articular cartilage (Hayami et al.).

Animals and humans both lose articular cartilage from the surface and deep regions of articular cartilage. The animals can also replicate the variability in onset and progression of articular cartilage degeneration experienced in human osteoarthritis. This is commonly avoided in animal studies because it requires a larger sample size and hampers the assessment of cartilage degradation (Glasson et al., 2007). The current models of inducing osteoarthritis in rodents may represent unique subsets of human osteoarthritis (Appleton, Pitelka, Henry, & Beier, 2007)

Interestingly, the rat model has supported a theory for a hormonal influence on human osteoarthritis. Ma et al. (2007) demonstrated that ovariectomized female mice had significantly more joint degeneration than healthy female mice. This may explain one reason why human males tend to represent a greater proportion of the osteoarthritis population under the age of 50. Estrogen may serve a protective mechanism in both mice and humans (Ma et al.).

Distinctions from Humans

While rodent models of osteoarthritis share common characteristics to humans and represent an opportunity to observe early joint degeneration, they have several short comings. Most studies of joint degeneration in rodents are performed in homogenous male populations (Ma et al., 2007).

Males tend to have the highest prevalence of osteoarthritis in rodents; however, humans only show this trend up until 45 years of age. Beyond the age of 45, post-menopausal women become the majority of osteoarthritis patients. In rodents, ovariectomized female mice still have a lower severity of joint degeneration than male mice (Ma et al.). Estrogen serves a protective effect in humans and mice; however, female mice may have other unique protective pathways not present in humans or male mice.

In spontaneous models in which osteoarthritis naturally progresses, the selected breeds of rodents tend to have an incidence of osteoarthritis significantly higher than humans. Several studies have reported that breeds of mice that spontaneously develop degenerative changes have a prevalence around 80% compared to 50% in humans (however, the human prevalence rate is highly debated; Blaney Davidson et al., 2006; National Institute of Arthritis and Musculoskeletal and Skin Disorders, 2002; Yamamoto et al., 2007).

To date, no animal models have been accepted as a means of testing disease modifying osteoarthritic drugs because they fail to predict successful outcomes in humans

(Glasson et al., 2007). Researchers continue to pursue new models capable of inducing joint degeneration and capable of predicting successful outcomes of DMOADs in humans.

Repetitive Movements on Extra-articular Structures

A voluntary task rat model has previously been reported to promote inflammation and tissue degeneration. When rats were required to perform a high-repetition (4 to 9 reaches/min), negligible force (< 5% maximum grip force; HRNF) reaching and grabbing task (2 hr/day, 3 days/week for 3 to 8 weeks), behavioral changes coincided with increased inflammation (Barbe et al., 2003). The rats exhibited a decrease in reach rate and task duration between weeks 3 to 7, but statistical significance was only reached at weeks 5 and 6 (Barbe et al.). By week 8, both behaviors tended to return towards baseline, suggesting that the rats may have been experiencing less pain, matching the reduction of some indicators of inflammation (Barbe et al., 2003; Barbe et al., 2008). When the rats were followed for 12 weeks they tended to decrease their reach rate between weeks 9 to 11 (Clark et al., 2003).

The HRNF reaching and grasping activity resulted in morphological changes in the anterior forelimb of the reach limb at sites where myofibers merge with tendon fibers. In

all of the weeks 6 and 8 rats, tendon fibrils appeared kinked at the myotendon junction, suggesting tendon fraying (Barbe et al., 2003). These morphological findings occurred in conjunction with increased ED1 macrophages (infiltrating macrophages) in tendon, muscle, and loose connective tissue (Barbe et al.). ED1 macrophages were present in musculotendinous and connective tissues throughout the body (e.g., palm, forearm, shoulder, back, and hindlimb). Peak concentrations of macrophages in musculotendinous tissues occurred at weeks 5 to 6 and then returned towards baseline at week 8 (Barbe et al.). Connective tissue in the palm and distal forearm contained a greater presence of ED1 macrophages than the musculotendinous structures (Barbe et al.). In contrast to ED1 macrophages, ED2 macrophages (resident macrophages associated with tissue repair) progressively increased in the anterior forelimb musculotendinous tissues through all 8 weeks of HRNF task performance. With the exception of ED2 macrophages, the HRNF model consistently showed a peak effect in musculotendinous tissues around week 5 with a gradual return to baseline around week 8.

The HRNF model induces an inflammatory response which the animal is capable of recovering from. This was further demonstrated in the median nerve at the carpal tunnel.

Immunoexpression of several key inflammatory mediators (i.e., IL-1α, IL-1β, TNF-α, IL-6, and IL-10) were increased in the median nerve at week 5 but not weeks at 3 or 8 (Al-Shatti, Barr, Safadi, Amin, & Barbe, 2005). In the epineural and perineural connective tissue and adjacent to axons, ED1 macrophages increased at weeks 5, 6, 8, and 12. Indications of epineural and intraneural fibrosis became evident between weeks 8 and 12 (Barr & Barbe, 2004; Clark et al., 2003). The active reach limbs consistently showed greater fibrotic changes in nerve and tendon than the nonreach limbs (Clark et al.). The fibrotic development coincided with reduced mean nerve conduction velocity of the median nerve between weeks 9 to 12 in the reach limb but not in the nonreach limb (Clark et al.). This progression mirrors the behavioral changes and ED1 macrophage increases, further supporting the theory that HRNF tasks result in local and systemic inflammation from which the rat can recover. However, if the task continues, fibrosis is likely to develop in the actively reaching limb (Al-Shatti et al.; Barr & Barbe, Clark et al.).

Similar to soft tissues, bone reacted to the HRNF task (Barr et al., 2003). After 4 to 6 weeks, ED1 mononuclear cells (likely macrophages) and osteoclasts were present in both the reach and nonreach limb along the periosteal-bone

interface, particularly at sites of muscle attachments (Barr et al.). By week 6, structural changes to the bone matrix included increased lamellar disorganization (Barr et al.). Osteocytes were more numerous and closely packed at weeks 6 and 12 (Barr et al.). Through week 6, collagen fibers in the periosteum lost their compacted state and parallel alignment, with periosteal cells increasing in number. However, by week 12 collagen fibers of the periosteum began to regain their closely packed parallel alignment (Barr et al.). Also, the number of ED1 cells at the periosteal bone interface had returned towards control levels, despite continuation of the HRNF task (Barr et al.). The bone matrix remained hypercellular at week 12 and did not appear to be as well organized as control animals (Barr et al.), suggesting that complete repair was not occurring, most likely due to continued performance of the task.

HRNF tasks consistently produce signs of local inflammation and systemic inflammation and remodeling/repair, although the animal is capable of recovering from this repetitive loading for up to 12 weeks. Based on repetitive injury theories, it has been hypothesized that high-repetition, high-force (HRHF; 8 reaches/min and 60% maximum grip force) activities may

prevent successful recovery and may lead to tissue degradation (e.g., joint degeneration). HRHF tasks may serve as a novel method for developing joint degeneration and assessing potential therapeutics (e.g., ibuprofen and electromagnetic energy).

Fundamental Bioelectromagnetics

Over the past century, the field of physiology has been advanced with a growing knowledge of biochemistry. It has become commonly accepted that life is dependent on an orchestra of chemical pathways. Researchers have pursued this understanding by evaluating the cause and effects of chemical pathways as well as the genetic expression dominating these processes. Unfortunately, it is commonly forgotten, especially by clinicians, that these chemical reactions are dependent upon the laws of physics. Many of life's reactions would not occur unless two atoms/smaller molecules combine to form larger molecules. The formation of these large compounds (i.e., lipids, carbohydrates, proteins) is dependent upon the principles of the electromagnetic force, one of the four fundamental forces in physics, which describes the influence of one charged particle on another. For millennia, clinicians have tried to relieve ailments/symptoms by altering physiological pathways with chemical compounds (e.g., pharmaceuticals,

elixirs, vitamins) and electromagnetic energy (e.g., electromagnetic stimulation, electrical stimulation, magnetic stones, electric eels). For the past century, use of chemical compounds is a mainstream of modern medicine, while the use of electromagnetic interventions has become an alternative medicine. During the past 3 decades, numerous studies have supported thousands of years of bioelectromagnetic medicine and demonstrated that electromagnetic energy is capable of profoundly altering physiology. Unfortunately, the full potential of electromagnetic energy remains elusive due to a lack of research examining the human body's natural electrical environment in healthy and pathologic states.

Bioelectromagnetics is the study of electromagnetic energy's endogenous generation and influence on biological structures. This field of study can be further separated into two major therapeutic delivery techniques: electrical currents and electromagnetic fields. Though modern bioelectromagnetics has only emerged in the past two centuries, its roots are over 4,000 years old.

Medical History

In 2000 BCE, The Yellow Emperor's Canon of Internal Medicine described the placement of lodestones (magnetic stones) on acupuncture points to relieve pain and other

complaints (Rosch, 2004). About this time, several Hindu texts described the therapeutic use of magnetic stones (Rosch). In the Western World, the Greek's, including Hippocrates, described the use of "lapus vivas" (live stones) for medicinal purposes. Furthermore, Egyptians, early Buddhists and Tibetan monks all described the use of magnetic stones for therapeutic purposes (Rosch). Although the early use of electrical stimulation was not as well documented, ancient Egyptians were the first to document use of electric catfish to treat a variety of illnesses (Rosch). In 40 AD, the Roman physician Scribonius Largus described a treatment for various ailments that included standing in shallow water with electric fish (Rosch).

Various clinicians over the past few centuries have proclaimed the therapeutic benefits of their energy-based medicine, but many were disproved by scientific inquiries. Late in the 17th century, bioelectromagnetic medicine was becoming increasingly popular around the world. In 1775, Frank Anton Mesmer published ***On the Medicinal Uses of the Magnet*** in which he described how he restored the health of a patient with uncontrollable seizures and numerous neurologic ailments using magnets. He later claimed that the healing forces actually resided in his own "animal magnetism". This was quickly hailed as a new force

analogous to Newtown's gravity. Mesmer's claim would eventually be disproved by a commission organized by Louis XVI, which included many of the top scientists of the day: Benjamin Frankin, Antoine Lavoiser, and Dr. JI Guillotin (Rosch, 2004). The commission concluded that the treatments were a combination of placebo and hypnosis (which is still occasionally called mesmerism; Rosch).

Magnetic therapy became popular in the United States during the Civil War and remained a popular therapeutic treatment until the turn of the century. During the 20th century, electromagnetic therapy declined because of the advancement of pharmacology. In the 1970s, electromagnetic therapy experienced a resurgence when treatments were found to promote healing in nonunion fractures (Becker, 1979; Becker & Spadaro, 1972; Marino, Cullen, Reichmanis, & Becker, 1979). The new interest in bioelectromagnetic medicine over the past 30 years has been strongly related to research started by Du Bois Reymond (1860), who demonstrated that the skin of a punctured finger had an electrical current (~10 μA). For the next 145 years, researchers examined the endogenous electrical signals of the human body, which, ultimately, lead to the development of bone stimulators and electrical stimulation protocols in an attempt to promote the healing response in decubitus

skin ulcers (Becker; Becker & Spadaro; Gentzkow, 1993; Lavine, & Grodzinsky, 1987; Marino et al.; Weiss, Kirsner, & Eaglstein, 1990).

Introduction to Electrical Potentials

Electrical potentials and charges are underlying concepts to many of the studies discussed hereafter. A charge is an intrinsic property of protons and electrons. Only two types of charge have been discovered: positive and negative. The smallest amount of free charge is 1.6×10^{-19} C (present in electrons and protons), therefore, charges of larger magnitudes are formed by adding or removing electrons. An electrical potential (V) is the potential energy (EPE) of a small test charge (q; $V = EPE/q$) and is reported in volts (joules/coulomb). Electrical potentials and the potential energy of a test charge cannot be directly measured. Instead the differences in potentials between two points are measured ($\Delta V = V_B - V_A$).

In an electrical circuit the reported voltage is the difference in potentials between two points and can be calculated using Ohm's Law (volts = current intensity x resistance). Current intensity (I) is the amount of charge crossing a surface during a period of time (t; $I = \Delta q/\Delta t$). Resistance (R) is determined by the resistivity of a material (ρ) multiplied by its length (D) and divided by

the cross-sectional area (A; $R = \rho(D/A)$). The term volt can also be used define the electromotive force, the maximal potential difference of a battery. The concepts of electrical potentials can also be applied to physiologic models.

Passive diffusion of ions across a membrane is dependent on a chemical force (concentration gradient across the membrane) and an electrical force (electrical potential difference across the membrane). The Nernst equation is used to determine the Nernst potential (E_x), which represents the equilibrium potential of an ion that is present on both sides of a membrane permeable to that ion ($E_x = \{(RT)/(zF)\} \ln \{[X]_o/[X]_i\}$). The equation accounts for the universal gas constant ($R = 8.31\ J \times mol^{-1} \times K^{-1}$), temperature in Kelvin (T), the valence of the ion (z), Faraday's constant ($F = 9.65 \times 10^4\ C$), and the natural logarithm of the ratio between the ion concentration inside ($[X]_i$) and outside ($[X]_o$) of the membrane. Based on this equation, the Nernst potential is positive when the exterior cation (positive ions) concentration is greater than the internal concentration or when the internal anion (negative ions) concentration is greater than the external anion concentration. While the Nernst equation is effective for calculating a single ion at a time, Goldman's

equation can determine the electrical potential across a membrane by accounting for the concentrations of multiple ions and the ion permeability (P) of the membrane ($E = \{(RT)/F\} \ln \{(P_K[K+]_o + P_{Na}[Na+]_o + P_{Cl}[Cl-]_i)/(P_K[K+]_i + P_{Na}[Na+]_i + P_{Cl}[Cl-]_o)\}$). A positive voltage can occur when a high concentration of cations are present outside the membrane and/or a high concentration of anions are on the interior of the membrane. Many bioelectrical potentials (e.g., electromyography, electroencephalography, electrocardiography, skin potentials) are dependent on these membrane potentials.

Generation of Endogenous Electrical Signals Associated with Injury and Healing

Several theories have been developed to explain the causes of the endogenous signals associated with injury and healing. Becker in the 1960s reported that the nervous system was generating and responding to changes in the electrical activity throughout the body (Becker, 1961). Then in the early 1980s it was proposed that the skin and its multilayers created endogenous signals (Barker, Jaffe, & Vanable, 1982; Jaffe & Vanable, 1984). Today, two types of endogenous electrical signals are commonly discussed: biologically closed electrical circuits (electrochemical gradients) and strain generated potentials.

Biologically Closed-Electrical Circuits

In the past 20 years, a new theory about the electrical nature of biological matter has been proposed based on biologically closed-electrical circuits. Biologically closed-electrical circuits have become the proposed mechanism permitting energy to flow and influence physiological functions (Nordenström, 1992). Biologically closed-electrical circuit systems are closed circuits found in all multi-cell organisms, including humans, in various forms and are controlled by the flow of ions in electrical field gradients found across the body. These closed circuits produce secondary electric and magnetic influences on surrounding biological material. The vascular closed circuit is an example of a biologically closed-electrical circuit in which the veins and arteries function as insulated conducting cables for ions aided by the high resistance of their walls (Nordenström, 1992, 1994). This theory has been used to explain the ability of rapid exchange between interstitial space and capillaries (Nordenström, 1992). The vascular-interstitial closed circuit is another important circuit aiding the mechanical movement of blood and lymph. It was once thought that diffusion, filtration, and osmotic pressure differences could fulfill the need for the exchange from the

capillaries. This is not the case at high demands (e.g., at exercise), where they cannot sufficiently manage the rapid bidirectional exchange of positive and negative ions in the same channels. This is possible by the vascular-interstitial closed circuit system (Nordenström, 1992).

Using the theory of biologically closed-electrical circuits, Nordenström described the electrical properties of injured tissue (Nordenström, 1992, 1994). These injured tissues are initially positively charged but then their charge varies in a slowly fluctuating fashion under attenuation towards equilibrium (Nordenström, 1992, 1994). Nordenström explained that injured tissue must get rid of both positive and negative ions and get new materials (ions) for healing. An electropositive tissue will guide cations (positive ions) out and anions (negative ions) into the tissue, after which a reversed gradient causes an opposite flow of ions to occur. The fluctuations of potentials are explained as a statistical representation of the different speed of migration and diffusion of anions and cations. The primary biologically closed-electrical circuit system being used during an injury is the vascular-interstitial closed circuit (Nordenström, 1992, 1994). The flow of current in the vascular-interstitial closed circuit channels influence movable cells such as leukocytes, which

carry a surplus of fixed negative charges on their surfaces (Nordenström, 1992, 1994). The biologically closed-electrical circuits theory proposes that the injured tissue is initially electropositive, however, some literature suggests that the tissue is negatively charged immediately after an injury and would therefore first repel negative ions (Betz & Caldwell, 1984; Craib, 1928; Driban, Swanik, Huxel, & Balasubramanian, 2004). Based on Nordenström's (1992, 1994) theory, there must be a reversal in tissue charge between the time of injury and the early inflammatory stage. This early reversal in charge has not been demonstrated but is needed to attract negatively charged inflammatory cells. Nordenström's (1992, 1994) general theory supports an assumption that the application of electrical stimulation can alter the movement of ions within the biologically closed-electrical circuits to repel inflammatory cells and attract fibroblasts. Further studies need to be performed however to determine the appropriate parameters, since different tissues seem to behave distinctly.

Strain Generated Potentials

Previous literature has demonstrated that trauma to any biological matter causes transient-electrical behaviors (Barker et al., 1982; Barnes, 1945; Becker, 1967; Betz &

Caldwell, 1984, Jaffe & Vanable, 1984; Nordenström, 1992, 1994). Strain generated potentials, however, are another method of generating transient electrical changes. These endogenous potentials (naturally produced potentials) are generated when bone and connective tissues are deformed by compression, distraction, bending and rotational forces (Black, 1987; Charman, 1990b). The source of these potentials is still unclear, although four theories have emerged: piezoelectricity, pressure-sensitive semiconductor junctions, internal fluid transfer, and internal dipole rotation (Black). The greater the degree of deformation the greater the resulting strain generated potentials. The polarity of the strain generated potentials is determined by the deformation (Black; Becker; Charman). In areas of compression, the strain generated potentials are always negative, while areas of tension are positive. It is theorized that these strain generated potentials signal cells in bone and connective tissues to respond to external forces in a manner consistent with Wolff's Law, allowing these tissues to grow and adapt to daily stresses (Black; Charman).

Transient Electrical Properties

Transient electrical properties/changes include a variety of electrical measurements designed to evaluate endogenous electrical signals. Transient electrical properties represent the electrical activity of a particular region under observation during a specific period. Transient electrical changes are the changes in electrical activities that accompany a change in physiologic state (i.e., during acute trauma). Transient electrical properties include electrical potentials and current intensity. Resistance, impedance and/or conductance may also be included but are typically described when measuring skin and will be discussed later.

Current Intensity: A Theoretical Representation Of Cellular Trauma

A resting membrane potential exists at the cellular level. This potential difference is caused by the unequal concentration of ions present on both sides of the membrane. Most living cells are internally negative with respect to their extra-cellular environment by 50 to 90 mV (Borgens, 1982; Charman, 1990a). When a cell membrane is torn, an injured cell demonstrates an inward flow of positive ions and an outward flow of negative ions (Betz & Caldwell, 1984). Betz and Caldwell demonstrated this

activity in frog cutaneous pectoris muscle tissue following the impalement of the cell membrane. They found an immediate inward current located at the impalement site, which diminished after several minutes. The convention for describing the direction of a current is based on the movement of positive charges which was once the prevailing theory; however, it is the movement of negative charges that have been found to cause current (Cutnell & Johnson, 1998). Betz and Caldwell believed this electrical phenomenon reflected an incomplete sealing of the cell membrane around the impaling intracellular pipette, allowing an injury current to flow into the cell at the site of penetration. As the membrane gradually seals around the pipette, the inward current declines until it is no longer present. These findings indicate that during the acute period after the cell membrane is traumatized a steady ionic current is produced to initiate the inflammatory process (Nordenström, 1992). Once the cell membrane reseals, bioelectrical potentials at the injury site reflect the presence of charged molecules and cells and no longer the ionic injury current across the open membrane. The established electrical field, which

represents the existing cellular activity in the healing tissue, influences the migration and activity of the charged molecules and cells around the injured tissue.

Bioelectrical Potentials

Bioelectrical potentials are considered to be a representation of the biochemical environment. Marino et al. (1994) reported "that potentials were primarily determined by Nernst potentials generated in the vicinity of the electrodes" (p. 151). Typically these measurements are performed by observing the difference in potentials at a normal point and a pathologic region. Changes in the bioelectrical potentials may be a result of strain generated potentials or a disturbance in the biochemical environment (e.g., altered ion distribution, changes in the concentration of proteins/ cells). Bioelectrical potential gradients, or lateral voltage gradients, have been described in traumatized skin and muscle. In the skin, an incision may alter the potentials along the epidermis 2 to 3 mm away from the wound and have an average value of 140 ± 20 mV/mm (Barker et al., 1982; Jaffe & Vanable, 1984). In vitro skeletal muscle has also been shown to have a lateral voltage gradient similar to skin but with the muscle becoming more positive closer to the wound. When a probe is within 2 to 3 mm of the incision, the region becomes

isopotential and more negative as the wound is examined closer (Craib, 1928). These potentials are likely a result of a change in tissue resistance and alterations in the ion balance of the region (by disrupting cell membranes and extracellular matrix). These gradients are believed to help guide the inflammatory process by signaling inflammatory cells and stimulating the production of inflammatory cytokines

An underappreciated influence on the local potential of a region may be fluctuations in the pH (concentration of hydrogen ions). Variations in pH can lead to changes in the polarity of a protein, including key inflammatory markers. The isoelectric point is the pH at which a protein takes on a neutral charge. It is well documented that inflammatory conditions typically expose cells to relatively hypoxic, acidic, and nutrient-depleted microenvironments (Swallow, Grinstein, Sudsbury, & Rotstein, 1991). Lardner (2004) attributed this local acidosis to increased lactic acid production by anaerobic glycolytic activity of infiltrated neutrophils. Furthermore, a strong correlation (r = -.92) was found between increasing white blood cell count and pH (Ward & Steigbigel, 1978). Though pH may not commonly shift enough

to alter the measured potentials, it should be considered as a potential covariate when inflammatory environments are being analyzed.

Anatomy of the Skin

The skin is the largest organ in the body and serves a protective role blocking harmful ultraviolet light and infectious agents. It is composed of five major layers: dermis, germinating, granular, stratum lucidum, and corneum. The innermost layer is the dermis, which is largely composed of connective tissue and also contains tactile elements, sebaceous glands (oil producing), hair roots, the neurovascular supply, the bodies of the sweat glands, and most of their ducts. Since this stratum has large intercellular spaces and an extensive network of blood vessels, it has a high electrical conductivity (Edelberg, 1977). Next, the germinating layer is the deepest level of reproducing cells. The germinating layer cells are separated by narrow spaces, filled with a fluid in which free diffusion or perhaps circulation may take place. The cells in the upper region contains numerous deeply staining granules, from which the name of the third layer is derived (granular layer). Above this third layer is the corneum, a compact stratum of flattened dead cells. A thin glistening layer separates this layer from the

granular layer (stratum lucidum; Edelberg, 1977). The layers of the skin compose a living semipermeable barrier which is covered by a denser layer of dead cells (the horny layer of the corneum), and is underlaid by a layer of loose, freely conducting connective tissues (dermis; Edelberg, 1968). Approximately, 80% of the resistance of the skin is encountered above the level of the germinating layer of the epidermis (Edelberg, 1968).

The dermis has a neurovascular network. Most importantly to the measurement of the transient electrical properties, is the autonomic innervation of this layer. In humans, most sympathetic fibers to the sweat glands are under alpha-adrenergic control and, therefore, increase the sweat rate (Iversen, Iversen, & Saper, 1991). In addition to the influence on the sweat glands, the sympathetic nervous system may also lead to the vasoconstriction of small arterioles (Iversen et al.). The parasympathetic stimulation has a smaller effect on the peripheral blood flow but can lead to some vasodilation (e.g., blushing). Changes in skin blood flow and sweat rate have been demonstrated to have a profound effect on the measurement of transient electrical properties (Edelberg, 1972). As a result of the influence of the autonomic nervous system, the skin is very responsive to acute changes in the

environment. As the local environment becomes warmer the resistance of the skin begins to decrease (~3%/°C; Edelberg & Wright, 1964). Furthermore, the skin can undergo a sudden decrease in hydration as a result of cognitive activities such as listening to instructions (Edelberg & Wright, 1964). These findings lead to the popularity of skin measurements among psychophysiologist and the development of lie detectors.

Diagnostic Bioelectric Skin Markers

Conductance, Resistance, and Impedance

Conductance, resistance, and impedance are all closely related and describe the characteristic of an object to permit or resist an electrical current. Electrical resistance is the opposition a material provides to the flow of an electrical current. Impedance is similar to electrical resistance in that it is a measurement of the opposition to current flow, but impedance is specific to alternating currents. In contrast to the others, conductance is a measurement of the ability of a material to conduct electricity, the reciprocal of resistance. These three measurements are dependent on the ion permeability of the tissue and may be mediated by two separate components, one from the sweat glands and the second arising from the epidermal layer of the skin

(Holmquest & Edelberg, 1964). Skin impedance is known to be influenced by the chemical composition of the skin, including water, electrolyte content, blood supply, the emotional state of the individual, as well as environmental variables such as room temperature and humidity (autonomic influence; Fujita, Fujii, Okada, Miyauchi, & Takagi, 2001).

Current Intensity

Upon acute cellular trauma there is a brief period (several minutes) of free flowing ions in and out of the cells, leading to an observable electrical current. The skin is commonly referred to as a battery because of the potential energy stored in a chemical form deep to the dermis. This potential energy is capable of generating an electromotive force as determined by the electrical current generated when the stratum corneum is cut (Borgens, 1982; Jaffe & Vanable, 1984). The current increases as the incision approaches the glistening layer of the epidermis and the resistance to current flow from the keratinized layers is reduced (Borgens; Jaffe & Vanable). The intensity then decreases as the cut is deepened through the living layer, which is considered the layer that generates the current (Barker et al., 1982; Jaffe & Vanable). Jaffe and Vanable reported that mammalian skin has a current driving capacity in the order of 1 μA/mm of wound length.

It is believed that the generated current is an electrical marker of the onset of the inflammatory process and helps signal the body that cellular trauma has occurred.

Skin Potentials

The measurement of skin potentials has been described as a representation of the neural activity, vascular related streaming potentials, and the Nernst potentials across various tissue membranes (Marino et al., 1994). Skin potentials once were commonly used for measuring transient electrical properties but never flourished. Much like the resistance measurements, skin potentials can be sensitive to changes in the stimulation of the autonomic nervous system (Edelberg, 1977). In 1977, Edelberg discussed the generation of skin potentials from a psychophysiological perspective and defined two possible mechanisms: potentials commonly arise as a consequence of unequal mobility of oppositely charged ions due either to steric or electrosteric drag imposed by the membrane, and the potentials may originate from the epithelial lining of the sweat ducts, secretory tubule, and the cell membranes of the granular and germinative layers. The true source of bioelectrical potentials in the skin may have several sources however, as it is commonly believed to be influenced by Nernst potentials and autonomic activity.

In 1994, Marino et al. evaluated the skin potentials measured on breasts and control sites of 110 women with palpable breast masses. The tumor sites were reported to be significantly electropositive when compared with control sites, but only when the tumor was cancer as determined by subsequent biopsy. No significant differences were found among the ipsilateral and contralateral control points. Marino et al. were among the first to report the diagnostic ability of skin potentials to differentiate between deep pathologic conditions. Most of the skin potential research prior to this study was conducted either in psychophysiology or healing skin wounds (Edelberg 1977, Burr, Harvey, & Taffel, 1939; Burr, Taffel, & Harvey, 1940; Barnes, 1945).

The use of skin measurements for monitoring transient electrical properties has been limited because of concern about extraneous factors interfering with accurate measurements. The reasons that these measurements have been dismissed (i.e., autonomic stimulation and measurement error) are the reasons for this reevaluation. Since the 1960s and 1970s bioelectrical instrumentation have improved. Electrodes, amplifiers, and computers have helped decrease motion artifact, ambient noise, and increase the sensitivity of the measures. In recent years,

advancements in science have also led to a new understanding of the relationship between the inflammatory process and the autonomic nervous system. The major clinical manifestations of inflammation (redness, heat, swelling, and pain) are associated with the autonomic nervous system.

Cellular Adaptations to Electromagnetic Energy

Research has demonstrated that cells produce a steady ionic current when the membrane is disrupted; however, little is understood about their response to electromagnetic energy (Betz & Caldwell, 1984). Borgens (1982) found that cells change their ionic concentrations, especially intracellularly, when exposed to a steady current. These changes in ionic concentrations within the cytoplasm can profoundly alter the physiology and the structure of the cells by stimulating the organelles and activating/inactivating enzymes found throughout the cell (Borgens). Robinson (1985) and Borgens both demonstrated that cells are strongly influenced by weak electromagnetic energy, leading to structural and physiological changes within the cell. Therefore, it can be predicted that the steady ionic current produced by an injury will affect the local tissue and inflammatory cells, initiating the healing process. Nordenström (1994) noted the effects of a small

current on human blood. Specifically, he found that the application of both anodic (positive) and cathodic (negative) currents transformed blood cells which then fused into larger conglomerates. Given these findings, Nordenström concluded that current flowing between cells could produce various structural modifications. The flow of current in a tissue can also produce entirely new structures of tissue such as fibrous membranes and organ capsules (Nordenström). The production of these structures demonstrates the extent to which electromagnetic energy can influence tissue development and tissue repair.

Jaffe and Vanable (1984) described that cell membrane components can be redistributed in voltage gradients of 1-10 mV per cell diameter. While research has shown how cells respond to electrical energy, it remains unknown how they sense and respond to voltage differences as small as .1 mV across the cell diameter (Jaffe & Vanable, 1984; Nordenström, 1994; Robinson, 1985). Robinson in his 1985 article noted, "It would be surprising if the cells involved in the healing response were not responding to such large fields" (p. 2026). Large voltage gradients may induce a cellular response be creating a difference in the membrane potentials established by the field, and the consequences of this difference on passive calcium entry

into the cathode- and anode-facing sides of the cells (Jaffe & Vanable; Robinson). The change in intracellular calcium levels can profoundly alter enzyme activity within the cell and alter the cell's metabolism. More recently, it has been found that the electrical field can cause a redistribution of charged proteins and lipids in the plasma membrane of nearby cells, including ion channels, thereby increasing the local fluxes of ions. Furthermore, the presence of a local electrical field can alter the membrane potentials leading to an increased number of open ion channels and increase the electromotive force driving those ions through the channels. Both of these outcomes can lead to changes in the cellular activity and structure, such as the stimulation of protein kinase A, an enzyme responsible for the phosphorylation of many substrates with in a cell (Nishimura, Isseroff, & Nuccitelli, 1996; Pullar, Isseroff, & Nuccitelli, 2001). Protein kinase A has been found to help regulate the migration of a cell while under the influence of an electric field (Pullar et al.).

It has been demonstrated that electromagnetic fields can have a profound effect on the physiology of various cell types. There have been very few studies, however, that have evaluated the physical side effects of electromagnetic energy on cells or tissues in vivo. Litke

and Dahners (1994) exposed rat ligaments (***in vivo***) to three electrical stimulation parameters: the lowest two settings (~0.65 µA and ~0.038 µA) had no impact and the third parameter (~8.6 µA) promoted healing. Higher current intensities produced visible tissue damage at the electrodes. The most effective current intensity for promoting healing was the highest intensity that could be tolerated without producing tissue damage (Litke & Dahners). Considering the findings of this study, it is important to avoid haphazardly selecting treatment protocols which may either fail to reach the required stimulus for optimal stimulation or provide conditions which lead to tissue degradation. It is also important to evaluate the need to individualize treatment protocols to account for the patient's unique characteristics (e.g., body composition, skin resistance, body girth, inflammatory reaction).

Individual Parameters

Throughout the literature, the effectiveness of many bioelectromagnetic clinical protocols has been inconclusive. Baker et al. (1997) summarized the status of electrical stimulation on wound healing: "the characteristics of stimulation that most affect the healing process are unknown. Whereas a variety of clinically based

procedures have been developed, they lack physiological rationale or experimental support" (p. 405). This gap in the literature is not exclusive to skin healing or to electrical stimulation, yet everyday clinicians are applying "cook book" electromagnetic parameters to patients without a clear appreciation of the physiological effects of these protocols. Clinicians often ignore the fundamental principles that influence the use of electromagnetic stimulation (e.g., body composition, treatment area, girth, skin resistance). It is often neglected that patients produce an individualized response to traumatic events and chronic overuse. This need for individualized care is further supported by the reaction patients have to various medications. No one anti-inflammatory drug can be used successfully on every patient.

In the 1990s ultrasound bone stimulators were introduced to the orthopaedic community and provided improved bone healing over the traditional electrical/electromagnetic bone stimulators (Aaron, Ciombor, & Simon, 2004; Nolte et al., 2001). The enhanced healing may be partially associated with the influence of low-intensity ultrasound to stimulate an endogenous electrical signal rather than the standard exogenous

electrical currents induced by earlier bone stimulators (Nolte et al.). The endogenous signals represent the body's own natural response to the stress placed on the bone and may have a greater impact on the healing process because of its individuality. The success of low intensity ultrasound bone stimulators and the lack of effectiveness of current electromagnetic protocols appears to further support the need for individualized treatment protocols.

In the past few years, the United States Department of Defense has been funding a research study to generate a new portable electrical stimulation patch (Henry, nd). The proposed unit is intended to treat acute skin wounds by measuring the transient electrical properties in and around the wound and selecting the optimal stimulation protocol. Once marketed, this stimulation unit will represent the first electromagnetic therapeutic intervention with individualized treatment parameters. While skin and bone research has been conducted for decades, it is important to evaluate the transient electrical properties associated with other tissues and pathologies to pursue the ultimate goal of indivualized parameters to optimize healing conditions.

Purpose of Dissertation

The purpose of this dissertation was to assess the biochemical and electrical changes associated with joint inflammation and degeneration associated with osteoarthritis. An animal study was conducted to evaluate the use of a novel HRHF task rat model, which has been theorized to induce joint inflammation and degeneration. Ibuprofen, a NSAID, was adminstered to elucidate the significance of inflammation in early joint degeneration. This animal model may be useful in evaluating the disease modifying effects of therapeutic interventions in early osteoarthritis; however, no diagnostic test has been accepted in humans as an indicator of early joint degeneration. The human phase of the dissertation assessed if bioelectrical analyses can differentiate between late-stage osteoarthritic and non-osteoarthritic knees. This is the first step towards assessing the use of bioelectrical analyses as a noninvasive method of diagnosing early stage osteoarthritis. These two studies elaborated on the underlying electrochemical mechanisms leading to the onset and progression of joint degeneration and may result in the development of a diagnostic test and intervention for early osteoarthritis.

Conceptual Framework for Dissertation

It has been theorized that osteoarthritis results from several initial triggers (e.g., macro-loading trauma, repetitive micro-loading). Regardless of the mechanism and originating tissue (e.g., subchondral bone, articular cartilage) the initial phases of joint degeneration are associated with low-grade inflammation, proteoglycan loss, local fissuring of the articular cartilage, focal bone resorption, and osteophyte formation (Blaney Davidson et al., 2006; Collins & McElligott, 1960; Custers et al., 2007; Fernihough et al., 2004; Hayami et al., 2006; Hu et al., 2006; Meng et al., 2005; Outerbridge, 1961). As the degenerative changes progress, a theorized point of no return is reached when gene expression in chondrocytes become altered throughout the joint and multiple tissues become compromised (Aigner et al., 2006; 2007). Lesions of articular cartilage deepen and progress to other regions within the joint, subchondral bone volume increases (sclerosis), and articular cartilage progressively calcifies in the deep zone (Blaney Davidson et al., Collins & McElligott, Custers et al., Fernihough et al., Hayami et al., Hu et al., Meng et al., Outerbridge). This progression is mediated by an interaction between

inflammation, which compromises tissue integrity, and biomechanical factors which propogate the inflammation and lead to further joint degeneration.

The figure in Appendix A summarizes the progression of osteoarthrititis. The figure also indicates an optimal phase for disease modifying osteoarthritis therapeutic intervention in early osteoarthritis, before the entire joint becomes compromised.

The low-grade inflammation associated with osteoarthritis is characterized by increased catabolic proteins and inflammatory cells (Fernandes et al., 2002; Haynes et al., 2002; Kaneyama, Segami, Nishimura, Suzuki, & Sato, 2002; Nishimura, Segami, Kaneyama, Suzuki, & Miyamaru, 2002; Sezgin et al., 2005; Takashi et al., 1998; Ushiyama, Chano, Inoue, & Matsusue, 2003). Anabolic proteins also increase in an attempt to recover joint integrity but their concentrations fail to compare to the catabolic proteins (see Appendix B; Fernandes et al.). The elevated concentration of proteins within the osteoarthritic joint leads to a negative electrical potential within the joint. The electrochemical environment (biochemical and bioelectrical conditions) within tissues has been theorized to help mediate wound healing, bone healing, and regulate bone adaptation

(Wolff's Law; Barker et al., 1982; Black, 1987; Charman, 1990b; Jaffe & Vanable, 1984; Nishimura, Isseroff, & Nuccitelli, 1996; Nordenström, 1992, 1994; Pullar et al., 2001; Robinson, 1985). The role of electrochemical changes in osteoarthritis has not been explored; however, early research suggests that pulsed electromagnetic fields may be a disease modifying osteoarthritic intervention (Brighton et al., 2008; Ciombor et al., 2003; Wang et al., 2004).

CHAPTER 2

A NOVEL MODEL FOR INDUCING JOINT INFLAMMATION AND DEGENERATION WITH A PHARMACOLOGICAL INTERVENTION TO REDUCE ITS EFFECTS

Introduction

Work-related musculoskeletal disorders (WMSD), also known as repetitive strain injuries, are estimated to account for 30% of lost work-day injuries in the United States private industry (Bureau of Labor Statistics, 2004). These disorders include: carpal tunnel syndrome, low back pain, rotator cuff syndrome, DeQuervain's syndrome, trigger finger, tarsal tunnel syndrome, sciatica, epicondylitis, tendinitis, hand-arm vibration syndrome, herniated spinal disks, and osteoarthritis (Barr & Barbe 2002; Barr, Barbe, & Clark, 2004; Feuerstein, Miller, Burrell, & Berger, 1998).

A positive relationship exists between the severity of WMSD and the performance of highly repetitive and/or forceful work tasks for extended periods (Barr & Barbe; Bernard, 1997; Latko et al., 1999; Moore & Garge, 1994).

Among WMSD, osteoarthritis is a growing concern because of an aging United States population. Osteoarthritis was estimated to affect 27 million United States citizens in 2005 compared to 21 million in 1995 (Lawrence et al., 2008). Radiographic evidence of osteoarthritis is predicted to be present in over 10% of the United States population by 2030 (National Institute of Arthritis and Musculoskeletal and Skin Diseases, 2002). Unfortunately, the future prevalence of osteoarthritis may be even greater due to recent changes in lifestyle (e.g., obesity). Osteoarthritis is a heterogeneous low-grade inflammatory disease, characterized by multi-tissue organ failure in diarthrodial joints. In spite of numerous epidemiological studies evaluating WMSD and osteoarthritis, the pathophysiology is poorly understood because of the inability to observe early degenerative changes in humans.

Several theories have been proposed to explain the progression of WMSD, including osteoarthritis. The multifactorial conceptual model theorizes that internal tissue tolerances are exceeded by external loads (macro-loading or repetitive micro-loading; National Research Council & Institute of Medicine, 2001), inducing physiological responses, which, in turn, influence tissue tolerance (National Research Council & Institute of

Medicine). Based on the cumulative load theory of musculoskeletal disorder development, tissues undergo progressive mechanical degradation as a result of load accumulation over time (Kumar, 2001). Furthermore, the overexertion theory of musculoskeletal development hypothesizes that tissue tolerance may be sufficient up to a certain threshold, below which its integrity is preserved and above which injury results (Kumar). Combined effects of risk factors are more than additive in exceeding tissue tolerance thresholds. When physical tasks are superimposed upon injured and inflamed tissues, a cycle of injury, inflammation, and motor dysfunction ensues, further jeopardizing the structural integrity of the tissues.

Several animal models have been used to explore the development of joint degeneration, with the goal of studying the progression of early osteoarthritis and effects of therapeutic interventions. In rodents, these consist of: (a) instability induced osteoarthritis (e.g., anterior cruciate ligament transection, destabilization of medial meniscus, bacterial collagenase; Blaney Davidson et al., 2006; Glasson et al., 2007; Hayami et al., 2006; Ma et al., 2007); (b) meniscal resections (Fernihough et al., 2004; Meng et al., 2005); (c) spontaneous development (e.g., transgenic mice, knock out mice; Blaney Davidson et

al.; Hu et al., 2006; Morko et al., 2004; Yamamoto et al., 2005); and (d) other models, including the injection of sodium iodacetate (inhibits glycolysis, promoting chondrocyte death; Fernihough et al.). While all of these models lead to a degenerative progression similar to humans, the initiating factor is not representative of the general population. Osteoarthritis in humans is not generally due to a Mendelian trait (similar to knock out mice) and is often (88% of lower extremity osteoarthritis; Brown, Johnston, Saltzman, Marsh, & Buckwalter, 2006) without an identified traumatic event (similar to instability induced models).

Recently, a novel voluntary HRHF task rat model has been shown to induce inflammation, fibrosis, and degenerative changes in nerve, muscle, tendon, and bone (Al-Shatti et al., 2005; Barbe et al., 2003; Barbe et al., 2008; Barr et al., 2003; Clark, Al-Shatti, Barr, Amin, & Barbe, 2004; Clark et al., 2003; Elliott et al., 2008). The model requires adult animals to voluntarily and repetitively grasp and pull a handle while the contralateral limb supports the body. Both repetition rate and force are controlled by a force transducer, which triggers a food reward when the rat completes the desired

task successfully. The HRHF model also allows for a controlled assessment of an intervention on inflammation and degenerative joint changes. This model may serve as a potential method for exploring disease modifying interventions in early joint degeneration.

Many theories have been developed to explain the onset and progression of osteoarthritis. Most describe an interaction between inflammation and biomechanical changes. Unfortunately, human tissue is not readily available in the early stages of osteoarthritis, and the aforementioned animal models of osteoarthritis represent unique subsets of osteoarthritis patients. Performance of a HRHF task by animals may serve as an ideal model to explore the onset of degenerative joint changes without surgical trauma or the constraints of spontaneous onset models. Furthermore, a lack of understanding between the interaction of inflammation and degenerative joint changes has hindered the development of DMOADs.

Combining the performance of a HRHF task with a secondary therapeutic intervention (e.g., ibuprofen) may lead to new DMOADs and an exploration of disease modifying effects of current anti-inflammatories. Ibuprofen is commonly used as an anti-inflammatory or analgesic, functioning as a nonselective NSAID. It is available as an

over the counter or prescription medication. The influence of ibuprofen on joint degeneration is unclear (Dingle, 1999; Gineyts et al., 2004; McKenzie et al., 1976). A steady dose of ibuprofen should result in decreased joint inflammation. Its ability to slow or halt the progression of joint degeneration is yet to be determined. The outcome of this study is intended to add to the body of knowledge for the purpose of advancing disease modifying interventions for osteoarthritis.

Statement of Purpose

The purposes of this study were to evaluate the potential of a HRHF rat model to induce joint inflammation and degeneration as well as to determine the effect of ibuprofen on joint inflammation and degeneration.

Specific Aims

1. To determine if twelve weeks of a voluntary HRHF task induces joint inflammation in female, young adult animals.

2. To determine if twelve weeks of a voluntary HRHF task induces joint degeneration in female, young adult animals.

3. To determine if eight weeks of ibuprofen can attenuate the effect of a HRHF task on inflammatory mediators in joint tissues of female, young adult animals.

4. To determine if eight weeks of ibuprofen can attenuate the effect of a HRHF task on joint degeneration in female, young adult animals.

Hypotheses

1. Twelve weeks of a voluntary HRHF task will increase mediators of inflammation (i.e., IL-1α, IL-1β, TNF-α, and IL-10) in the wrist joints (i.e., reach and support) of female, young adult rats.

2. Twelve weeks of a voluntary HRHF task will increase histopathological scores of radiocarpal joint degeneration (i.e., reach and support) in female, young adult rats.

3. Eight weeks of ibuprofen will attenuate the effect of a HRHF task on inflammatory mediators (i.e., IL-1α, IL-1β, TNF-α, and IL-10) in the wrist joints (i.e., reach and support) of female, young adult rats.

4. Eight weeks of ibuprofen will attenuate the effect of a HRHF task on histopathological scores of radiocarpal joint degeneration (i.e., reach and support) in female, young adult rats.

Methods

Research Design

A randomized controlled trial design was used in this study. Three components were used to address the purposes of the study: (a) biochemical analyses to assess joint inflammation with and without the use of ibuprofen, (b) histopathological analyses to assess joint degeneration with and without the use of ibuprofen, and (c) a biochemical analysis to assess a serum marker of cartilage degradation with and without the use of ibuprofen. Seven groups were analyzed in various components of this study and are presented in Table 1.

For the biochemical analyses of inflammatory markers, three independent variables were assessed: group, region, and limb. Group consisted of five levels: (a) NORM, (b) HRHF6, (c) HRHF12, (d) HRHF6+IBU, and (e) HRHF12+IBU. Limb consisted of two levels: preferred reach, the limb primarily used to perform the repetitive pulling task; and preferred support, the limb primarily used for postural support (see Figure C-1). Region consisted of two levels: wrist joints and radioulnar diaphyses. The primary dependent variables were inflammatory mediator concentrations to assess inflammation: IL-1α, IL-1β, TNF-α, and IL-10.

Table 1. Animal Group Definitions

Group	Training	Weeks of Task	Treatment
NORM	No Training	0	No Ibuprofen
TR CON	Trained	0	No Ibuprofen
TR CON+IBU	Trained	0	Ibuprofen
HRHF6	Trained	6	No Ibuprofen
HRHF6+IBU	Trained	6	Ibuprofen
HRHF12	Trained	12	No Ibuprofen
HRHF12+IBU	Trained	12	Ibuprofen

Note. NORM = normal control; TR CON = trained controls; TR CON+IBU = trained controls plus ibuprofen; HRHF6 = high-repetition, high-force for 6 weeks; HRHF6+IBU = high-repetition, high-force for 6 weeks plus ibuprofen; HRHF12 = high-repetition, high-force for 12 weeks; and HRHF12+IBU = high-repetition, high-force for 12 weeks plus ibuprofen.

For the histopathological analyses, three independent variables were assessed: group, limb, and zone. Group consisted of four levels: (a) TR CON, (b) TR CON+IBU, (c) HRHF12, and (d) HRHF12+IBU. NORM animals were analyzed, but were not included in the statistical analysis. These latter animals served as a reference group. Limb consisted of two levels: preferred reach and support limb. Zone consisted of four regions, progressing from the radial margin of the distal radius articular cartilage to the

ulnar margin. The dependent variables were histopathological scores, used to assess severity of joint degeneration, and epiphyseal plate staining and immunohistochemical observations to assess which cells were present (e.g., osteoclasts and macrophages).

For the biochemical analysis of a serum a marker for collagen types 1 and 2 degeneration (i.e., C1,2C concentrations), two independent variables were assessed: time and treatment. Time consisted of three levels: (a) 0 weeks of task performance, (b) 6 weeks of task performance, and (c) 12 weeks of task performance. Treatment consisted of two levels: ibuprofen and control, no ibuprofen. These two variables were used to create six independent treatment levels: (a) NORM, (b) HRHF6, (c) HRHF12, (d) TR CON+IBU, (e) HRHF6+IBU, and (f) HRHF12+IBU. The primary dependent variable was serum C1,2C concentration.

Animals

Adult female Sprague-Dawley rats (3.5 months of age at onset of experiments) were obtained from ACE Animals Inc. (Boyertown, PA). The animals were housed in the Central Animal Facility on the Health Sciences Campus at Temple University. They were housed in separate cages in a 12 hr light/dark cycle. All trained animals were food restricted for no longer than 1 week to no less than 80% of full body

weight during an initial shaping period when they first began learning the task. During the remaining four weeks of shaping, rat weights were measured and then maintained at ± 5% of yoked free access to food control rats. Trained animals were weighed once per week, provided rat chow daily to supplement the sucrose pellets used for food reward, and given free access to water throughout the experiment. Age-matched TR CON and TR CON+IBU were yoked to HRHF and HRHF+IBU animals by weight and diet (i.e., fed both sucrose and rat chow to matched experimental animals with similar diet and weight) and were sacrificed at matched time points. Animal care and use was monitored by Temple University Animal Care and Use Committee to assure compliance with the provisions of Federal Regulations and the National Institute of Health "Guide for the Care and Use of Laboratory Animals." Animals were randomly assigned to one of the seven groups.

Behavioral Apparatus, Training Procedures, and Task Performance

Behavioral Apparatus

The force apparatus was custom-designed (by Dr. Ann Barr and Custom Medical Research Equipment, Glendora, NJ) and integrated into an existing commercially available operant training system (Med Associates, Georgia, VT). The

force apparatus consisted of a machined aluminum, U-shaped platform block that was affixed externally to the base of the training chamber, such that its upright side was oriented parallel to the chamber wall (see Figure C-1). A miniature tension-compression load cell (Model LCFA-500g, Omega Engineering, Stamford, CT), with a threaded load axis, was mounted to the upright side of the metal base so that its load axis was oriented perpendicular to the chamber wall. A threaded aluminum rod, approximately 76 mm in length, was attached to the load axis of the load cell and threaded through a cylindrical channel in the side of the platform block next to the chamber wall. This channel prevented off-axis loading of the load cell. A small aluminum bar, 1.5 mm in diameter, was attached to the free end of the aluminum rod and served as the force handle. The handle was positioned 2.5 cm from the chamber wall and oriented so that it formed a 45 deg angle from vertical in the direction of pronation (which was adjustable, depending on the preferred limb of the animal). The load cell output was interfaced with a strain-gauge signal conditioner (Analog Devices, Norwood, MA), which amplified and filtered the load cell signal before it was sampled digitally at 100 Hz, using ForceLever software (version 1.03.02, Med Associates). An oval aperture, 1.5 cm wide by 2 cm high,

in the Plexiglass test chamber wall was located at the animal's shoulder height, allowing access to the force handle by reaching through the aperture with the forepaw. The 2.5 cm distance of the handle from the exterior chamber wall required the animal to fully elevate the shoulder and extend the elbow to grasp the force handle, giving a postural constraint to this task.

Training Procedures

All of the animals were handled for 1 to 2 weeks prior to entry into the study. The HRHF6 (n = 5), HRHF12 (n = 21), HRHF6+IBU (n = 5), HRHF12+IBU (n = 16), TR CON (n = 8), and TR CON+IBU (n = 9) animals learned to reach for the food during an initial 5 to 6 weeks training period. During this period, the animals were first encouraged to reach through open bars for food pellets placed on an elevated platform for 5 min/day. When they began to reach freely for the food, they were transferred to the test chamber until they could reach into the tube dispenser with no specified reach rate for 10 to 20 min/day. The training animals were then trained to achieve at least 8 reaches/min for 10 to 20 min/day. Most of the animals tended to overreach and averaged 12 reaches/min.

Task Performance

When the animals were able to perform the task consistently, typically after a total training period of 3 to 6 weeks, the HRHF and HRHF+IBU animals began the task regimen at the rate of 12 reaches/min at 60% maximum grip strength, for 2 hr/day, 3 days/week (Monday, Wednesday, Friday) for 12 weeks. The high force task was previously defined by Barr and Barbe (2002), based on a review of the literature, and Clark et al. (2004). The daily task was divided into four, 0.5-hr training sessions separated by 1.5 hr. Animals were allowed to use their preferred limb to reach. The side used to reach was recorded for each session. The contralateral limb was used as a postural support limb throughout the reach and pull task (see Figure C-1).

To perform the task, animals were cued to reach every 5 sec and pull a force handle between 55 to 65% of their maximum for at least 50 ms. If the force and time criteria were met, a reward light turned on and a food pellet was dispensed into a trough. The animal could only reach the reward by releasing the handle. Maximum pulling force was determined on the last day of the initial training period during a 5 min session in which the force criterion for a food reward was gradually increased. Animals were observed

carefully for their maximum force generating ability during this 5 min session, and maximum pulling force was selected as the highest force resulting in a successful reach (i.e., food pellet reward) that could be repeated 3 times. In general, maximum pulling force was approximately 80% of maximum grip strength and was considered a more accurate representation of maximum voluntary contraction. Force threshold criteria established a window in which force was maintained for at least 50 msec for animals to obtain a food reward. If they either "undershot" the minimum criterion or "overshot" the maximum criterion, no food reward was delivered. Since this was a blind reach with no knowledge of performance, but only knowledge of results (i.e., a light signal and food reward), the task constraints were reasonably selected to allow for successful motor performance. The target force criterion for the high force conditions was 60% maximum pulling force. Therefore, the criteria boundaries, taking into account estimates of force variability, were 60 ± 5% maximum pulling force.

Intervention Procedures: Ibuprofen Administration

The effectiveness of oral ibuprofen, a nonselective cyclooxygenase inhibitor, as a secondary intervention to reduce wrist joint inflammation and degeneration associated

with a HRHF task regimen was assessed. Based on previous research, animals performing the HRHF task regimen showed the first signs of behavioral degradation between 3 to 6 weeks after task onset (Clark et al., 2004). These behavioral changes were observed as decreases in reach rate as well as duration and degradation of reach movement patterns. These previously observed behavioral indicators were used to guide the initiation of ibuprofen administration. In this study, at the end of the 4th week of task performance, the HRHF+IBU and TR CON+IBU animals were administered ibuprofen (Children's Motrin Grape Flavored, Johnson & Johnson Services, Inc., Langhorne, PA) in drinking water daily (45 mg/kg body weight). The amount of water consumed/day was tracked for each animal by measuring the amount given to amount consumed daily. Based on water consumption, the average weekly ibuprofen dose was significantly less among TR CON+IBU animals (38.7 ± 3.8 mg/Kg body weight) than HRHF6+IBU (48.1 ± 9.8 mg/Kg body weight; $p = .011$) and HRHF12+IBU (48.8 ± 6.3 mg/Kg body weight; $p = .003$) animals. The doses were lower than the maximum limit for gastrointestinal toxicity in animals, yet have been shown effective in reducing chronic inflammation (Adams et al., 1970). The HRHF+IBU animals continued to perform the HRHF task regimen along with the ibuprofen treatment for the remainder of the 12-week period.

Tissue Collection and Analyses

Tissue Collection for Histology

Following euthanasia by lethal overdose (Nembutol, 120 mg/kg body weight), animals were perfused transcardially with 4% paraformaldehyde in 0.1 M phosphate buffer (pH 7.4). The entire upper extremity and posterior thorax were postfixed "en bloc" by immersion overnight. Bilateral wrist joints and radioulnar diaphyses were collected from each animal. After postfixation, soft tissues were dissected away from bony tissues. Wrist joints were then decalcified and paraffin embedded before microtome sectioning into 8 µm longitudinal sections. The sections were mounted on coated slides (Ultrastick; Corning Inc., Corning, NY) for eventual histological and immunohistochemical analyses.

Histopathological Grading System for Degenerative Changes

Histological scores were assessed using paraffin embedded and sectioned joints and bones stained with Safranin O staining and fast green in HRHF12 (n = 15), HRHF12+IBU (n = 10), TR CON (n = 8), TR CON+IBU (n = 9), and NORM (n = 4). The osteoarthritic severity in the articular cartilage of the distal radius was assessed in a blinded manner by 2 independent raters using an adaptation

of a modified Mankin Scoring System (see Appendix D; van der Sluijs et al., 1992). The modified Mankin Scoring System was supplemented with half points for the subscores. Each radiocarpal joint was assessed in four zones: (a) zone 1 was the radial edge of articular cartilage, (b) zone 2 was a radial area of articular cartilage ulnar to zone 1, (c) zone 3 was an area of articular cartilage ulnar to zone 2, and (d) zone 4 was the ulnar edge of the articular cartilage. Zones with tears were not scored (see Figure E-1). If a joint had a questionable appearance (e.g., tears or folds produced during slide preparation), other sections of the joint were evaluated. Additional sections to evaluate structure and cellular subscores included hematoxylin and eosin stained cross sections. Epiphyseal plate staining was assessed using a five-grade scoring system: 0 = normal staining, 1 = slight reduction, 2 = moderate reduction, 3 = severe reduction, and 4 = no dye noted. Reliability was assessed for the primary investigator for each zone: Zone 1 $ICC(3,1)$ = .91, Zone 2 $ICC(3,1)$ = .85, Zone 3 $ICC(3,1)$ = .66, Zone 4 $ICC(3,1)$ = .76, and epiphyseal plate $ICC(3,1)$ = .77.

Tissue Collection for Cytokine Assays and Analysis

Animals were euthanized with an overdose of sodium pentobarbital (Nembutal; 120 mg/kg body weight). Wrist joints and radioulnar diaphyses were collected from HRHF6 (n = 5), HRHF12 (n = 6), HRHF6+IBU (n = 5), HRHF12+IBU (n = 6), and NORM (n = 9). Tissues were flash-frozen and stored at -80 °C until homogenization. After thawing on ice, bones were crushed and powdered. All tissue samples were homogenized in a radioimmuno precipitation assay buffer and a protein extraction buffer, consisting of (a) 50 mM Tris-HCl, pH 7.5; (b) 135 mM NaCl; (c) 1% Triton X-100; (d) 0.1% sodium deoxycholate; (e) 2 mM EDTA; (f) 50 mM NaF; (g) 2 mM sodium orthovanadate; (h) 10 µg/ml aprotinin; (i) 10 µg/ml leupeptin; and (j) 1 mM PMSF. Homogenates were incubated for 60 min at 4 °C on a rocker, centrifuged, and then the supernatants were collected and stored at −80 °C. Total protein concentrations were measured using a bicinchoninic acid protein assay (Thermo Fisher Scientific Inc., Rockford, IL). Fifty µl tissue lysates were utilized for measuring cytokines, in duplicate, for each cytokine ELISA assay kit (Invitrogen Corporation, Carlsbad, CA), according to the manufacturer’s protocol.

Immunohistochemistry

Immunohistochemistry was performed to qualitatively assess which cells (e.g., osteoclasts and macrophages) were present in NORM animals and animals that performed the HRHF task for 12 weeks. An anti-ED1 antibody was selected to identify these cells. ED1 recognizes a 90 kDa lysosomal glycoprotein associated with lysomes in osteoclasts, phagocytic macrophages, and their progenitors (Chemicon International, Inc., Temecula, CA). For peroxidase staining, tissue sections were first exposed to 3% H_2O_2 in phosphate buffered saline to block endogenous peroxidase activity, washed, and treated with 0.05% pepsin in 0.01 N HCl for 20 min at room temperature. Pepsin was used to break down protein crosslinks formed during fixation and expose the targeted proteins. After two more washings, sections were incubated for 30 min in 4% goat serum/phosphate buffered saline to block non-specific binding sites. Sections were then incubated overnight at room temperature with primary antibodies diluted with serum/phosphate buffered saline (1:250). The primary antibody was visualized by standard indirect immunohistochemistry, using appropriate secondary antibodies conjugated to horseradish peroxidase (brown precipitate; Jackson ImmunoResearch Laboratories, Inc.,

Willow Grove, PA). For immunoperoxidase, a routine diaminobenzidine reaction was carried out using FAST Sigma peroxidase tablets. Negative control staining was performed by omitting the primary antibodies or omitting the second antibody. All slides were counter stained lightly with hematoxylin. Slides were dehydrated and coverslipped with a mounting media of distyrene, plasticizer, and xylene (DPX, Electron Microscopy Sciences, Hatfield, PA) and then examined using bright field microscopy.

Collection of Serum and Measurement of a Serum Marker of Collagen Types 1 and 2 Degeneration

To validate the histopathological findings an ELISA measured serum concentrations of carboxy terminus of the 3/4 peptide (C1,2C) generated by cleavage of types I and II collagens by matrix metalloproteinases. C1,2C serum concentrations reflect degradation of tendons, bone, and articular cartilage (Frisbie, Al-Sobayil, Billinghurst, Kawcak, & McIlwraith, 2008). Serum was collected from HRHF6 (n = 5), HRHF12 (n = 6), HRHF6+IBU (n = 7), HRHF12+IBU (n = 6), TR CON+IBU (n = 6), and NORM (n = 6) following euthanasia with sodium pentobarbital (Nembutal, 120 mg/kg body weight), 18 hrs after completion of the final task session. Blood was collected by cardiac

puncture using a 23-gauge needle and centrifuged immediately at 1,000 g for 20 min at 4 °C. Serum was collected, flash-frozen, and stored at -80 °C until analyzed. C1,2C was assayed in serum using commercially available ELISA kits (IBEX Technologies, Inc.; Montreal, Quebec). All samples were analyzed in duplicate in a blinded fashion and batched as much as possible to reduce potential inter-assay variability. Data are presented as ng/ml serum.

Statistical Analyses

All data were analyzed with descriptive and interferential statistics using SPSS 15.0 statistical package (Chicago, IL). Statistical significance was based on a $p \leq .05$. All measures of variance are reported as standard error of the mean.

Inflammatory Mediator ELISA Analyses

The ELISA data were analyzed using a 5 (group) x 2 (region) x 2 (limb) analysis of variance (ANOVA) to assess group differences at four regions/limbs of the body (i.e., reach wrist joint, support wrist joint, reach radioulnar diaphysis, and support radioulnar diaphysis). Each dependent variable was analyzed separately within a 5 x 2 x

2 ANOVA. Significant findings were assessed with appropriate follow-up ANOVAs and Bonferroni corrected independent t-tests.

Histopathological Analyses

Initially, histological total scores for each zone were analyzed using paired-sample t-tests with Bonferroni corrections to assess differences between zones (see Table G-1). All zones of articular cartilage were significantly different except between Zones 1 and 4. Because these two zones were on the margins of the articular cartilage and may represent a transitional region of articular cartilage, only Zones 2 and 3 were analyzed further. A 4 (group) x 2 (limb) x 2 (zone) ANOVA with zone treated as a within variable was performed to assess differences in histopathological articular cartilage scores between groups and limbs in the two zones of articular cartilage. A 4 (group) x 2 (limb) ANOVA was used to determine if group and limb differences existed in epiphyseal plate staining scores. Significant findings were assessed with appropriate follow-up one-way ANOVAs and Bonferroni corrected independent t-tests. Bonferroni corrections in SPSS are calculated by multiplying p values by the number of t-tests performed.

Serum a Marker of Collagen Types 1 and 2 Degeneration

A 3 (time) x 2 (treatment) ANOVA was performed to assess differences in C1,2C serum concentrations. Significant findings were assessed with follow-up Bonferroni corrected independent t-tests.

Results

All raw data are presented in Appendix F. All test statistics are presented in Appendix G.

Inflammatory Mediator Analyses

Group inflammatory mediator concentration means and standard error of the means are presented in Table 2. The 5 (group) x 2 (region) x 2 (limb) ANOVA for IL-1α concentrations demonstrated significant interaction effects for group x region and group x limb (see Figures H-1 and H-2). Follow-up one-way ANOVAs within each region revealed a significant main effect for group in both regions (i.e., radiocarpal joint and radioulnar diaphysis). Bonferroni corrected independent t-tests demonstrated that IL-1α concentrations were 191 to 582% higher in the HRHF12 group than in the other four groups in the radioulnar diaphyses. At the wrist, IL-1α concentrations were 222 to 477% greater in the HRHF12 group than in the other four groups. Follow-up one-way ANOVAs for IL-1α concentrations within each limb

Table 2. Inflammatory Mediator Concentrations in Radioulnar Diaphyses and Wrist Joints Collapsed among Groups

Variable	IL-1α	IL-1β	TNF-α	IL-10
NORM	0.314 ± 0.067*	0.470 ± 0.094*	0.720 ± 0.263*	0.337 ± 0.093*#
HRHF6	0.331 ± 0.066*	0.314 ± 0.013*	0.171 ± 0.010*	0.595 ± 0.037*
HRHF6+IBU	0.374 ± 0.081*	0.276 ± 0.017*	0.099 ± 0.006*	0.528 ± 0.047*
HRHF12	1.418 ± 0.209	1.041 ± 0.154	4.293 ± 0.580	1.741 ± 0.190
HRHF12+IBU	0.407 ± 0.067*	0.429 ± 0.042*	0.141 ± 0.018*	0.904 ± 0.091*

Note. NORM = normal controls (*N* = 9); HRHF6 = high-repetition, high-force for 6 weeks (*N* = 5); HRHF12 = high-repetition, high-force for 12 weeks (*N* = 6); HRHF6+IBU = high-repetition, high-force for 6 weeks plus ibuprofen (*N* = 5); and HRHF12+IBU = high-repetition, high-force for 12 weeks plus ibuprofen (*N* = 6). All data are reported in pg/µg/ml. All values are reported in means and standard error of the mean.
* Significantly different from HRHF: $p \leq .05$. # Significantly different from HRHF12+IBU: $p \leq .05$.

revealed a significant main effect for group in both limbs (i.e., reach and support limb). Bonferroni corrected independent t-tests demonstrated IL-1α concentrations in reach limbs were 348 to 517% greater in the HRHF12 group than in the other four groups. IL-1α concentrations in support limbs were 160 to 227% greater in the HRHF12 group group than in the other four groups. The 5 (group) x 2 (region) x 2 (limb) ANOVA for IL-1α concentrations demonstrated significant main effect for region. IL-1α concentrations were 170% greater at wrists compared to radioulnar diaphyses.

The 5 (group) x 2 (region) x 2 (limb) ANOVA for IL-1β, TNF-α, and IL-10 concentrations revealed a significant main effect for group. Bonferroni corrected independent t-tests demonstrated that IL-1β concentrations were 121 to 277% higher in the HRHF group than in the other four groups (see Figure H-3). Bonferroni corrected independent t-tests demonstrated that TNF-α concentrations were 496 to 4,236% higher in the HRHF group than in the other four groups (see Figure H-4). Bonferroni corrected independent t-tests demonstrated that IL-10 concentrations were 93 to 417% higher in the HRHF group than in the other four groups. IL-10 concentrations were 168% greater in the HRHF12+IBU group than in the NORM group (see Figure H-5).

Histopathological Analyses

Histopathological score means and standard error of the means are presented in Table 3. The 4 (group) x 2 (limb) x 2 (zone) ANOVA with zone as a within measure demonstrated significant main effects for zone and group. Histopathological scores for zone 2 was 19% greater than zone 3. Follow-up Bonferroni corrected independent t-tests demonstrated that HRHF12 was greater than TR CON, TR

Table 3. Histopathological Scores in Zones 2 and 3 among Groups

Limb	Zone 2	Zone 3	Combined Score
TR CON	3.5 ± 0.6	3.3 ± 0.6	3.4 ± 0.5*
TR CON+IBU	3.4 ± 0.7	1.9 ± 0.7	2.7 ± 0.6*
HRHF12	5.6 ± 0.5	5.1 ± 0.4	5.4 ± 0.4
HRHF12+IBU	3.6 ± 0.6	3.2 ± 0.5	3.4 ± 0.5*
Total	4.0 ± 0.3	3.4 ± 0.3#	

Note. TR CON = trained controls (***N*** = 8); TR CON+IBU = trained controls plus ibuprofen limb (***N*** = 6); HRHF12 = high-repetition, high-force for 12 weeks (***N*** = 14); HRHF12+IBU = high-repetition, high-force for 12 weeks plus ibuprofen (***N*** = 10). All values are reported in means and standard error of the mean.
* Significantly different from HRHF12: $p \leq .05$.
# Significantly different between zones 2 and 3: $p \leq .05$.

CON+IBU, and HRHF12+IBU (59, 101, 59%, respectively; see Figure I-1). Typical representations for histological characteristics of each group are shown in Figure E-2.

The histopathological subscores (i.e., structure, cellular, and staining) are presented in Figures I-2 to I-4. Structural subscores ranged from 25 to 43% greater in the HRHF12 group than in the three other groups. Cellular scores were 46 to 58% greater in the HRHF12 group than in the other groups. Staining subscores were 79 to 257% greater in the HRHF12 group than in the other groups.

The 4 (group) x 2 (limb) ANOVA on epiphyseal staining scores demonstrated a significant main effect for group only (see Figure I-5). An example of epiphyseal plates from TRCON+IBU and HRHF12 animal are shown in Figure E-3. HRHF12 epiphyseal staining scores were greater than TR CON+IBU and HRHF12+IBU (77 and 178%, respectively). TR CON epiphyseal plate staining scores were 150% greater than HRHF12+IBU.

Serum Marker of Collagen Types 1 and 2 Degeneration

C1,2C serum concentration means and standard error of the means are presented in Table 4. The 3 (time) x 2 (treatment) ANOVA demonstrated a significant interaction. Bonferroni corrected independent t-tests revealed no

Table 4. C1,2C Serum Concentrations between Time and Treatment

Group	Time	Treatment	C1,2C (ng/ml)
NORM	0 week	No Ibuprofen	381.762 ± 28.473
HRHF6	6 week	No Ibuprofen	470.433 ± 47.729
HRHF12	12 week	No Ibuprofen	546.281 ± 74.261
TR CON+IBU	0 week	Ibuprofen	396.063 ± 54.275
HRHF6+IBU	6 week	Ibuprofen	414.905 ± 33.827
HRHF12+IBU	12 week	Ibuprofen	281.984 ± 35.520

Note. NORM = normal controls (*N* = 6); TR CON+IBU = trained controls plus ibuprofen limb (*N* = 6); HRHF6 = high-repetition, high-force task for 6 weeks (*N* = 5); HRHF6+IBU = high-repetition, high-force for 6 weeks plus ibuprofen (*N* = 7); HRHF12 = high-repetition, high-force task for 12 weeks (*N* = 6); and HRHF12+IBU = high-repetition, high-force for 12 weeks plus ibuprofen (*N* = 6). All values are reported in means and standard error of the mean.

significant differences within the interaction. The 3 (time) x 2 (treatment) ANOVA on C1,2C serum concentrations also demonstrated a significant main effect for treatment. Animals receiving no treatment (465.907 ± 34.121 ng/ml) had serum concentrations of C1,2C that were 27% greater than ibuprofen animals (366.980 ± 26.423 ng/ml).

ED1 Immunohistochemical Staining

HRHF reach limbs and NORM limbs were evaluated for the presence of ED1+ cells (e.g., macrophages, osteoclasts, and their progenitors). In HRHF reach limbs, ED1+ mononucleated cells were identified in the subchondral bone adjacent to articular cartilage in the distal radius (see Figure J-1). ED1+ mononucleated cells, presumably osteoclast progenitors, were found in multiple regions of the carpal bones (see Figure J-1). None of the NORM or HRHF+IBU limbs had ED1+ cells in the subchondral bone of the radius or carpal bones. ED1+ cells were identified in the outer synovium of the radiocarpal joint in HRHF reach limbs, but not in other groups (see Figure J-2).

Discussion

The development of DMOADs has been hindered by the inability of degenerative joint animal models to accurately represent human responses to therapeutic interventions. The HRHF task was selected because it is a nonsurgical-voluntary repetitive task previously associated with soft tissue and bone inflammation and degeneration. The purpose of this study was to assess the HRHF task as a novel animal model theorized to generate joint inflammation and degeneration and to determine the effect of ibuprofen on these outcomes. After 12 weeks of a HRHF task, animals

demonstrated evidence of joint inflammation (i.e., elevated IL-1α, IL-1β, TNF-α, and IL-10 concentrations) and joint degeneration (i.e., elevated histopathological scores). Eight weeks of ibuprofen reduced joint inflammation and joint degeneration. An additional finding of this study was that radioulnar diaphyses also showed an increase in inflammation following 12 weeks of a HRHF task, which was attenuated by 8 weeks of ibuprofen use.

Inflammatory Protein Analyses

High-Repetition, High-Force Tasks Induce Wrist Joint and and Diaphysis Inflammation

A primary aim of this study was to assess if a HRHF task could lead to inflammatory response at the wrist joint and radioulnar diaphyses. The results of this study revealed that IL-1α, IL-1β, TNF-α, and IL-10 concentrations were all elevated after 12 weeks of a HRHF task regardless of limb (i.e., reach or support). In contrast, six weeks of the HRHF task did not produce an increase in inflammatory mediator concentrations. All four proteins have been reported to be expressed in osteoarthritic articular cartilage (i.e., chondrocytes; Doss et al., 2007; Hulejova et al., 2007; Iannone et al., 2001; Tchetina, Squires, & Poole, 2005; Wang, Verdonk, Elewaut, Veys, &

Verbruggen, 2003), synovial membranes (e.g., macrophages, synovial fibroblasts, and plasma cells; Bondeson et al., 2006; Doss et al.; Fiorito, Magrini, Adrey, Mailhe, Broute-Boye, 2005; Hulejova et al.), and subchondral bone (e.g., osteoblasts; Hopwood, Tsykin, Findlay, Fazzalari, 2007; Hulejova et al.; Sanchez et al., 2008).

Signs of behavioral changes (e.g., decrease in reach rate, decrease reach duration, and degradation of reach movement patterns) have been shown to occur with HRHF tasks between 3 to 6 weeks (Clark et al., 2004). Because this task represents a voluntary activity, the animals may have responded by decreasing their activity as pain or discomfort increased. The HRNF task typically results in the animals decreasing their participation between 5 and 6 weeks and then again between 9 and 11 weeks (Barbe et al., 2003; Clark et al., 2003). At 6 weeks, the decrease in activity may provide an opportunity to decrease wrist joint and diaphyseal inflammation. However, at 12 weeks, the second rest phase is apparently not sufficient to eliminate the inflammatory response. Furthermore, the histopathological scoring demonstrated significant joint degeneration at 12 weeks. The onset of these early degenerative joint changes may enhance inflammation at 12 weeks. For example, IL-1α concentrations, a key

inflammatory cytokine in rats, were greater in HRHF12 animals' wrist joints compared to their radioulnar diaphyses.

Ibuprofen Attenuates Wrist Joint and Diaphysis Inflammation

The results of this study confirmed that ibuprofen has an anti-inflammatory effect at 12 weeks of a HRHF task, regardless of limb (i.e., reach or support). The lack of a significant finding at 6 weeks may be attributed to the concentrations of the inflammatory mediators (comparable to NORMS) or because ibuprofen concentrations were just establishing a steady state dose. After 12 weeks of a HRHF task, all of the inflammatory mediator concentrations were lower in the animals that received ibuprofen for 8 weeks than for the HRHF12 animals. In contrast to IL-1α, IL-1β, and TNF-α, IL-10 concentrations did not return to baseline levels (NORM). IL-10 is a cytokine associated with anti-inflammatory and protective articular properties (Fernandes et al., 2002). In contrast to the other three proteins, the pathways promoting IL-10 expression may not be as influenced by ibuprofen. The results of this study support an anti-inflammatory role for ibuprofen in limbs exposed to 12 weeks of a HRHF task.

Histopathological Analyses

High-Repetition, High-Force Tasks Induce Radiocarpal Joint Degeneration

The results of this study revealed that 12 weeks of HRHF tasks increased histopathological scores of radiocarpal joint degeneration in female, young adult Sprague-Dawley rats. The HRHF task represents a new voluntary animal model capable of inducing joint degenerative changes within 12 weeks. Previous studies have shown that this animal model can induce inflammation and degeneration in soft tissue and bone (Al-Shatti et al., 2005; Barbe et al., 2003; Barbe et al., 2008; Barr et al., 2003; Clark et al., 2004; Clark et al., 2003; Elliott et al., 2008). The increase in histopathological scores in the HRHF12 group compared to other groups may be primarily attributed to changes in the staining and cellular subscores. Only three HRHF12 limbs had signs of definite structural changes (e.g., pannus). The observed changes represent an early stage of joint degeneration (Blaney Davidson et al., 2006; Yamamoto et al., 2005). Histopathological scores were higher in the radial zone compared to the ulnar zone of articular cartilage. Based on previous animal and human research, if the HRHF task continued beyond 12 weeks, the degenerative changes would

presumably propagate throughout the joint (Hayami et al., 2006; Pelletier et al., 2007). The radial region of articular cartilage appears to be the initial site of joint degeneration in reach limbs. This site is most likely affected first because the task is performed with radial deviation of the wrist, which would increase the loading on this region of the articular cartilage.

In addition to degenerative changes in the distal radius articular cartilage, HRHF12 carpal bones showed signs of degenerative changes compared to TR CON, TR CON+IBU, and HRHF12+IBU carpal bones. Unfortunately, the histopathological scoring system could not be used to score the articular cartilage morphology of rat carpal bones. Future research should use a scoring system which accounts for the unique superficial changes (e.g., cellular changes, and superficial layer irregularities) associated with carpal articular cartilage degeneration.

Radiocarpal degenerative joint changes in the HRHF12 animals were supported by the presence of ED1+ mononucleated cells in the carpal bones and the subchondral bone adjacent to the articular cartilage in the distal radius. These osteoclast progenitor cells are indicators

of subchondral bone remodeling in the HRHF12 group, a common feature of early osteoarthritis (Hayami et al., 2006).

Other nonsurgical joint degeneration models (e.g., spontaneous or knock-out models) promote proteoglycan depletion and superficial cell clustering at 8 to 12 weeks and structural changes at 6 months of age (Blaney Davidson et al., 2006; Hu et al., 2006). This new model follows a similar time to onset but does not require the time and expense to breed spontaneous or knock-out animals. Furthermore, most joint degeneration models only include male rats because female rats develop degenerative changes slower than males, but in the current study females showed changes after 12 weeks of a HRHF task.

Ibuprofen Attenuates Radiocarpal Joint Degeneration

The results of this study revealed that 8 weeks of ibuprofen had a protective effect. Histopathological scores were lower in HRHF12+IBU animals than in HRHF12 animals. Ibuprofen functions as an analgesic and anti-inflammatory. Joint degeneration has been associated with low-level inflammation within a joint. Reduction of joint inflammation should attenuate the degenerative progression. Ibuprofen has been previously implicated with catabolic

changes in articular cartilage but the anti-inflammatory effects should prevent joint degeneration (Dingle, 1999; Gineyts et al., 2004; McKenzie et al., 1976). The histopathological scoring data from this animal model supports a protective role for ibuprofen in joint degeneration. The histopathological data were confirmed with C1,2C serum concentrations, a marker of collagen types 1 and 2 degeneration, and in soft tissue, bone, and articular cartilage. C1,2C serum concentrations were significantly reduced in animals receiving ibuprofen. Furthermore, the distal epiphyseal plate of the radius had less proteoglycan loss in HRHF12+IBU animals than their no treatment counterparts (i.e., TR CON and HRHF12). Local bone and articular cartilage scoring and systemic markers indicate the ibuprofen has a protective effect on radiocarpal joint degeneration associated with HRHF tasks.

Conclusion

Twelve weeks of a voluntary HRHF task represents a successful model for inducing joint inflammation and degeneration. IL-1α, IL-1β, TNF-α, and IL-10 concentrations, as well as histopathological joint scores were elevated after 12 weeks of HRHF. Furthermore, ED1+ cells were identified in the synovium (indicative of joint inflammation) and subchondral bone (indicative of

subchondral bone remodeling) in HRHF radiocarpal joints. IL-1α, IL-1β, TNF-α, and IL-10 concentrations, as well as histopathological joint scores were lower in the animals that underwent 12 weeks of a HRHF task with ibuprofen than those not receiving ibuprofen. Based on the current model, ibuprofen appears to be not only an anti-inflammatory but also a chondroprotective drug. The HRHF task model leads to joint degeneration and provides an opportunity to observe the effects of pharmaceutical interventions (e.g., NSAIDs and DMOADs).

CHAPTER 3

ANALYSIS OF THE ELECTROCHEMICAL ENVIRONMENT OF OSTEOARTHRITIC KNEES

Introduction

Osteoarthritis is a significant health problem, affecting over 50% of Americans 65 years of age and older (National Institute of Arthritis and Musculoskeletal and Skin Diseases, 2002). Radiographic evidence of osteoarthritis is estimated to be present in 10% of the United States population by 2030 (National Institute of Arthritis and Musculoskeletal and Skin Diseases). The World Health Organization estimates that 10% of the world population over 60 years of age has symptomatic osteoarthritis (70.85 million osteoarthritic patients; Symmons et al., 2006; US Census Bureau, 2007). In 2007, the United Nations announced that the world population would increase by 2.5 billion between 2005 and 2050. Half of the increase is attributed to the population over 60 years of age. This increase alone represents 125 million

new osteoarthritic patients, which may be an underestimate as developing nations' life styles change and the prevalence of obesity increases.

Classified as a degenerative disease, osteoarthritis is associated with the inflammatory process and characterized by an increase in catabolic proteins (e.g., pro-inflammatory cytokines and metalloproteinases) and a decrease in anabolic proteins (e.g., anti-inflammatory cytokines; Baddour & Bradley, 1999; Fernandes et al., 2002; Kaneyama et al., 2002; Shi et al., 2004). Osteoarthritis results in articular cartilage and subchondral bone destruction, synovial membrane thickening, and decreased synovial fluid viscosity of the affected joint (Baddour & Bradley). A wide variability in the biochemical environment occurs throughout the osteoarthritic degenerative process across the general population (Sezgin et al., 2005).

Symptomatic osteoarthritic patients present a challenge to treat non-operatively as evidenced by the 23 non-operative treatment options that exist currently (American College of Rheumatology, 2000). While total joint arthroplasty is a typical beneficial treatment for end-stage degeneration, early-stage management includes: (a) therapeutic exercises (Roddy et al., 2005), (b)

activity modification (Buckwalter et al., 2001), (c) external load reductions (Richards, Sanchez-Ballester, Jones, Darke, & Livingstone, 2005), (d) oral and injectable pharmacological interventions (Buckwalter et al.), and (e) electromagnetic stimulation (Trock et al., 1993; Trock et al., 1994; Pipitone & Scott, 2001). Evidence for support of these interventions has not been established across the general population. This is most evident among the pharmacological agents where various oral and injectable prescription options exist (e.g., hyaluronan, cortisone-like steroids, naproxen sodium, nabumetone). Furthermore, interventions designed to prevent or reverse the progression of osteoarthritis have had limited success (Trock et al.). One possible reason for the limited success is that treatment protocols are not directed to the biochemical conditions of an individual's osteoarthritic joint.

Common assessments currently used to diagnose osteoarthritis include radiographs (Vilalta et al., 2004) and magnetic resonance imaging (Guermazi et al., 2003; Phan et al., 2005). These diagnostic assessments do not reflect, however, the individual's symptoms or help determine which treatment options are most effective (Jordan et al., 1997; McAlindon, Cooper, Kirwan, & Dieppe,

1993). Analyses of certain synovial cytokines and metalloproteinases have been reported to reflect pre-radiological osteoarthritic changes and correlate to the patient's symptoms (Kubota, Imamura, Kubota, Shibata, & Murakami, 1997; Kubota, Kubota, Matsumoto, Shibata, & Murakam, 1998; Punzi et al., 2003; Fang, Ma, Ma, & Fu, 1999; Takahashi et al., 1998). The relationships between the biochemical markers and patient symptoms suggest that they reflect the individual nature of the osteoarthritic joint and may allow for the development of improved individualized diagnoses and treatments. The use of synovial protein analyses to assess osteoarthritis in its early stages has influenced researchers to pursue treatment options to block certain proteins, with the goal of preventing further deterioration of the articular cartilage (Punzi et al.; Shinoda & Takaku, 2000).

Bioelectrical analysis of the skin, or skin potentials, may further improve earlier assessment of osteoarthritis. These potentials are a noninvasive method that represent the differences between two regions' skin resistance and electrical fields generated by deep physiological processes (Edelberg, 1972). Skin potential measurements have been used extensively since the 1920s to examine an array of physiological processes, including

brain activity (electroencephalography), muscle activity (electromyography), cardiac function (electrocardiography), and the body's response to trauma and psychological stimuli (Barker et al., 1982; Barnes, 1945; Burr et al., 1939, 1940; Edelberg; Jaffe & Vanable, 1984). Early studies assessing the role of skin potentials as a diagnostic tool for trauma have established that skin potentials around a wound correlate with the healing process (Burr et al., 1939, 1940). Marino et al. (1994) demonstrated that skin potentials can differentiate between benign and malignant cancerous breast lesions deep to the recording electrodes. Similarly, an increase in negative skin potentials may be capable of representing the gross biochemical environment within the osteoarthritic joint and facilitating the early diagnosis of osteoarthritis.

Advancement in the clinical treatment of osteoarthritis will rely on discovering new diagnostic tools to facilitate implementation of more effective treatments in the disease process. Skin potentials may have that utility, allowing clinicians to more effectively diagnose the stage and select appropriate therapeutic interventions, returning the joint to a normal physiologic cycle of remodeling (see Appendix B). The outcomes of this

study are intended to enhance early diagnosis and improve the understanding of the variability of osteoarthritic knees. These measures may eventually be used to define the need for more individualized treatment protocols.

Statement of the Purpose

The purpose of this study was to determine if bioelectrical analysis can be used to differentiate between osteoarthritic and non-osteoarthritic normal knees.

Specific Aims

1. To determine if skin potentials can differentiate between osteoarthritic and non-osteoarthritic normal knees.

2. To determine if protein concentrations in knee synovial fluid are significantly different between osteoarthritic and non-osteoarthritic normal knees.

3. To determine if skin potentials correlate with synovial protein concentrations in knees.

4. To determine if skin potentials and intra-articular potentials correlate in knees.

Hypotheses

1. Skin potentials will be 20% more negative in the osteoarthritic than in the non-osteoarthritic normal knees.

2. Synovial protein concentrations will be 50% greater in the osteoarthritic knees than in the non-osteoarthritic normal knees.

3. A significant negative moderate (r = .5 to .75) correlation will exist between skin potentials and synovial protein concentrations in knees.

4. A significant positive strong ($r \geq .76$) correlation will exist between skin and intra-articular potentials in knees.

Methods

Research Design

A cross-sectional design was used in this study. The independent variable was group: osteoarthritic knee, comprising osteoarthritic participants' osteoarthritic knee; and normal knee, comprising non-osteoarthritic participants' knee. The dependent variables were skin and intra-articular potentials, as well as knee synovial protein concentrations. Potential covariates were knee effusion, lifetime physical activity, self-rated health, skin resistance, smoking habit, and history of cardiovascular disease.

Participants

Eight participants (35 years of age and older) were recruited to participate in this study. The four osteoarthritic participants (2 males, and 2 females) were recruited from the outpatient orthopaedic practice at Temple University Department of Orthopaedics at

Northeastern Hospital and Temple University Hospital, Philadelphia, PA. The four osteoarthritic participants were selected based on a diagnosis of knee osteoarthritis. The diagnosis was based on clinical symptoms of knee inflammation (e.g., chronic joint effusion); and bilateral standing radiographic evidence, using the Kellgren-Lawrence Grading System (LaValley, McAlindon, Chaisson, Levy, & Felson, 2001). Inclusion criterion was a Kellgren-Lawrence osteoarthritis score of ≥ 3 (moderate to severe osteoarthritis). Two of the osteoarthritic participants had a history of cardiovascular disease, but none of the osteoarthritic knee participants were current smokers.

The four normal knee group participants were recruited in office areas at Temple University, Philadelphia, PA (3 males, and 1 female). These participants had no history of knee osteoarthritis based on bilateral standing radiographs. Bilateral anteroposterior standing knee radiographs were used to select participants with bilateral Kellgren-Lawrence grading scores of ≤ 1. Normal knees were arbitrarily selected. None of the normal knee participants had a history of cardiovascular disease, but one of the normal knee participants was a current smoker.

All participants were screened for general exclusion factors. Exclusion criteria were: (a) any joint pathology other than osteoarthritis (e.g., rheumatoid arthritis, gout, pseudo-gout), (b) uncontrolled metabolic/ immunological disorders, (c) cancer, (d) skin irritation or dermatological conditions (e.g., abscess, cellulitis) around the injection site, (e) prior history of a fracture within 12 months of entering the study, (f) consistent use of an anti-inflammatory medication for 14 to 90 days, (g) use of an antibiotic within 1 month prior to the study, and (h) prior history of injury within 3 months of the study.

Potential participants in both groups were excluded if they presented any additional contraindications for arthrocentesis: bacteremia, knee prosthesis, or bleeding disorders. A participant on an anticoagulant has a minimal risk of hemorrhaging, but, for this study, only those already scheduled for arthrocentesis were included to minimize risk to the participant (Thumboo & O'Duffy, 1998). Finally, participants in both groups were not included if the study physician observed any pathological conditions other than osteoarthritis (e.g., crystals, blood, sepsis) in the synovial fluid. If found, the sample was not used for the study but underwent a separate analysis for

diagnostic purposes. Participation in the study was not based on gender, ethnicity, anthropometric variables, or demographic variables. The study was approved by Temple University Institutional Review Board, and the Health Insurance Portability and Accountability Act guidelines were adhered to throughout testing. Participants signed an informed consent form prior to inclusion (see Appendix J).

Instrumentation

Health History Questionnaire and Anthropometric Measures

A Health History Questionnaire (see Appendix K), developed by the investigator, was used to assess for inclusion and exclusion criteria. The first 17 questions addressed the medical history directly related to the participants' knees and current medications. Each of these questions provided space for the participants to further expand on their answers or add requested details (e.g., list of medications, frequency of effusions, date of injury, date of surgery). The final 34 yes - no questions were used to assess the participant's global health history. At the conclusion of this section, participants were asked to provide any additional information they deemed important.

Body weight and height were measured and recorded on the Health History Questionnaire. Body weight was recorded to the nearest pound and converted to kilograms. Height was measured to the nearest centimeter using a fiberglass metric tape measure (CR100, Martin) and converted to meters. Body mass index was calculated for each participant using the formula kilograms divided by meters squared.

X-ray and Osteoarthritis Grading System

The degree of joint degeneration was determined by assessing bilateral standing anteroposterior knee radiographs. A lead shield was used to protect the rest of the participant's body during the x-rays. Standard knee radiograph procedures were followed, except the film was rotated 90 deg to include both knees. The associated radiation dose for the bilateral standing anteroposterior knee view x-ray required for this study had a total effective dose equivalent of 1 mrem and a partial skin exposure of 45 mrad.

The Kellgren-Lawrence Osteoarthritis Grading System is a 5-grade scale and was used to radiographically assess the degree of joint degeneration associated with osteoarthritis (LaValley et al., 2001). The scoring was based on the

presence of joint space narrowing, osteophytes, and sclerosis of the subchondral bone. The 5-level stratification of radiographic characteristics that define the degrees of joint degeneration is presented in Appendix L. The Kellgren-Lawrence score was used to determine group assignment: 0 or 1 were considered little or no degeneration (i.e., normal knees), and 3 or 4 were classified as moderate or severe joint degeneration (i.e., osteoarthritic knees). This system is considered by the World Health Organization as the gold standard for cross-sectional and longitudinal epidemiological studies on osteoarthritis (American Academy of Orthopaedic Surgeons, 2002).

Modified Historical Leisure Activity Questionnaire

The Modified Historical Leisure Activity Questionnaire (see Appendix M) is a self-administered questionnaire designed to assess the physical activity of participants at various stages throughout the participant's lifetime: ages 14 to 21, 22 to 34, 35 to 50, 51 to 65; and past year (Chasan-Taber, Erickson, McBride et al., 2002). The survey focuses on recreational and household activities. The survey was used to account for lifetime physical activity. The questionnaire provides for a list of activities,

stratified into five columns, one each for the five time periods. Within each of the time periods, the participant provided information on the "typical number of hours per week", "typical number of months per year", and "number of years" they performed a particular activity. Lifetime physical activity was calculated as described by Chasan-Taber et al. First, the average hours of an activity per week is recorded and then multiplied by the metabolic equivalent assigned to the task, providing an average weekly energy expenditure for each activity. Next, each of the activities' weekly expenditures is multiplied by the number of weeks each task is performed and then summed, providing a total energy expenditure in an age category (Standard Metabolic Equivalent x hours). A summary lifetime activity score is then determined by calculating a weighted (years per time period) average of each life period's energy expenditure and dividing the average by the total number of years reported on the questionnaire. Higher scores represent a greater degree of physical activity over the individual's lifetime. The lifetime score were used as a potential covariate. The validity (r = .15 to .52) and reliability (ICC = .61 to .86) of this questionnaire has been determined for women (Chasan-Taber, Erickson, McBride et al.; Chasan-Taber, Erickson, Nasca,

Chasan-Taber, & Freedson, 2002). The questionnaire is modified for males by changing the final column to read "between the ages of 12 to 21 years" rather than "between age of menstruation to 21 years" (L. Chasan-Taber, personal communication, October 21, 2005). To account for the emphasis on lifetime leisure and household activities, the Health History Questionnaire has questions regarding former occupations and athletic participation.

Acute Form of the Short Form-36v2™ Health Survey

The Acute Form of the Short Form-36v2™ Health Survey (QualityMetric, Inc., Lincoln, RI) was used to assess the participants' self-rated health, a potential covariate. This survey is a self-administered questionnaire and consists of 36 items divided into three parts: 19 questions with a Likert Scale, 10 questions with three possible responses (i.e., "limited a lot", "limited a little", and "not limited at all"), and 7 yes – no questions. The survey is used to evaluate eight domains of health: (a) physical functioning, (b) role limitations due to physical health, (c) bodily pain, (d) general health perceptions, (e) vitality, (f) social functioning, (g) role limitations due to emotional problems, and (h) mental health. Responses to the questions are based on the general quality

of life for the week prior to administration of the survey. The SF-36v2™ was scored with two summary scores: physical component score (focusing on pain and physical function) and mental component score (focusing primarily on mental health and vitality). The instrument is scored on a 0 to 100 point scale (closer to 100 representing higher quality health), with a score of 50 representing the average of the general population in the United States (Beaton & Schemitsch, 2003). The validity (*Cronbach's alpha* = .75 to .91) and reliability (r = -.19 to -.67) of this survey has been determined for osteoarthritic patients (Beaton & Schemitsch; Kosinski, Keller, Hatoum, Kong, & Ware, 1999). The SF-36 series health survey is one of the most widely reported general health tools used in the medical literature (Beaton & Schemitsch). Permission to use the Acute Form of the Short Form-36v2™ Health Survey was acquired from QualityMetric, Inc.

Biopac MP150 Data Acquisition System

The Biopac MP150 data acquisition system (BIOPAC Systems, Inc., Goleta, CA) was used measure both the skin and intra-articular bioelectrical potentials (millivolts). The system includes a high-input impedance (10^{15} ohms), low noise (2.1 µV) differential amplifier (MCE100C), and a 50

dB notch filter at 50/60 Hz (Biopac Systems, Goleta, CA). Filters for the hardware were set with a low-pass filter at 3 kHz and a high-pass filter at direct current. The Biopac system was connected via an ethernet cable to a Dell Inspiron E1405 laptop (Round Rock, TX) with AcqKnowledge 3.7.3 Software (Biopac Systems, Goleta, CA). The applied software provides real-time data analysis and digital filtering.

Two types of electrodes were used to complete the bioelectrical analysis. For the skin potentials, floating silver/silver-chloride wet gel surface electrodes (Blue Sensor N, Ambu Inc., Glen Burnie, MD) were utilized. The surface electrodes have a sensor area of 15 mm^2 with a typical alternating current impedance of 600 Ω. A disposable solid monopolar needle electrode was used to measure intra-articular potentials. Though this electrode has a different offset potential than the surface electrode, its material was held constant throughout testing, minimizing interference with the correlation or group comparisons. The needle electrode is a 50 mm, 26-gauge stainless steal Teflon™ coated solid monopolar needle. Prior to testing, all of the leads and electrodes were visually inspected to ensure the equipment was in working order. After data collection, off-set potentials

were recorded between the ground surface and needle electrodes. The off-set potential was used to adjust the recorded intra-articular potentials.

A standardized protocol was used for skin potentials. The areas around the lateral joint line, medial joint line, control point (15 cm proximal to the patella), and the anterior surface of the midshaft of the tibia were shaved with a disposable razor and cleaned lightly with alcohol. A surface electrode was then placed over the midshaft of the tibia, lateral joint line, medial joint line, and control point. The resistance between electrodes was recorded with a standard multimeter (22-813 Radio Shack, Fort Worth, TX). A timer was started once the electrodes were in place to maintain a consistency among participants for the length of time between attachment of the electrodes and measurements. The electrode on the anterior midshaft of the tibia served as the ground/reference electrode. The lateral and medial joint line electrodes were the active sites. The control point served as a comparative point, allowing the difference between the pathologic and normal skin measurements to be calculated (Marino et al., 1994). Prior to each testing session, the Biopac system was warmed up for at least 15 min and calibrated to within ± 0.05 mV to minimize error. The skin potentials were recorded for

90 s at a sampling rate of 10 measures/s. The 90 s were divided into three 30 s segments, which were individually averaged. The time period with the smallest coefficient of variation was used in the statistical analysis. Following the 90 s of recording, the active lead was attached to the second active site and then to the proximal control point, using the recording methods previously described. After the data were collected, the electrodes over the two active and control sites were removed and the skin was cleaned with alcohol. The ground fault interrupter helped prevent the participant from being exposed to any significant accidental current.

A standardized protocol was used for intra-articular potentials. To initiate the intra-articular potential measurement, the disposable solid needle electrode was run through a disposable 18-gauge 38 mm hypodermic needle (Becton, Dickinson, & Company, Franklin Lakes, NJ). The synovial fluid was aspirated, following the standard protocol. For the control participants, 7 to 14 mL of sterile saline was injected into the knee to recover a synovial fluid sample. Once the synovial fluid was aspirated, the needle electrode was glided into the knee via the larger needle and exposed to the joint cavity. The free end of the needle electrode was then connected to the

active measuring lead. The intra-articular potentials were then recorded for 90 s, using a sample rate of 10 measures/s. The data reduction was the same as for the skin potentials. All of the bioelectrical potential measurements were analyzed after the testing session and reported in millivolts.

These methods represent a new use for the Biopac system, which has been used to collect an array of physiological measures in humans (Blumenthal & Flaten, 1994; Glass & Armstrong, 1997; Shin, Minamitani, Onishi, Yamazaki, & Lee, 1997). The specifications (e.g., input impedance, and sensitivity) were similar to the electrometer and high-impedance electrometers used in previous research (Marino et al., 1994; Barker, Jaffe, & Vanable, 1982). This system combined the convenience of a high-input impedance voltmeter with real time data acquisition and filtering. Reliability for skin potentials were assessed by the primary investigator prior to the study on healthy volunteers (ICC [3,1] = .99). Data from six of the eight participants in this study were used to determine the reliability of intra-articular potentials (ICC [3,1] = .63).

Custom Human SearchLight Proteome Array

To quantify the cytokine/metalloproteinase concentrations, at least 120 µL of synovial fluid was shipped to the Thermo Scientific SearchLight Sample Testing Laboratory (Pierce Biotechnology, Inc., Rockford, IL) for analysis. The lab used a custom human SearchLight Proteome Multi-plex Protein Array (Pierce Biotechnology, Inc., Rockford, IL) to determine the cytokine and metalloproteinase concentrations in the synovial fluid. The SearchLight multi-plex protein array provides the ability to assess multiple cytokines and other proteins, including metalloproteinases, simultaneously in the same sample. The array was a quantitative multiplexed sandwich Enzyme-Linked Immunosorbent Assay, containing up to 16 different antibodies. These 16 proteins (see Table 5) have been reported in previous studies to be altered in the synovial fluid of osteoarthritic joints (Baddour & Bradley, 1999; Fernandes et al., 2002; Kaneyama et al., 2002; Shi et al., 2004).

Synovial fluid samples were sealed in a sterile test tube, placed in dry ice, and shipped to Thermo Scientific SearchLight Sample Testing Laboratory. The deliveries were shipped priority overnight and packaged as specified by the

Table 5. Antibodies' Sensitivity and Detectable Range

Antibody	Detectable Range	Sensitivity
Adiponectin	19.5 - 20,000.0	39.1
IL-1α	0.4 - 400.0	0.8
IL-1β	0.2 - 200.0	0.4
IL-1ra	7.8 - 8,000.0	15.6
IL-4	0.8 - 800.0	1.6
IL-10	0.4 - 400.0	0.8
IL-13	0.2 - 200.0	0.4
Leptin	15.6 - 16,000.0	31.2
MMP-2	31.3 - 32,000.0	62.5
MMP-3	9.8 - 10,000.0	19.5
MMP-13	9.8 - 10,000.0	19.5
OPG	0.2 - 200.0	0.4
RANKL	1.0 - 1,000.0	2.0
TIMP-1	4.9 - 5,000.0	9.8
TIMP-2	4.9 - 5,000.0	9.8
TNF-α	2.3 - 2,400.0	4.7

Note: All values reported in pg/mL. IL Interleukin, MMP = Matrix Metalloproteinase, OPG = Osteoprotegerin, RANKL = Receptor Activator of Nuclear Factor-κB Ligand, TIMP = Tissue Inhibitor Matrix Metalloproteinase, and TNF = Tumor Necrosis Factor.

United States Department of Transportation and the carrier company. The staff at the Thermo Scientific SearchLight Sample Testing Laboratory noted any complications (e.g., insufficient dry ice, broken containers, and irregular number of samples) upon receiving the samples.

The arrays were produced by spotting a 4 x 4 pattern, using 16 different antibodies. Each antibody captures specific proteins present in the standards and samples. The bound proteins were detected with a biotinylated detection antibody, followed by the sequential addition of streptavidin-horseradish peroxidase and, SuperSignal Enzyme-Linked Immunosorbent Assay Femto Chemiluminsecent substrate. The luminescent signal produced from the streptavidin-horseradish peroxidase-catalyzed oxidation of the substrate was measured by imaging the plate with the SearchLight Imaging System (Pierce Biotechnology, Inc., Rockford, IL), which is a cooled charge-coupled device camera. The data were then analyzed using ArrayVision customized software. The amount of luminescent signal produced is proportional to the amount of each protein present in the standard. All of the samples were tested in duplicate, and a final report summarizing each protein concentration per sample (pg/mL) was electronically forwarded to the investigator. The data were normalized to

the total protein of each sample, determined by a bicinchoninic acid assay (Thermo Fisher Scientific, Inc., Rockford, IL). Normalized results were reported in pg/µg. Validity and reliability of the SearchLight proteome array's has been established through the cytokines' spiked recovery rates. Recovery rates range from 75 to 136% (mean recovery ranges from 96 to 111%).

Procedures

Clinical Examination and Recruitment

Osteoarthritic patients of Dr. Easwaran Balasubramanian were recruited following their clinical examination during a follow-up visit. Dr. Balasubramanian is a board-certified orthopaedic surgeon with over 25 years of clinical experience in knee osteoarthritis. Each patient underwent a standard orthopaedic evaluation (i.e., physician consultation and functional assessment). If x-rays had not been taken in the previous 6 months, new standing radiographs were ordered per the attending physician's standard of care. The study physician evaluated the standing bilateral anteroposterior knee x-rays to determine the Kellgren-Lawrence score. Patients who met the radiographic criteria (moderate to severe osteoarthritis) were informed of and asked to participate

in the study. Those willing to participate signed an informed consent, completed the three questionnaires (i.e., Health History Questionnaire, Acute Form of the Short Form-36v2™ Health Survey, and Modified Historic Leisure Activity Questionnaire) and had their height and weight measured and recorded by the investigator. The osteoarthritic participants who met all of the eligibility criteria progressed to the bioelectrical/synovial analyses. If the patient had any exclusionary criteria, the patient was excluded from the study, but their standard health care continued unaltered.

Normal participants received a free orthopaedic assessment and radiograph to ensure they had no significant signs of osteoarthritis or prevailing joint conditions. They completed the informed consent and the three study questionnaires prior to being evaluated by the orthopaedic surgeon. Their height and weight were measured and recorded by the investigator.

Radiographic Procedures

Participants who meet all of the inclusion criteria were x-rayed for a standing anteroposterior film. Upon entering the Radiology Department, they were supervised by a radiology technician employed by the hospital. Only one bilateral standing anteroposterior x-ray was performed,

minimizing the participants' exposure to x-rays. Once the x-rays were digitized, the study physician evaluated each x-ray to ensure the radiographic criterion of the study was met.

Data Collection

After the participants were cleared for study participation by the investigator and study physician, a hypodermic needle was inserted into the knee and a 20-mL syringe was placed on the hypodermic needle to remove a sample of the synovial fluid. Approximately 0.5 to 1.5 mL of synovial fluid was extracted from the joint by the study physician. A greater amount of synovial fluid was withdrawn, if present, to reduce the patient's discomfort. The control participants' synovial fluid was extracted by injecting 7 to 14 mL of sterile saline. The amount of saline injected was individualized by the study physician, based on the ability to aspirate synovial fluid following every 2 mL of saline. Once the synovial fluid was extracted, a visual analysis of the fluid was performed by the study physician to check for the aforementioned pathological conditions. If the sample appeared yellow and translucent, the sample was placed in a sterile test tube, which was then placed in an insulated container with ice for transport. The investigator then collected all of the

skin potential measurements and managed the Biopac system during the intra-articular potential measurements. All of the bioelectrical measurements were completed in an examination room with climate controls. A constant environment was maintained throughout testing by monitoring room temperature (21.31 ± 1.99 °C, range 17.28 to 23.44 °C), humidity (41.99 ± 12.28%, range 23.00 to 61.50%), and atmospheric pressure (762.13 ± 2.18 mmHg, range 759.46 to 766.31 mmHg). Skin potentials were recorded at each active site in a randomized order for each participant. The control site was measured after the active sites. Intra-articular potentials were measured after the skin potentials.

Once the bioelectric measures were completed, the solid needles were removed by the study physician. At the conclusion of each data collection session, the synovial fluid sample was sent to Dr. Mary Barbe's lab on Temple University's Health Science Campus, Philadelphia, PA. The synovial fluid was flash frozen and stored at -80 °C. After all of the samples were collected a portion of the stored synovial fluid was shipped to Thermo Scientific SearchLight Sample Testing Laboratory. Another portion of each sample was analyzed in Dr. Mary Barbe's laboratory for total protein content, using a bicinchoninic acid assay.

Data Analyses

Data were analyzed with descriptive and interferential statistics using SPSS 15.0 statistical package (Chicago, IL). Independent sample t-tests were used to analyze the descriptive data, potential covariates, skin potentials, intra-articular potentials and synovial protein concentrations between osteoarthritic and normal knees. SPSS corrected test statistics were reported if Levene's Test for Equality of Variances revealed the knee groups did not have equal variance. Three of the osteoarthritic participants had bilateral osteoarthritis data recorded. Only the more effused knee was included in the independent t-tests. Cohen effect sizes (d) were manually calculated for each t-test. Cohen effect sizes were defined as low (d = 0.20), medium (d = 0.50) and large (d = 0.80). Statistical trends were defined as t-tests with a Cohen effect size $\geq$ 2.00.

Multiple correlations were performed to determine the relationships among the variables: skin potentials, intra-articular potentials, and 16 synovial protein concentrations. Correlations included three additional osteoarthritic knees that were collected bilaterally among osteoarthritic participants. Correlations were defined as

low (.00 to .25), fair (.26 to .50), moderate (.51 to .75), and strong (> .75; Portney & Watkins, 2000). Statistical significance was based on a $p \leq .05$.

Results

Descriptive Group Characteristics

Raw data are presented in Appendix N. Descriptive characteristics of and potential covariates for the osteoarthritic and normal knee groups are presented in Tables 6 to 8. Independent t-tests demonstrated no significant differences in age, weight, height, BMI, lifetime physical activity, Acute Form of the Short Form-36v2™ Health Survey mental component scores, and resistance measurements between the two groups. A significant group difference existed in the Acute Form of the Short Form-36v2™ Health Survey physical component scores, with the osteoarthritic knee group having a 40% lower score than the normal knee group. The osteoarthritic knee group had 20 ± 10 mL knee joint effusion while none of the normal knee group had an effusion. Three of the four osteoarthritic knee group participants had severe osteoarthritis (Kellgren-Lawrence Score = 4), while the fourth had moderate

Table 6. Descriptive Characteristics of the Osteoarthritic and Normal Knee Groups

Characteristic	Osteoarthritic Knee	Normal Knee	T-test Statistic	P-value	Effect Size
Age (years)	64.78 ± 5.72	53.55 ± 10.33	-1.901	.106	1.09
Weight (kg)	97.27 ± 17.11	77.69 ± 15.09	-1.717	.137	1.14
Height (m)	1.71 ± 0.11	1.70 ± 0.04	-0.130	.901	0.09
BMI (kg/m^2)	33.31 ± 5.89	26.66 ± 4.00	-1.866	.111	1.13

Note. Osteoarthritic N = 4 and normal N = 4. BMI = body mass index. All values are reported in means and standard deviations.

Table 7. Potential Covariates for the Osteoarthritic and Normal Knee Groups

Covariate	Osteoarthritic Knee	Normal Knee	T-test Statistic	P-value	Effect Size
Lifetime PA (MET x hrs)	1336.68 ± 980.69	2912.19 ± 1941.90	-1.448	.198	0.81
SF36 PCS	31.31 ± 1.75	50.11 ± 8.69	-4.213	.020*	3.00
SF36 MCS	52.23 ± 8.32	51.84 ± 6.13	0.073	.945	0.05
R Lat-G (MΩ)	5.80 ± 6.59	0.44 ± 0.32	1.622	.203	1.15
R Med-G (MΩ)	10.68 ± 15.01	0.59 ± 0.52	1.343	.272	0.95
R Con-G (MΩ)	5.56 ± 6.35	0.70 ± 0.51	1.524	.224	1.08

Note. Osteoarthritic N = 4 (SF36 Scores N = 3) and normal N = 4. PA = physical activity, SF36 PCS = Acute Form of the Short Form-36v2™ Health Survey physical component score, SF36 MCS = Acute Form of the Short Form-36v2™ Health Survey mental component score, R Lat-G = electrical resistance between lateral and ground electrodes, R Med-G = electrical resistance between medial and ground electrodes, R Con-G = electrical resistance between control and ground electrodes. All values are reported in means and standard deviations.
* $p \leq .05$.

Table 8. Descriptive Characteristics of the Participant Knees

Participant	Limb	K-L Scores	Effusion (mL)
KneeOA1	Right	4	5
	Left	4	7*
KneeOA2	Right	4	4
	Left	4	25*
KneeOA3	Right	3	30*
	Left	3	22
KneeOA4	Left	4	20
Normal1	Right	0	0
Normal2	Left	0	0
Normal3	Right	0	0
Normal4	Left	0	0

Note. KneeOA# = Osteoarthritic knee group participant, Normal# = nonosteoarthritic normal knee group participant, K-L Scores = Kellgren-Lawrence Scores. * = more effused knee selected for group comparisons.

osteoarthritis (Kellgren-Lawrence Score = 3). All of the normal knees had no radiographic signs of osteoarthritis (Kellgren-Lawrence Score = 0).

Bioelectrical Potential Measurements

Skin and intra-articular potentials means, standard deviations, test statistics, effect sizes, and 95% confidence intervals for the osteoarthritic and normal knee groups are presented in Tables 9 and 10. Independent t-tests demonstrated no significant differences between the two groups for any of the bioelectrical potentials.

Table 9. Bioelectrical Potentials for the Osteoarthritic and Normal Knee Groups

Location	Osteoarthritic Knee	Normal Knee	T-test Statistic	P-value	Effect Size
Skin					
Lateral	-3.3 ± 4.1	6.1 ± 13.9	-1.307	.239	0.68
Medial	6.4 ± 5.5	14.1 ± 15.4	-0.942	.383	0.50
Control	-8.5 ± 13.7	5.1 ± 14.1	-1.380	.217	0.96
Lateral-Control	5.1 ± 13.4	1.0 ± 20.5	-0.338	.747	0.20
Medial-Control	14.9 ± 19.0	9.0 ± 24.5	-0.381	.716	0.24
Intra-articular	64.8 ± 65.6	-13.7 ± 66.0	-1.375	.241	1.19

Note. Osteoarthritic knees *N* = 4 (intra-articular *N* = 2) and normal knee *N* = 4. Lateral = skin potentials at lateral joint, Medial = skin potentials at medial joint line, Control = skin potentials at control site, Lateral-Control = lateral skin potential corrected for the control site potentials, and Medial-Control = medial skin potential corrected for the control site potentials. All data are reported in mV. All values are reported in means and standard deviations.

Table 10. Bioelectrical Potentials 95% Confidence Intervals for the Osteoarthritic and Normal Knee Groups

Measurement	Osteoarthritic Knee	Normal Knee
Skin		
Lateral	-7.40 – 0.7	-7.48 – 19.71
Medial	1.06 – 11.78	-0.97 – 29.18
Control	-21.91 – 4.98	-8.73 – 18.98
Lateral-Control	-8.01 – 18.25	-19.08 – 21.06
Medial-Control	-3.70 – 33.47	-15.02 – 32.98
Intra-articular	-25.98 – 155.49	-78.47 – 50.98

Note. Osteoarthritic knees ***N*** = 4 (intra-articular ***N*** = 2) and normal knee ***N*** = 4. Lateral = skin potentials at lateral joint, Medial = skin potentials at medial joint line, Control = skin potentials at control site, Lateral-Control = lateral skin potential corrected for the control site potentials, and Medial-Control = medial skin potential corrected for the control site potentials. All data are reported in mV.

Synovial Protein Concentrations

Synovial protein concentrations means, standard deviations, test statistics, effect sizes, and 95% confidence intervals for the osteoarthritic and normal knee groups are presented in Tables 11 to 14. Independent t-tests demonstrated IL-13, OPG, and IL-1β concentrations

Table 11. Anti-inflammatory/Protective Protein Concentrations for Osteoarthritic and Normal Knee Groups

Location	Osteoarthritic Knee	Normal Knee	T-test Statistic	P-value	Effect Size
IL-4	0.0002 ± 0.0001	0.0009 ± 0.0004	-3.089	.052	2.40
IL-10	0.0002 ± 0.0001	0.0009 ± 0.0004	-3.037	.053	2.40
IL-13	0.0001 ± 0.0000	0.0006 ± 0.0002	-4.245	.005*	2.50
IL-1ra	0.0236 ± 0.0078	0.1878 ± 0.2445	-1.343	.272	0.95
OPG	0.0006 ± 0.0004	0.0050 ± 0.0022	-3.886	.008*	2.00

Note. Osteoarthritic knees $N = 4$ and normal knees $N = 4$. IL = interleukin, ra = receptor antagonist, and OPG = osteoprotegerin. All data are reported in pg/µg. All values are reported in means and standard deviations.
* $p \leq .05$.

Table 12. Pro-inflammatory/Catabolic and Adipokine Protein Concentrations for Osteoarthritic and Normal Knee Groups

Location	Osteoarthritic Knee	Normal Knee	T-test Statistic	P-value	Effect Size
IL-1α	0.0001 ± 0.0001	0.0003 ± 0.0002	-2.510	.077	1.26
IL-1β	0.0002 ± 0.0001	0.0006 ± 0.0001	-7.652	.001*	4.00
TNF-α	0.0007 ± 0.0005	0.0024 ± 0.0039	-0.829	.466	0.61
RANKL	0.0001 ± 0.0000	0.0005 ± 0.0003	-1.856	.160	1.88
Leptin	0.5910 ± 0.3866	0.0980 ± 0.0142	2.549	.084	1.80
Acrp	95.1944 ± 76.8100	15.0323 ± 9.7633	2.071	.084	1.04

Note. Osteoarthritic knees ***N*** = 4 and normal knees ***N*** = 4. IL = interleukin, TNF = tumor necrosis factor, RANKL = receptor activator of nuclear factor-kappaB ligand, and Acrp = adiponectin. All data are reported in pg/µg. All values are reported in means and standard deviations. * ***p*** < .001.

Table 13. Matrix Metalloproteinases and Inhibitor Protein Concentrations for Osteoarthritic and Normal Knee Groups

Location	Osteoarthritic Knee	Normal Knee	T-test Statistic	P-value	Effect Size
TIMP-1	257.7233 ± 222.9196	3.1310 ± 1.7974	2.284	.107	1.62
TIMP-2	34.6271 ± 12.6397	2.2194 ± 1.6396	5.085	.014*	3.60
MMP-2	102.3384 ± 41.0003	6.6046 ± 2.5433	4.661	.018*	3.30
MMP-3	120.4708 ± 59.5160	5.0544 ± 4.0930	3.869	.030*	2.74
MMP-13	0.0188 ± 0.0097	0.0347 ± 0.0164	-1.669	.146	0.97

Note. Osteoarthritic knees $N = 4$ and normal knees $N = 4$. TIMP = tissue inhibitor of metalloproteinase, and MMP = matrix metalloproteinase. All data are reported in pg/µg. All values are reported in means and standard deviations. * $p \leq .05$.

Table 14. Synovial Protein Concentrations 95% Confidence Intervals for Osteoarthritic and Normal Knee Groups

Measurement	Osteoarthritic Knee	Normal Knee
IL-4	0.00016 - 0.00026	0.00045 - 0.00125
IL-10	0.00014 - 0.00026	0.00043 - 0.00128
IL-13	0.00006 - 0.00013	0.00036 - 0.00082
IL-1ra	0.01592 - 0.03122	0.00000 - 0.42743
OPG	0.00030 - 0.00099	0.00280 - 0.00709
IL-1α	0.00006 - 0.00015	0.00016 - 0.00051
IL-1β	0.00009 - 0.00021	0.00046 - 0.00063
TNF-α	0.00024 - 0.00124	0.00000 - 0.00617
Leptin	0.21211 - 0.96985	0.08412 - 0.11188
Acrp	19.92063 - 170.46825	5.46424 - 24.60039
TIMP-1	39.26205 - 476.18446	1.36945 - 4.89244
TIMP-2	22.24016 - 47.01397	0.61249 - 3.82620
MMP-2	62.15817 - 142.51871	4.11216 - 9.09703
MMP-3	62.14518 - 178.79651	1.04328 - 9.06557
MMP-13	0.00927 - 0.02825	0.01858 - 0.05075

Note. Osteoarthritic knees *N* = 4 and normal knees *N* = 4. IL = interleukin, ra = receptor antagonist, OPG = osteoprotegerin, TNF = tumor necrosis factor, RANKL = receptor activator of nuclear factor-kappaB ligand, Acrp = adiponectin, TIMP = tissue inhibitor of metalloproteinase, and MMP = matrix metalloproteinase. All data in pg/µg.

were significantly greater in the normal than in the osteoarthritic knee group (500, 733, and 200% respectively). TIMP-2, MMP-2, and MMP-3 concentrations were significantly greater in the osteoarthritic than in the normal knee group (1,460, 1,450 and 1,206%, respectively). No other synovial protein concentrations met the .05 alpha level requirement for statistical significance.

Bioelectrical Potentials and Synovial Protein Concentrations Correlations

Bioelectrical potentials and synovial protein concentrations Pearson Correlation Statistics are presented in Tables 15 to 17. Two synovial protein concentrations (RANKL and TNF-α) had significant strong positive correlations to lateral skin potentials. Five synovial protein concentrations (i.e., IL-4, IL-10, IL-13,IL-1ra, and IL-1α) had significant positive moderate correlations to medial skin potentials. Four synovial protein concentrations (i.e., adiponectin, leptin, MMP-2, TIMP-2) had positive correlations to intra-articular potentials (***N*** = 8). IL-1β had a significant negative moderate correlation to intra-articular potentials.

Table 15. Biolectrical Potentials and Synovial Anti-inflammatory/Protective Protein Concentrations Pearson Correlation Matrix

Measurements	IL-4	IL-10	IL-13	IL-1ra	OPG
Skin					
Lateral	.130	.056	.215	-.203	.410
Medial	.741*	.703*	.683*	.711*	.590
Control	.339	.382	.313	-.051	.537
Lateral-Control	-.228	-.323	-.139	-.102	-.208
Medial-Control	.285	.230	.262	.526	.048
Intra-articular	-.513	-.444	-.626	-.483	-.463

Note. Osteoarthritic knees *N* = 7 (intra-articular *N* = 4) and normal knees *N* = 4. IL = interleukin, ra = receptor antagonist, and OPG = osteoprotegerin. Lateral = skin potentials at lateral joint, Medial = skin potentials at medial joint line, Control = skin potentials at control site, Lateral-Control = lateral skin potential corrected for the control site potentials, and Medial-Control = medial skin potential corrected for the control site potentials. * Significant Pearson correlation $p \leq .05$.

Table 16. Bioelectrical Potentials and Synovial Pro-inflammatory/Catabolic and Adipokines Protein Concentrations Pearson Correlation Matrix

Measurements	IL-1α	IL-1β	TNF-α	RANKL	Adiponectin	Leptin
Skin						
Lateral	-.038	.484	.756*	.783*	-.145	-.233
Medial	.677*	.532	.014	.228	-.547	-.466
Control	.396	.447	.024	.113	.031	-.227
Lateral-Control	-.408	-.067	.541	.477	-.138	.043
Medial-Control	.203	.068	-.007	.082	-.399	-.170
Intra-articular	-.319	-.740*	-.612	-.706	.831*	.756*

Note. Osteoarthritic knees *N* = 7 (intra-articular *N* = 4) and normal knees *N* = 4. IL = interleukin, TNF = tumor necrosis factor, and RANKL = receptor activator of nuclear factor-kappaB ligand. Lateral = skin potentials at lateral joint, Medial = skin potentials at medial joint line, Control = skin potentials at control site, Lateral-Control = lateral skin potential corrected for the control site potentials, and Medial-Control = medial skin potential corrected for the control site potentials. * Significant Pearson correlation $p \leq .05$.

Table 17. Bioelectrical Potentials and Synovial Matrix Metalloproteinases and Inhibitors Concentrations Pearson Correlation Matrix

Measurements	TIMP-1	TIMP-2	MMP-2	MMP-3	MMP-13
Skin					
Lateral	-.288	-.135	-.133	-.195	-.034
Medial	-.358	-.571	-.564	-.540	.549
Control	-.262	.099	.079	-.016	.239
Lateral-Control	.036	-.196	-.175	-.130	-.254
Medial-Control	-.072	-.461	-.443	-.362	.219
Intra-articular	.528	.734*	.706*	.682	-.465

Note. Osteoarthritic knees N = 7 (intra-articular N = 4) and normal knees N = 4. TIMP = tissue inhibitor of metalloproteinase, and MMP = matrix metalloproteinase. Lateral = skin potentials at lateral joint, Medial = skin potentials at medial joint line, Control = skin potentials at control site, Lateral-Control = lateral skin potential corrected for the control site potentials, and Medial-Control = medial skin potential corrected for the control site potentials. * Significant Pearson correlation $p \leq .05$.

Skin and Intra-articular Potentials Correlations

Skin and intra-articular potentials Pearson Correlation Statistics are presented in Table 18. No significant correlations existed among these skin potentials.

Discussion

The purpose of this study was to determine if skin potentials can differentiate between osteoarthritic and normal knees. Secondary aims were to determine factors that influence skin potentials. The results revealed that the skin potentials did not differentiate between the osteoarthritic and normal knee groups in spite of the skin potentials having moderate to high correlations with seven synovial protein concentrations (i.e., RANKL, TNF-α, IL-4, IL-10, IL-13, IL-1ra, and IL-1α). Six of the synovial protein concentrations (i.e., IL-13, OPG, IL-1β, TIMP-2, MMP-2, and MMP-3) were statistically different between osteoarthritic and normal knee groups.

Bioelectrical Potential Measurements

One obstacle to the development and implementation of DMOADs has been the absence of an early diagnostic marker for osteoarthritis. This study evaluated if skin potentials were a novel noninvasive marker for

Table 18. Skin and Intra-articular Potentials Pearson Correlation Matrix

Measurements	1	2	3	4	5	6
Skin						
Lateral (1)		.049	.331	---	-.188	-.673
Medial (2)			-.080	.113	---	-.514
Control (3)				---	---	-.127
Lateral-Control (4)					.553	-.490
Medial-Control (5)						-.324
Intra-articular (6)						

Note. Osteoarthritic knees $N = 7$ (intra-articular $N = 4$) and normal knees $N = 4$. --- = Pearson Correlations were not calculated because the adjusted potentials were calculated based on the lateral, medial, and control sites. * Significant Pearson correlation $p \leq .05$.

osteoarthritis. Skin potentials have been previously used to differentiate between benign and malignant breast tumors (Marino et al., 1994). The inflammatory and catabolic biochemical conditions in osteoarthritic knees were theorized to promote bioelectrical potential differences within the knee joint and superficially on the skin. The results of this study revealed that skin potentials could not differentiate between osteoarthritic and normal knees. The lack of significant findings is attributed to a low

sample size and the effect sizes being below an acceptable threshold for diagnostic sensitivity and specificity. Potential diagnostic markers should have a Cohen effect size greater than 3.0 (Zakanis, 2001).

The current findings are also limited due to high variability of the bioelectrical potentials. The average coefficient of variation among the skin potentials was 1.64. Normal knees had a greater average coefficient of variation than osteoarthritic knees (2.05 vs 1.24, respectively). The large variability, especially among normal knees, may be related to factors that influence the skin (e.g., participants' age, relative humidity). To account for the variability, skin potentials at the active sites (i.e., medial and lateral sites) were corrected using skin potentials at the control site. This technique was previously described by Marino et al. (1994) and resulted in significant differences between cancerous and benign breast tumors. Similar to the previous study, the coefficient of variation increased with the correction, although in the current study no significant differences were found. Cancerous lesions compared to osteoarthritis may produce a greater localized change in deep electrochemical conditions or a more profound change in

autonomic influences on the skin. The variability in skin potentials may be associated with a variable electrochemical environment within the knee joint.

Intra-articular potentials were expected to be representative of the biochemical conditions within the joint. If skin potentials were significantly different between the osteoarthritic and normal knee groups, one cause for the differences was theorized to be intra-articular potentials deep to the active electrodes. However, neither skin nor intra-articular potentials were significantly different between the two groups. While a large effect size existed for intra-articular potentials, only two osteoarthritic knees were included, limiting the interpretation of the effect size. Large coefficient of variations existed with intra-articular and skin potentials. The average intra-articular potential coefficient of variation (2.92) was 1.78 times greater than for the skin potentials. While these potentials could be influenced by the skin, it is probable that the increased variability was associated with the biochemical conditions within each knee.

Synovial Protein Concentrations

In the conceptual model, skin potentials were expected to be significantly different between the osteoarthritic and normal knee groups because of biochemical differences. Sixteen synovial protein concentrations were analyzed to determine if intra-articular biochemical differences existed between the two knee groups. The biochemical analyses of knee synovial fluid revealed IL-1β was 200% greater in the normal knee group than in the osteoarthritic knee group. This differs from previous research, which demonstrated elevated IL-1β in osteoarthritic synovial fluid (Kaneyama et al., 2002; Kubota et al., 1997, 1998). The contradictory findings may be related to the normalization of IL-1β to total protein content. Synovial fluid total protein content has been reported to be greater in osteoarthritic than in normal joints (Fujimara et al., 2006; Kaneyama et al.; Takahashi et al., 1998). Another reason for the normal knees having elevated IL-1β concentrations was because they could have been in an asymptomatic pre-radiologic stage of osteoarthritis. Radiographs do not detect osteoarthritis until significant joint space narrowing, osteophyte formation, and/or subchondral bone sclerosis develops (Punzi et al., 2003).

It is possible that some of the normal knees represented early osteoarthritis and that IL-1β was a sensitive indicator of this early phase.

Two synovial protein concentrations associated with anabolic or protective roles in the joints were elevated in normal knees (i.e., IL-13, OPG). IL-4 and IL-10 concentrations, associated with anabolic or protective roles in the joints, had statistical trends towards being elevated in normal joints. OPG, an inhibitor of RANKL, has been reported to be lower in osteoarthritic joints than in normal joints (Wakita, Mogi, Kurita, Kuzushima, & Togari, 2006). IL-4, IL-10, and IL-13 have been reported to be elevated in osteoarthritis, however, in relationship to other proteins (e.g., pro-inflammatory cytokines), they do not maintain concentrations sufficient for a homeostatic balance (Fernandes et al., 2002). When these synovial protein concentrations are normalized to total protein concentrations they appear greater in normal knees. Furthermore, one or more of the normal knees may have had early pre-radiological osteoarthritis, raising the cytokine levels.

Two MMPs (i.e., MMP-2, MMP-3) and one associated inhibitor (TIMP-2) were elevated in osteoarthritic knees. All three proteins have been previously demonstrated to be

elevated in osteoarthritic joints (Kanayama et al., 2002; Kubota et al., 1998). MMP-2 is associated with denaturing of collagen while MMP-3 has been implicated in proteoglycan degradation (Burrage, & Brinckerhoff, 2007; Roach et al., 2007). TIMP-2 is a natural inhibitor to MMPs and its elevation in osteoarthritic joints represents the chondrocytes failed attempt to maintain a homeostatic balance between catabolic and anabolic processes.

While the differences between the two groups represent a critical aspect to using synovial protein concentrations as potential diagnostic tests, the electrical potentials could be influenced by synovial protein concentrations with large variability. For example, IL-1ra and TNF-α had a coefficient of variation greater than 1.0 in the normal knees. Both of these synovial protein concentrations had strong to moderate correlations with skin potentials.

Bioelectrical Potentials and Synovial Protein Concentrations Correlations

Skin potentials could not differentiate between osteoarthritic and normal knees, however, seven synovial protein concentrations (i.e., RANKL, TNF- α, IL-4, IL-10, IL-13, IL-1ra, and IL-1α) were correlated with skin potentials at active sites. These correlations indicate that skin potentials, while not diagnostic, may reflect

biochemical changes in the knee joint. As certain synovial protein concentrations increased skin potentials increased. All of the synovial proteins concentrations associated with skin potentials were either trending towards being greater in the normal knees or revealed no significant differences between the two groups. Five of the correlations were associated with the medial site, two with the lateral site, and none with the control site. The medial site, which represented the majority of significant skin correlations, is the side associated with initial degenerative changes and fastest rate of progression of knee osteoarthritis (Pelletier et al., 2007). Four of the five significant correlations on the medial side were among synovial proteins concentrations associated with anabolic or protective roles (i.e., IL-4, IL-10, IL-13, and IL-1ra). Synovial protein concentrations correlated with skin potentials at active sites and not the control site, demonstrating that skin potentials are influenced by biochemical conditions deep to the electrodes.

Skin potentials may indirectly relate to the biochemical conditions within the knee joint, however, intra-articular potentials were measured directly in the intra-articular biochemical environment. Intra-articular potentials correlated with four of the six proteins with

the highest synovial concentrations. Intra-articular potentials may be influenced by local biochemical conditions with greatest protein concentrations having the most profound effect. The intra-articular potentials correlated primarily with the synovial protein concentrations that were greater in osteoarthritic knees or had no significant group differences. The exception was IL-1β, which was greater in normal knees; however, this was the only significant negative correlation. Skin potentials and intra-articular potentials had opposing patterns of correlations. Skin potentials had positive correlations with synovial protein concentrations that were either greater in normal knees or were not significantly different. In contrast, intra-articular potentials had positive correlations with synovial proteins concentrations greater in osteoarthritic knees (i.e., adiponectin, leptin, TIMP-2, and MMP-2), while maintaining a negative correlation with IL-1β; which was greater in normal knees. There were no synovial protein concentrations with significant correlations between skin and intra-articular potentials. Skin potentials may react to systemic changes (e.g., IL-1 α, IL-10, TNF-α), while intra-articular

potentials are influenced directly by intra-articular biochemical conditions (e.g., adiponectin, leptin, MMP-2, TIMP-2).

Skin and Intra-articular Potentials Correlations

In the conceptual model for this study skin potentials were expected to be significantly different between osteoarthritic and normal knees because of electrochemical differences within knee joints. Skin potentials did not differ between the two knee groups; however, they did correlate to seven synovial protein concentrations. No synovial protein concentrations had correlations with both skin and intra-articular potentials. Furthermore, no significant correlations existed between skin and intra-articular potentials. Skin potentials may be mediated by systemic effects of the biochemical changes associated with osteoarthritis with a minor contribution from deeper bioelectrical potentials. Trends for moderate negative correlations existed between skin potentials at active sites and intra-articular potentials. No significant correlations existed between the control site and intra-articular potentials. The negative moderate correlations may represent an association between these two measurements but they respond uniquely to the biochemical environment.

Skin potentials may react to systemic changes (e.g., changes in autonomic influence), while intra-articular potentials are influenced by the intra-articular biochemical conditions.

Conclusion

The results of this study revealed that skin and intra-articular potentials did not differentiate between osteoarthritic and normal knees in spite of the skin potentials having moderate to high correlations with several synovial protein concentrations. Although biochemical differences existed between the two knee groups, skin potentials do relate to changes in biochemical conditions in knees. Future research needs to determine the mechanism that produces this relationship with the goal of developing an early diagnostic marker for osteoarthritis.

CHAPTER 4

CONCLUSIONS

The development of DMOADs has been hindered by an inability to diagnose osteoarthritis at an early stage, prior to a degenerative point of no return. Furthermore, none of the current animal models for joint degeneration have been capable of predicting successful disease modifying outcomes in humans (Glasson et al., 2007). The first part of this dissertation was to determine if a novel voluntary HRHF animal model was capable of increasing wrist joint inflammation and promoting joint degeneration. The model induced inflammation and tissue degeneration in soft tissues and bone. In the current study, 12 weeks of the HRHF task led to elevated inflammatory mediator concentrations and histopathological scores indicative of early joint degeneration (e.g., cellular reaction and decreased proteoglycan staining). The model demonstrated that ibuprofen has an anti-inflammatory and a chondroprotective effect. The HRHF task may be a successful model for studying early osteoarthritis and potential DMOADs.

In addition to assessing early osteoarthritis and DMOADs in animals, it is important to find a reliable method for diagnosing osteoarthritis in early stages. The primary goal of the second part of the dissertation was to assess the diagnostic properties of skin potentials. Skin potentials can differentiate between benign and cancerous breast tumors but has not been previously used to differentiate between osteoarthritic and normal knee groups. The biochemical changes associated with osteoarthritis were predicted to alter skin potentials. The results of this study revealed that skin potentials can not differentiate between osteoarthritic and normal knee groups but they do relate to changes in biochemical conditions in knee synovial fluid (i.e., IL-4, IL-10, IL-13, IL-1ra, IL-1α, TNF-α, and RANKL).

The four inflammatory mediator concentrations measured in the animal model were also measured in the human study. IL-10, IL-1α, and TNF-α were not significantly different in humans but were elevated in the animal model. IL-1β was elevated in the animal model but lower in osteoarthritic knees compared to normal knees. Contradictory biochemical findings between the animal and human data may be related to the examined tissues. In humans, only the synovial fluid was analyzed while in the animal model the joint was

homogenized and included synovial fluid, bone, and articular cartilage. Joint degenerative stage may be another reason for different biochemical findings between the animal model and humans. After 12 weeks of a HRHF task, most animals were representative of early osteoarthritis while all of the human osteoarthritic knees were in a moderate to late stage of joint degeneration.

The results of this dissertation support further evaluation of a voluntary HRHF task in animals as a model for inducing joint inflammation and degeneration. Skin potentials are not a diagnostic criterion for osteoarthritis although they do correlate to biochemical changes. Continued pursuit of diagnostic tools for early osteoarthritis and animal models to explore therapeutic interventions represent the key to developing disease modifying osteoarthritis therapeutic interventions.

Decisions on Hypotheses

Chapter 2

1. Twelve weeks of a voluntary HRHF task led to higher concentrations of mediators of wrist joint inflammation (i.e., IL-1α, IL-1β, TNF-α, and IL-10) in female, young adult rats. Hypothesis 1 was not rejected.

2. Twelve weeks of a voluntary HRHF task led to higher histopathological scores in radiocarpal articular cartilage of female, young adult rats. Hypothesis 2 was not rejected.

3. Eight weeks of ibuprofen attenuated the effect of a HRHF task on inflammatory mediators (i.e., IL-1α, IL-1β, TNF-α, and IL-10) in wrist joints of female, young adult rats. Hypothesis 3 was not rejected.

4. Eight weeks of ibuprofen attenuated the effect of a HRHF task on histopathological scores in radiocarpal articular cartilage in female, young adult rats. Hypothesis 4 was not rejected.

Chapter 3

1. Skin potentials were not significantly different between osteoarthritic knees and normal knees. Hypothesis 1 was rejected.

2. TIMP-2, MMP-2, and MMP-3 synovial fluid concentrations were greater in osteoarthritic than in normal knees. IL-1β, IL-13, and OPG synovial fluid concentrations were greater in normal than in osteoarthritic knees. Ten other synovial protein concentrations were not significantly different between the two knee groups. Hypothesis 2 was rejected.

3. Skin potentials had positive strong to moderate correlations with a select set of synovial protein concentrations in knees (i.e., IL-4, IL-10, IL-13, IL-1ra, IL-1α, TNF-α, and RANKL). Hypothesis 3 was rejected.

4. No significant correlations existed between skin potentials and intra-articular potentials in knees. Hypothesis 4 was rejected.

Future Research

Chapter 2

1. In the current study, 12 weeks of a HRHF task led to increased concentrations of inflammatory mediators. Future studies should assess the contribution of the training period on inflammatory mediator concentrations. The initial 3 to 6 weeks of training, used to learn the task, may promote an early inflammatory response. Furthermore, future studies should be conducted for a longer period of time to determine how inflammatory changes fluctuate as joint degeneration progresses and animals adapt their behaviors.

2. Twelve weeks of a HRHF task led to increased concentrations of IL-1α, IL-1β, TNF-α, and IL-10. Future studies should assess a larger array of proteins, using

multiplex ELISAs or proteomic techniques to develop a more complete profile of the inflammatory and degenerative mediators associated with this degenerative model.

3. After 12 weeks of a HRHF task, inflammatory mediators were elevated in both the wrist joint (i.e., reach and support) and radioulnar diaphyses (i.e., reach and support). Future studies should assess joints in the tail to determine if inflammation is present in a region not contributing to the task. Furthermore, serum measurements of inflammatory and catabolic mediators as well as markers of articular cartilage degradation (e.g., cartilage oligomeric matrix protein) should be assessed.

4. In the current study, a HRHF task led to increased histopathological scores in radiocarpal articular cartilage in reach limbs. Future studies should include a longer follow-up time to determine if the joint degeneration progresses and the time course of joint degeneration. Because male rats typically develop joint degeneration quicker than female rats, future studies may include males and females to determine if this model demonstrates a similar trend.

5. Ibuprofen reduced inflammation and histopathological scores in animals performing a HRHF task. Future studies may assess the efficacy of ibuprofen when

the task is performed over a longer period of time. This will determine if prolonged exposure to a HRHF task with ibuprofen attenuates further inflammation and degeneration.

6. If future studies continue to demonstrate a protective benefit of a consistent dose of ibuprofen in animals, intervention studies should be pursued with humans (e.g., high risk work environment for developing osteoarthritis).

4. Ibuprofen may attenuate inflammation and degenerative joint changes in the radiocarpal joint. Future studies should provide animals with ibuprofen prior to initiating a HRHF task to determine if ibuprofen can prevent the onset of degenerative changes.

Chapter 3

1. In the current study, high variability hindered the diagnostic ability of skin potentials. New measuring techniques that eliminate the skin as a source of variability (e.g., microneedle arrays, ultra high impedance electrical field probes, and electrode arrays) should be assessed to determine if they can differentiate between osteoarthritic and normal knees.

2. New intra-articular potential measuring techniques (e.g., saline referenced electrodes, and improved reference skin-electrode interfaces) should be explored to determine if they are capable of differentiating between osteoarthritic and normal knees.

3. After determining new skin and intra-articular potential techniques the correlational aspect of the current study should be repeated with a larger sample size. To enhance recruitment, any patient with knee osteoarthritis should be included. Recruitment should be performed within an orthopaedic department and a network of primary care physicians who frequently see patients with early osteoarthritis. To enhance this study further, no controls should be recruited so that both raw and normalized protein concentrations can be assessed. Proteomic techniques should be considered to increase the number of proteins analyzed. Fragments of extracellular matrix should be included to maximize the biochemical profile of the synovial fluid. Blood samples should be collected to determine if synovial protein concentrations that correlate with skin potentials are also present in the blood.

4. With a small sample size the current study found significant differences and trends among synovial protein concentrations. These findings should be confirmed with a larger sample size. Furthermore, larger sets of proteins should be analyzed using multiplex ELISAs and proteomic techniques to examine other proteins that may differ between osteoarthritic and normal knees. With a large enough sample size, synovial protein concentrations may be assessed across various grades of severity.

5. In future studies, normal knees with electrochemical characteristics associated with osteoarthritic knees should be followed up with additional testing. It should be determined if the knees are truly nonosteoarthritic, have asymptomatic osteoarthritis, or developed osteoarthritis within two years of recruitment; the minimum time to detect radiographic changes in osteoarthritis.

REFERENCES

Aaron, R. K., Ciombor, D. M., & Simon, B. J. (2004). Treatment of nonunions with electric and electromagnetic fields. ***Clinical Orthopaedics and Related Research, 419,*** 21-29.

Adams, S. S., Bough, R. G., Cliffe, E. E., Dickinson, W., Lessel, B., McCullough K. F., et al. (1970). Some aspects of the pharmacology, metabolism, and toxicology of ibuprofen. I. Pharmacology and metabolism. ***Rheumatology and Physical Medicine***, 10, S9-26.

Aigner, T., Fundel, K., Saas, J., Gebhard, P. M., Haag, J., Weiss, T., et al. (2006). Large-scale gene expression profiling reveals major pathogenetic pathways of cartilage degeneration in osteoarthritis. ***Arthritis and Rheumatism, 54,*** 3533-3544.

Aigner, T., Soder, S., Gebhard, P. M., McAlinden, A., & Haag, J. (2007). Mechanisms of disease: Role of chondrocytes in the pathogenesis of osteoarthritis--structure, chaos and senescence. ***Nature Clinical Practice. Rheumatology, 3,*** 391-399.

Al-Shatti, T., Barr, A. E., Safadi, F. F., Amin, M., & Barbe, M. F. (2005). Increase in inflammatory cytokines in median nerves in a rat model of repetitive motion injury. ***Journal of Neuroimmunology, 167,*** 13-22.

Alaaedine, N., Olee, T., Hashimoto, S., Creighton-Achermann, L., & Lotz, M. (2001). Production of the chemokine RANTES by articular chondrocytes and role in cartilage degradation. ***Arthritis and Rheumatism, 44,*** 1633-1643.

American Academy of Orthopaedic Surgeons (2002). Using the AAOS osteoarthritis of the knee fact sheets. Retrieved November 4, 2005 from http://www3.aaos.org/research/imca/OAkneeContents/OA_knee_m3_5.htm.

American College of Rheumatology (2000). Recommendations for the medical management of osteoarthritis of the hip and knee. ***Arthritis and Rheumatism, 43,*** 1905-1915.

Appleton, C. T. G., McErlain, D. D., Henry, J. L., Holdsworth, D. W., & Beier, F. (2007). Molecular and histological analysis of a new rat model of experimental knee osteoarthritis. ***Annals of the New York Academy of Science, 1117,*** 165-174.

Appleton, C. T. G., McErlain, D. D., Pitelka, V., Schwartz, N., Bernier, S. M., Henry, J. L., et al. (2007). Forced mobilization accelerates pathogenesis: Characterization of a preclinical surgical model of osteoarthritis. ***Arthritis Research and Therapy, 9,*** R13.

Appleton, C. T., Pitelka, V., Henry, J., & Beier, F. (2007). Global analyses of gene expression in early experimental osteoarthritis. ***Arthritis and Rheumatism, 56,*** 1854-1868.

Arokoski, J., Kiviranta, I., Jurvelin, J., Tammi, M., & Helminen, H. J. (1993). Long-distance running causes site-dependent decrease of cartilage glycosaminoglycan content in the knee of beagle dogs. ***Arthritis and Rheumatism, 36,*** 1451-1459.

Baddour, V. T., & Bradley, J. D. (1999). Clinical assessment and significance of inflammation in knee osteoarthritis. ***Current Rheumatology Reports, 1,*** 59-63.

Baker, L. L., Chambers, R., DeMuth, S. K., & Villar, F. (1997). Effects of electrical stimulation on wound healing in patients with diabetic ulcers. ***Diabetes Care, 20,*** 405-412.

Barbe, M. F., Barr, A. E., Gorzelany, I., Amin, M., Gaughan, J. P., & Safadi, F. F. (2003). Chronic repetitive reaching and grasping results in decreased motor performance and widespread tissue responses in a rat model of MSD. ***Journal of Orthopaedic Research, 21,*** 167-176.

Barbe, M. F., Elliot, M. B., Abdelmagid, S. M., Amin, M., Popoff, S. N., Safadi, F. F., & Barr, A. E. (2008) Serum and tissue cytokines and chemokines increase with repetitive upper extremity tasks. *Journal of Orthopaedic Research*, Epub ahead of print.

Barker, A. T., Jaffe, L. F., & Vanable Jr, J. W. (1982). The glabrous epidermis of cavies contains a powerful battery. *The American Journal of Physiology, 242,* R358-R366.

Barnes, T.C. (1945). Healing rate of human skin determined by measurement of the electrical potential of experimental abrasions*. The American Journal of Surgery, 69,* 82-88.

Barr, A. E., & Barbe, M. F. (2002). Pathophysiological tissue changes associated with repetitive movement: a review of the evidence. *Physical Therapy, 82,* 173-187.

Barr, A. E., & Barbe, M. F. (2004). Inflammation reduces physiological tissue tolerance in the development of work-related musculoskeletal disorders. *Journal of Electromyography and Kinesiology*, *14,* 77-85.

Barr, A. E., Barbe, M., & Clark, B. D. (2004). Systemic inflammatory mediators contribute to widespread effects in work-related musculoskeletal disorders. *Exercise and Sports Science Reviews, 32,* 1-8.

Barr, A. E., Safadi, F. F., Gorzelany, I., Amin, M., Popoff, S. N., & Barbe, M. F. (2003). Repetitive, negligible force reaching in rats induces pathological overloading of upper extremity bones. *Journal of Bone and Mineral Research, 18,* 2023-2032.

Beaton, D. E., & Schemitsch, E. (2003). Measures of health-related quality of life and physical function. *Clinical Orthopaedics and Related Research, 413*, 90-105.

Becker, R. O. (1961). The bioelectric factors in amphibian-limb regeneration. *The Journal of Bone and Joint Surgery, 43-A,* 643-656.

Becker, R. O. (1967). The electrical control of growth. *Medical Times, 95,* 657-669.

Becker, R. O., & Spadaro, J. A. (1972). Electrical stimulation of partial limb regeneration in mammals. *Bulletin of the New York Academy of Medicine, 48,* 627-641.

Becker, R. O. (1979). The significance of electrically stimulated osteogenesis. *Clinical Orthopaedics and Related Research, 141,* 266-274.

Bernard, B. P. (Ed.), 1997. Musculoskeletal Disorders (MSDs) and Workplace factors: A Critical Review of Epidemiological Evidence for Work-related Musculoskeletal Disorders of the Neck, Upper Extremity, and Low Back. U.S. Department of Health and Human Services, Public Health Service, Centers for Disease Control, National Institute for Occupational Safety and Health. Washington, DC, Publication no. 97-141.

Betz, W. J., & Caldwell, J. H. (1984). Mapping electric currents around skeletal muscle with a vibrating probe. *The Journal of General Physiology, 83,* 143-156.

Black J. (1987). *Electrical Stimulation: Its Role in Growth, Repair, and Remodeling of the Musculoskeletal System*. New York: Praegar Publishers.

Blaney Davidson, E. N., Vitters, E. L., van der Kraan, P. M., & van den Berg, W. B. (2006). Expression of transforming growth factor-beta (TGFbeta) and the TGFbeta signalling molecule SMAD-2P in spontaneous and instability-induced osteoarthritis: Role in cartilage degradation, chondrogenesis and osteophyte formation. *Annals of the Rheumatic Diseases, 65,* 1414-1421.

Blumenthal, T. D., & Flaten, M. A. (1994). Selective effects of attentional direction on the startle reflex at different stages of processing, *Psychobiology, 22*, 338-346).

Bondeson, J., Wainwright, S. D., Lauder, S., Amos, N., & Highes, C. E. (2006*).* The role of synovial macrophages and macrophage-produced cytokines in driving aggrecanses, matrix metalloproteinases and other destructive and inflammatory responses in osteoarthritis. *Arthritis Research and Therapy, 8,* R187.

Borgens, R. B. (1982). What is the role of naturally produced electric current in vertebrate regeneration and healing? *International Review of Cytology, 76,* 245-298.

Borzi, R. M., Mazzetti, I., Cattini, L., Uguccioni, M., Baggiolini, M., & Facchini, A. (2000). Human chondrocytes express functional chemokine receptors and release matrix-degrading enzymes in response to C-X-C and C-C chemokines. *Arthritis and Rheumatism, 43,* 1734-1741.

Brighton, C. T., Wang, W., & Clark, C. C. (2008). The effect of electrical fields on gene and protein expression in human osteoarthritic cartilage explants. *Journal of Bone and Joint Surgery*, 90-A, 833-48.

Brown, T. D., Johnston, R. C., Saltzman, C. L., Marsh, J. L., & Buckwalter, J. A. (2006). Posttraumatic osteoarthritis: A first estimate of incidence, prevalence, and burden of disease. *Journal of Orthopaedic Trauma, 20,* 739-744.

Buckwalter, J. A., Stanish, W. D., Rosier, R. N., Schenck, R. C. Jr, Dennis, D. A., & Coutts, R. D. (2001). The increasing need for nonoperative treatment of patients with osteoarthritis. *Clinical Orthopaedics and Related Research, 385*, 36-45.

Bureau of Labor Statistics (2006). Nonfatal occupational injuries and illnesses requiring days away from work. United States Department of Labor New, USDL 07-1741. Retrieved November 8, 2007 from http://www.bls.gov/iif/home.htm.

Burr, H. S., Harvey, S. C., & Taffel, M. (1939). Bio-electric correlates of wound healing. *Yale Journal of Biology and Medicine, 11,* 103-107.

Burr, H. S., Taffel, M., & Harvey, S. C. (1940). An electrometric study of the healing of wound in man. *Yale Journal of Biology and Medicine, 12,* 483-485.

Burrage, P. S., & Brinckerhoff, C. E. (2007). Molecular targets in osteoarthritis: Metalloproteinases and their inhibitors. *Current Drug Targets, 8,* 293-303.

Charman, R. A. (1990a). Bioelectricity and electrotherapy-Towards a new paradigm? Part 1: The electric cell. *Physiotherapy, 76,* 503-508.

Charman, R. A. (1990b). Part 4: Strain generated potentials in bone and connective tissue. *Physiotherapy, 76,* 725-730.

Chasan-Taber, L., Erickson, J. B., McBride, J. W., Nasca, P. C., Chasan-Taver, S., & Freedson, P. S. (2002). Reproducibility of a self-administered lifetime physical activity questionnaire among female college alumnae. *American Journal of Epidemiology, 155*, 282-89.

Chasan-Taber, L., Erickson, J. B., Nasca, P. C., Chasan-Taver, S., & Freedson, P. S. (2002). Validity and reproducibility of a physical activity questionnaire in women. *Medicine and Science in Sports and Exercise, 34*, 987-992.

Ciombor, D. M., Aaron, R. K., Wang, S., & Simon, B. (2003). Modification of osteoarthritis by pulsed electromagnetic field-a morphological study. *Osteoarthritis and Cartilage, 11,* 455-462.

Clark, B. D., Al-Shatti, T. A., Barr, A. E., Amin, M., & Barbe, M. F. (2004). Performance of a high-repetition, high-force task induces carpal tunnel syndrome in rats. *Journal of Orthopaedic and Sports Physical Therapy, 34(5),* 244-53.

Clark, B. D., Barr, A. E., Safadi, F. F., Beitman, L., Al-Shatti, T., Amin, M., et al. (2003). Median nerve trauma in a rat model of work-related musculoskeletal disorder. *Journal of Neurotrauma, 20,* 681-695.

Collins, D. H., & McElligott, T. F. (1960). Sulphate (35SO4) uptake by chondrocytes in relation to histological changes in osteoarthritic human articular cartilage. *Annals of the Rheumatic Diseases, 19:318-30*.

Cox, S. R., Gall, E. P., Forbes, K. K., Gresham, M., & Goris, G. (1991). Pharmacokinetics of the R(-) and S(+) enantiomers of ibuprofen in the serum and synovial fluid of arthritis patients. ***Journal of Clinical Pharmacology, 31,*** 88-94.

Craib, W. H. (1928). A study of the electrical field surrounding skeletal muscle. ***The Journal of Physiology, 66,*** 49-73.

Custers, R. J., Creemers, L. B., Verbout, A. J., van Rijen, M. H., Dhert, W. J., & Saris, D. B. (2007). Reliability, reproducibility and variability of the traditional Histologic/Histochemical Grading System vs the new OARSI Osteoarthritis Cartilage Histopathology Assessment System. ***Osteoarthritis and Cartilage, 15,*** 1241-1248.

Cutnell J. D., & Johnson K. W. (1998). Electric forces and electric fields. ***Physics*** (521-556). New York: John Wiley & Sons, Inc.

David, F., Farley, J., Huang, H., Lavoie, J. P., & Laverty, S. (2007). Cytokine and chemokine gene expression of IL-1β stimulated equine articular chondrocytes. ***Veterinary Surgery, 36,*** 221-227.

Davies, N. M. (1998). Clinical pharmokinetics of ibuprofen. The first 30 years. ***Clinical Pharmacokinetics, 34,*** 101-154.

Day, R. O., Williams, K. M., Graham, G. G., Lee, E. J., Knihinicki, R. D., & Champion, G. D. (1988). Stereoselective disposition of ibuprofen enantiomers in synovial fluid. ***Clinical Pharmacology and Therapeutics, 43,*** 480-487.

Diaz-Gallego, L., Prieto, J. G., Coronel, P., Gamazo, L. E., Gimeno, M., & Alvarez, A. I. (2005). Apoptosis and nitric oxide in an experimental model of osteoarthritis in rabbit after hyaluronic acid treatment. ***Journal of Orthopaedic Research, 23,*** 1370-1376.

Dingle J. T. (1999). The effect of NSAID on the matrix of human articular cartilages. ***Zeitschrift für Rheumatologie***, 58, 125-9.

Doss, F., Menard, J., Hauschild, M., Kreutzer, H.J., Mittlemeier, T., Muller-Steinhardt, M., et al. (2007). Elevated IL-6 levels in synovial fluid of osteoarthritis patients stem from plasma cells. *Scandinavian Journal of Rheumatology, 36,* 136-139.

Driban, J. B., Swanik, C. B., Huxel, K., & Balasubramanian, E. (2004). The transient electrical properties of muscle tissue immediately following trauma. *Journal of Athletic Training, 39,* S-92.

Echigo, R., Mochizuki, M., Nishimura, R., & Sasaki, N. (2006). Suppressive effect of hyaluronan on chondrocyte apoptosis in experimentally induced acute osteoarthritis in dogs. *The Journal of Veterinary Medical Science, 68,* 899-902.

Edelberg, R., & Wright, D. J. (1964). Two galvanic skin response effector organs and their stimulus specificity. *Psychophysiology, 62,* 39-47.

Edelberg, R. (1968). Biopotentials from the skin surface: the hydration effect. *Annals of New York Academy of Sciences, 148,* 252-262.

Edelberg, R. (1972). Electrical activity of the skin: Its measurement and uses in psychophysiology. In N. S. Greenfield & R. A. Sternback (Eds.), *Handbook of Psychophysiology* (pp. 367-418). New York: Holt, Rinehart and Winston, Inc.

Edelberg, R. (1977). Relation of electrical properties of skin to structure and physiologic state. *The Journal of Investigative Dermatology, 69,* 324-327.

Elliot, M. B., Barr, A. E., Kietrys, D. M., Al-Shatti T, Amin, M., & Barbe, M. F. (2008) Peripheral neuritis and increased spinal cord neurochemicals are induced in a model of repetitive motion injury with low force and repetition exposure. Brain Research, doi: 10.1016/j.brainres.2008.04.029.

Fajardo, M., & Di Cesare, P. E. (2005). Disease-modifying therapies for osteoarthritis: Current status. *Drugs & Aging, 22,* 141-161.

Fang, P. K., Ma, X. C., Ma, D. L., & Fu, K. Y. (1999). Determination of interleukin-1 receptor antagonist, interleukin-10, and transforming growth factor-beta1 in synovia fluid aspirates of patients with temporomandibular disorders. *Journal of Oral and Maxillofacial Surgery, 57,* 922-8.

Fernandes, J. C., Martel-Pelletier, J., & Pelletier, J. P. (2002). The role of cytokines in osteoarthritis pathophysiology. *Biorheology, 39,* 237-246.

Fernandez-Madrid, F., Karvonen, R. L., Teitge, R. A., Miller, P. R., An, T., & Negendank, W. G. (1995). Synovial thickening detected by MR imaging in osteoarthritis of the knee confirmed by biopsy as synovitis. *Magnetic Resonance Imaging, 13,* 177-183.

Fernihough, J., Gentry, C., Malcangio, M., Fox, A., Rediske, J., Pellas, T., et al. (2004). Pain related behaviour in two models of osteoarthritis in the rat knee. *Pain, 112,* 83-93.

Feuerstein, M., Miller, V. L., Burrell, L. M., & Berger, R. (1998). Occupational upper extremity disorders in the federal workforce. Prevalence, health care expenditures, and patterns of work disability. *Journal of Occupational and Environmental Medicine, 40,* 546-55.

Fiorito, S., Magrini, L., Adrey, J., Mailhe, D., & Broute-Boye, D. (2005). Inflammatory status and cartilage regenerative potential of synovial fibroblasts from patients with osteoarthritis and chondropathy. *Rheumatology (Oxford), 44,* 164-171.

Fransen, M., McConnell, S., & Bell, M. (2003). Exercise for osteoarthritis of the hip or knee. *Cochrane Database Systematic Reviews, 3,* CD004286.

Frisbee, D. D., Al-Sobayil, F., Billinghurst, R. C., Kawcak, C. E., & McIlwraith, C. W. (2008). Changes in synovial fluid and serum biomarkers with exercise and early osteoarhritis in horses. *Osteoarthritis and Cartilage,* doi:10.1016/j.joca.2008.03.008.

Focht, B. C., Rejeski, W. J., Ambrosius, W. T., Katula, J. A., & Messier, S. P. (2005). Exercise, self-efficacy, and mobility performance in overweight and obese older adults with knee osteoarthritis. ***Arthritis and Rheumatism, 53, 659***-65.

Fujimura, K., Segami, N., Yoshitake, Y., Tsuruoka, N., Kaneyama, K., Sato, J., et al. (2006). Electrophoretic separation of the synovial fluid proteins in patients with temporomandibular joint disorders. ***Oral Surgery, Oral Medicine, Oral Pathology, Oral Radiology, and Endodontics, 101,*** 463-468.

Fujita, T., Fujii, Y., Okada, S. F., Miyauchi, A., & Takagi, Y. (2001). Fall of skin impedance and bone and joint pain. ***Journal of Bone and Mineral Metabolism, 19,*** 175-179.

Gentzkow, G. D. (1993). Electrical stimulation to heal dermal wounds. ***The Journal of Dermatologic Surgery and Oncology, 19,*** 753-758.

Gineyts, E., Mo, J. A., Ko, A., Henriksen, D. B., Curtis, S. P., Gertz, B. J., et al. (2004). Effects of ibuprofen on molecular markers of cartilage and synovium turnover in patients with knee osteoarthritis. ***Annals of the Rheumatic Diseases, 63,*** 857-861.

Glass, R. C., & Swannell, A. J. (1978). Concentrations of ibuprofen in serum and synovial fluid from patients with arthritis [proceedings]. ***British Journal of Clinical Pharmacology, 6,*** 453P-454P.

Glass, S. C., & Armstrong, T. (1997). Electromyographical activity of the pectoralis muscle during incline and decline bench presses, ***Journal of Strength and Conditioning Research, 11,*** 163-167.

Glasson, S. S., Blanchet, T. J., & Morris, E. A. (2007). The surgical destabilization of the medial meniscus (DMM) model of osteoarthritis in the 129/SvEv mouse. ***Osteoarthritis and Cartilage, 15,*** 1061-1069.

Godfrey, R. G., & de la Cruz, S. (1975). Effect of ibuprofen dosage on patient response in rheumatoid arthritis. ***Arthritis and Rheumatism, 18,*** 135-137.

Grau, S., Richards, P. J., Kerr, B., Hughes, C., Caterson, B., Williams, A. S., et al. (2006). The role of human HtrA1 in arthritic disease. *The Journal of Biological Chemistry, 281,* 6124-6129.

Guermazi, A., Zaim, S., Taouli, B., Miaux, Y., Peterfy, C. G., & Genant, H. K. (2003). MR findings in knee osteoarthritis. *European Radiology, 13*, 1370-1386.

Hayami, T., Pickarski, M., Zhuo, Y., Wesolowski, G. A., Rodan, G. A., & Duong, L. T. (2006). Characterization of articular cartilage and subchondral bone changes in the rat anterior cruciate ligament transection and meniscectomized models of osteoarthritis. *Bone, 38,* 234-243.

Haynes, M. K., Hume, E. L., & Smith, J. B. (2002). Phenotypic characterization of inflammatory cells from osteoarthritic synovium and synovial fluids. *Clinical Immunology*, 105, 315-25.

Henry, J. L. (2004). Molecular events of chronic pain: From neuron to whole animal in an animal model of osteoarthritis. *Novartis Foundation Symposium, 260,* 139-153.

Henry, K. A. (nd). PIC Persistence in Combat: "Medicine for Non-Medics" Toward an Accelerated Self-Healing Warfighter. Retrieved November 10, 2005 from http://www.darpa.mil/dso/thrust/biosci/picpublic.pdf.

Holmquest, D., & Edelberg, R. (1964). Problems in the analysis of the endosomatic galvanic skin response. *Psychophysiology, 62,* 48-54.

Honorati, M. C., Bovara, M., Cattini, L., Piacentini, A., & Facchini, A. (2002). Contribution of interleukin-17 to human cartilage degradation and synovial inflammation in osteoarthritis. *Osteoarthritis and Cartilage, 10,* 799-807.

Hopwood, B., Tsykin, A., Findlay, D. M., & Fazzalari, N. L. (2007). Microarray gene expression profiling of osteoarthritic bone suggests altered bone remodelling, WNT and transforming growth factor-beta/bone morphogenic protein signalling. *Arthritis Research and Therapy, 9,* R100.

Hsu, Y. H., Hsieh, M. S., Liang, Y. C., Li, C. Y., Sheu, M. T., Chou, D. T., et al. (2004). Production of the chemokine eotaxin-1 in osteoarthritis and its role in cartilage degeneration. ***Journal of Cellular Biochemistry, 93,*** 929-939.

Hu, K., Xu, L., Cao, L., Flahiff, C. M., Brussiau, J., Ho, K., et al. (2006). Pathogenesis of osteoarthritis-like changes in the joints of mice deficient in type IX collagen. ***Arthritis and Rheumatism, 54,*** 2891-2900.

Hulejova, H., Baresova, V., Klezl, Z., Polanska, M., Adam, M., & Senolt, L. (2007). Increased level of cytokines and matrix metalloproteinases in osteoarthritic subchondral bone. ***Cytokine, 38***, 151-6.

Hulmes, D. J., Marsden, M. E., Strachan, R. K., Harvey, R. E., McInnes, N., & Gardner, D. L. (2004). Intra-articular hyaluronate in experimental rabbit osteoarthritis can prevent changes in cartilage proteoglycan content. ***Osteoarthritis and Cartilage., 12,*** 232-238.

Iannone, F., DeBari, C., Dell'Accio, F., Covelli, M., Cantatore M., Patella, V., et al. (2001). Interleukin-10 and interleukin-10 receptor in human osteoarthritic and healthy chondrocytes. ***Clinical and Experimental Rheumatology, 19***, 139-145.

Iversen, S., Iversen, L., & Saper, C. B. (1991). The autonomic nervous system and the hypothalamus. In Kandel, E. R., Schwartz, J. H., & Jessel, T. M. (Eds.), ***Principles of Neural Science*** (2nd ed.) (pp. 960-996). New York: McGraw-Hill Company.

Jaffe, L. F., & Vanable Jr, J. W. (1984). Electric fields and wound healing. ***Clinics in Dermatology, 2,*** 34-44.

Jordan, J., Luta, G., Renner, J., Dragomir, A., Hochberg, M., & Fryer, J. (1997). Knee pain and osteoarthritis severity in self-reported task specific disability: The Johnston County Osteoarthritis Project. ***Journal of Rheumatology***, 24, 1344-1349.

Kaneyama, K., Segami, N., Nishimura, M., Suzuki, T., & Sato, J. (2002). Importance of proinflammatory cytokines in synovial fluid from 121 joints with temporomandibular disorders. ***British Journal of Oral and Maxillofacial Surgery, 40,*** 418-423.

Kiviranta, I., Tammi, M., Jurvelin, J., Arokoski, J., Saamanen, A., & Helminen, H. J. (1992). Articular cartilage thickness and glycosaminoglycan distribution in the canine knee joint after strenuous running exercise. ***Clinical Orthopaedics and Related Research, 283,*** 302-308.

Krohn, K. (2005). Footwear alterations and bracing as treatments for knee osteoarthritis. ***Current Opinion in Rheumatology, 17,*** 653-656.

Kosinski, M. M. A., Keller, S. D., Hatoum, H. T., Kong, S. X., & Ware, J. E. (1999). The SF-36 health survey as a generic outcome measure in clinical trials of patients with osteoarthritis and rheumatoid arthritis: Tests of data quality, scaling assumptions, and score reliability. ***Medical Care, 37,*** MS10-MS22.

Kotake, S., Udagawa, N., Takahashi N., Matsuzaki, K., Itoh, K., Ishiyama, S., et al. (1999). IL-17 in synovial fluid from patients with rheumatoid arthritis is a potent stimulator of osteoclastogenesis. ***The Journal of Clinical Investigation, 103,*** 1345-52.

Kubota, E., Imamura, H., Kubota, T., Shibata, T., & Murakami, K. (1997). Interleukin 1 beta and stromelysin (MMP3) activity of synovial fluid as possible markers of osteoarthritis in the temporomandibular joint. ***Journal of Oral and Maxillofacial Surgery, 55,*** 20-27.

Kubota, E., Kubota, T., Matsumoto, J., Shibata, T., & Murakami, K. I. (1998). Synovial fluid cytokines and proteinases as markers of temporomandibular joint disease. ***Journal of Oral and Maxillofacial Surgery, 56,*** 192-198.

Kumar, S. (2001). Theories of musculoskeletal injury causation. ***Ergonomics, 44,*** 17-47.

Lapvetelainen, T., Nevalainen, T., Parkkinen, J. J., Arokoski, J., Kiraly, K., Hyttinen, M., et al. (1995). Lifelong moderate running training increases the incidence and severity of osteoarthritis in the knee joint of C57BL mice. *The Anatomical Record, 242,* 159-165.

Lardner, A. (2001). The effects of extracellular pH on immune function. *Journal of Leukocyte Biology, 69,* 522-530.

Latko, W. A., Armstrong, T. J., Franzblau, A., Ulin, S. S., Werner, R. A., & Albers, J. W. (1999). Cross-sectional study of the relationship between repetitive work and the prevalence of upper limb musculoskeletal disorders. *American Journal of Industrial Medicine, 36,* 248-59.

LaValley, M. P., McAlindon, T. E., Chaisson, C. E., Levy, D., & Felson, D. T. (2001). The validity of different definitions of radiographic worsening for longitudinal studies of knee osteoarthritis. *Journal of Clinical Epidemiology, 54,* 30-39.

Lavine, L. S., & Grodzinsky, A. J. (1987). Electrical stimulation of repair of bone. *The Journal of Bone and Joint Surgery, 69-A,* 626-630.

Lawrence, R. C., Felson, D. T., Helmick, C. G., Arnold, L. M., Choi, H., Deyo, R. A., et al. (2007). Estimates of the prevalence of arthritis and other rheumatic conditions in the United States: Part II. *Arthritis and Rheumatism, 58,* 26-35.

Lindblad, S., & Hedfors, E. (1987). Arthroscopic and immunohistologic characterization of knee joint synovitis in osteoarthritis. *Arthritis and Rheumatism, 30,* 1081-8.

Litke, D. S., & Dahners, L. E. (1994). Effects of different levels of direct current on early ligament healing in a rat model. *Journal of Orthopaedic Research, 12,* 683-688.

Ma, H. L., Blanchet, T. J., Peluso, D., Hopkins, B., Morris, E. A., & Glasson, S. S. (2007). Osteoarthritis severity is sex dependent in a surgical mouse model. ***Osteoarthritis and Cartilage, 15,*** 695-700.

Marino, A. A., Cullen, J. M., Reichmanis, M., & Becker, R. O. (1979). Fracture healing in rats exposed to extremely low-frequency electric fields. ***Clinical Orthopaedics and Related Research, 145,*** 239-244.

Marino, A. A., Morris, D. M., Schwalke, M. A., Iliev, I. G., & Rogers, S. (1994). Electrical potential measurements in human breast cancer and benign lesions. ***Tumor Biology, 15,*** 147-152.

McAlindon, T. E., Cooper, C., Kirwan, J. R., & Dieppe, P. A. (1993). Determinants of disability in osteoarthritis of the knee. ***Annals of the Rheumatic Diseases***, 52, 258-262.

McAlindon, T. E., LaValley, M. P., Gulin, J. P., & Felson, D. T. (2000). Glucosamine and chondroitin for treatment of osteoarthritis: A systematic quality assessment and meta-analysis. ***Journal of the American Medical Association, 283,*** 1469-75.

McKenzie, L. S., Horsburgh, B. A., Ghosh, P., & Taylor, T. K. (1976). Effect of anti-inflammatory drugs on sulphated glycosaminoglycan synthesis in aged human articular cartilage. ***Annals of the Rheumatic Diseases, 35,*** 487-497.

Meng, J., Ma, X., Ma, D., & Xu, C. (2005). Microarray analysis of differential gene expression in temporomandibular joint condylar cartilage after experimentally induced osteoarthritis. ***Osteoarthritis and Cartilage, 13,*** 1115-1125.

Messier, S. P., Gutekunst, D. J., Davis, C., & DeVita, P. (2005). Weight loss reduces knee-joint loads in overweight and obese older adults with knee osteoarthritis. ***Arthritis and Rheumatism, 52***, 2026-32.

Moore J. S., & Garg A. (1994). Upper extremity disorders in a pork processing plant: Relationships between job risk factors and morbidity. *American Industrial Hygiene Association Journal, 55,* 703-715.

Morko, J. P., Soderstrom, M., Saamanen, A. M., Salminen, H. J., & Vuorio, E. I. (2004). Up regulation of cathepsin K expression in articular chondrocytes in a transgenic mouse model for osteoarthritis. *Annals of the Rheumatic Diseases, 63,* 649-655.

Myers, S. L., Brandt, K. D., Ehlich, J. W., Braunstein, E. M., Shelbourne, K. D., Heck, D. A., et al. (1990). Synovial inflammation in patients with early osteoarthritis of the knee. *The Journal of Rheumatology, 17,* 1662-9.

National Institute of Arthritis and Musculoskeletal and Skin Diseases (2002). *Handout on Health: Osteoarthritis*. Bethesda, MD: NIAMS/National Institutes of Health.

National Research Council and Institute of Medicine (2001). *Musculoskeletal Disorders and the Workplace.* Washington, DC: National Academy Press.

Nishimura, K. Y., Isseroff, R. R., & Nuccitelli, R. (1996). Human keratinocytes migrate to the negative pole in direct current electric fields comparable to those measured in mammalian wounds. *Journal of Cell Science, 109,* 199-207.

Nishimura, M., Segami, N., Kaneyama, K., Suzuki, T., & Miyamaru, M. (2002). Relationships between pain-related mediators and both synovitis and joint pain in patients with internal derangements and osteoarthritis of the temporomandibular joint. *Oral Surgery, Oral Medicine, Oral Pathology, Oral Radiology, and Endodontics, 94,* 328-332.

Nolte, P. A., van der Krans, A., Patka, P., Janssen, I. M. C., Ryaby, J. P., & Albers, G. H. R. (2001). Low-intensity pulsed ultrasound in the treatment of nonunions. *The Journal of Trauma, 51,* 693-703.

Nordenstrom, B. E. W. (1992). Impact of biologically closed electric circuits (BCEC) on structure and function. *Integrative Physiological and Behavioral Science, 27,* 285-303.

Nordenstrom, B. E. W. (1994). The paradigm of biologically closed electric circuits (BCEC) and the formation of an international association (IABC) for BCEC systems. *The European Journal of Surgery, Suppl 574,* 7-23.

Outerbridge, R. E. (1961). The etiology of chondromalacia patellae. *Journal of Bone and Joint Surgery, 43-B,* 752-757.

Pap, G., Eberhardt, R., Sturmer, I., Machner, A., Schwarzberg, H., Roessner, A., et al. (1998). Development of osteoarthritis in the knee joints of wistar rats after strenuous running exercise in a running wheel by intracranial self-stimulation. *Pathology Research and Practice, 194*, 41-47.

Pasquali R. I., Guerra, D., Taparelli, F., Boraldi, F., Bergamini, G., Mori, G., et al. (2001). Morphological analysis of knee synovial membrane biopsies from a randomized controlled clinical study comparing the effects of sodium hyaluronate (Hyalgan) and methylprednisolone acetate (Depomedrol) in osteoarthritis. *Rheumatology (Oxford), 40,* 158-169.

Pelletier, J. P., & Martel-Pelletier, J. (2007). DMOAD developments: Present and future. *Bulletin of the NYU Hospital for Joint Diseases, 65,* 242-248.

Pelletier, J., Raynauld, J., Berthiaume, M., Abram, F., Choquette, D., Haraoui, B., et al. (2007). Risk factors associated with the loss of cartilage volume on weight-bearing areas in knee osteoarthritis patients assessed by quantitative magnetic resonance imaging: A longitudinal study. *Arthritis Research and Therapy, 9,* R74-84.

Phan, C. M., Link, T. M., Blumenkrantz, G., Dunn, T. C., Ries, M. D., Steinbach, L. S., et al. (2006). MR imaging finding in the follow-up of patients with different stages of knee osteoarthritis and the correlation with clinical symptoms. *European Radiology, 16*, 608-618.

Pipitone, N., & Scott, D. L. (2001). Magnetic pulse treatment for knee osteoarthritis: A randomised, double-blind, placebo-controlled study. *Current Medical Research and Opinion, 17,* 190-196.

Poolsup, N., Suthisisang, C., Channark, P., & Kittikilsuth, W. (2005). Glucosamine long-term treatment and the progression of knee osteoarthritis: Systematic review of randomized controlled trials. *The Annals of Pharmacotherapy, 39*, 1080-87.

Portney, L. G., & Watkins, M. P. (2000). *Foundations of Clinical Research: Applications to Practice* (2nd ed.). Upper Saddle River, NJ: Prentice-Hall.

Presle, N., Pottie, P., Dumond, H., Guillaume, C., Lapicque, F., Pallum, S., et al. (2006). Differential distribution of adpiokines between serum and synovial fluid in patients with osteoarthritis. Contribution of joint tissues to their articular production. *Osteoarthritis and Cartilage, 14,* 690-695.

Pullar, C. E., Isseroff, R. R., & Nuccitelli, R. (2001). Cyclic AMP-dependent protein kinase A plays a role in the directed migration of human keratinocytes in a DC electric field. *Cell Motility and the Cytoskeleton, 50,* 207-217.

Pulsatelli, L., Dolzani, P., Piacentini, A., Silvestri, T., Ruggeri R., Gualtieri, G., et al. (1999). Chemokine production by human chondrocytes. *Journal of Rheumatology, 26,* 1992-2001.

Punzi, L., Oliviero, F., Ramonda, R., Valvason, C., Sfriso, P., & Todesco, S. (2003). Laboratory investigations in osteoarthritis. *Aging Clinical and Experimental Research, 15,* 373-379.

Revell, P. A., Mayston, V., Lalor, P., & Mapp, P. (1988). The synovial membrane in osteoarthritis: A histological study including the characterization of the cellular infiltrate present in inflammatory osteoarthritis using monoclonal antibodies. *Annals of Rheumatic Diseases, 47*, 300-7.

Richards, J. D., Sanchez-Ballester, J., Jones, R. K., Darke, N., & Livingstone, B. N. (2005). A comparison of knee braces during walking for the treatment of osteoarthritis of the medial compartment of the knee. ***Journal of Bone and Joint Surgery, 87,*** 937-939.

Robinson, K. R. (1985). The responses of cells to electrical fields: A review. ***The Journal of Cell Biology, 101,*** 2023-2027.

Roddy, E., Zhang, W., & Doherty, M. (2005). Aerobic walking or strengthening exercises for osteoarthritis of the knee? A systematic review. ***Annals of the Rheumatic Diseases, 64,*** 544-8.

Roach, H. I., Aigner, T., Soder, S., Haag, J., & Welkerling, H. (2007). Pathobiology of osteoarthritis: pathomechanisms and potential therapeutic targets. ***Current Drug Targets, 8,*** 271-282.

Roman-Blas, J. A., & Jimenez, S. A. (2006). NF-κB as a potential therapeutic target in osteoarthritis and rheumatoid arthritis, ***Osteoarthritis and Cartilage, 14,*** 839-848.

Rosch P. J. (2004). Preface. In PJ Rosch, & MS Markov (Eds.), ***Bioelectromagnetic Medicine*** (iii-v). New York: Marcel Dekker, Inc.

Sanchez, C., Deberg, M. A., Bellahcnee, A., Castronovo, V., Msika, P., Delcour, J. P., et al. (2008). Phenotypic characterization of osteoblasts from the sclerotic zones of osteoarthritic subchondral bone. ***Arthritis and Rheumatism. 58,*** 442-455.

Sezgin, M., Demirel, A. C., Karaca, C., Ortancil, O., Ulkar, G. B., Kanik, A., et al. (2005). Does hyaluronan affect inflammatory cytokines in knee osteoarthritis. ***Rheumatology International, 25,*** 264-269.

Shakibaei, M., Schulze-Tanzil, G., John, T., & Mobasheri, A. (2005). Curcumin protects human chondrocytes from IL-l1beta-induced inhibition of collagen type II and beta1-integrin expression and activation of caspase-3: An immunomorphological study. ***Annals of Anatomy, 187,*** 487-497.

Shi, J., Schmitt-Talbot, E., DiMattia, D. A., & Dullea, R. G. (2004). The differential effects of IL-1 and TNF-α on proinflammatory cytokine and matrix metalloproteinase expression in human chondrosarcoma cells. ***Inflammation Research, 53,*** 377-389.

Shikhman, A. R., Brinson, D. C., & Lotz, M. (2000). Profile of glycosaminoglycan-degrading glycosidases and glycoside sulfatases secreted by human articular chondrocytes in homeostasis and inflammation. ***Arthritis & Rheumatism, 43,*** 1307-1314.

Shin, K., Minamitani, H., Onishi, S., Yamazaki, H., & Lee, M. (1997). Autonomic differences between athletes an nonathletes: Spectral analysis approach. ***Medicine and Science in Sports and Exercise, 29,*** 1482-1490.

Shinoda, C., & Takaku, S. (2000). Interleukun-1 beta, interleukin-6, and tissue inhibitor of metalloproteinase-1 in the synovial fluid of temporomadibular joint with respect to cartilage destruction. ***Oral Diseases***, 6, 383-390.

Simopoulou, T., Malizos, K. N., Iliopoulos, D., Stefanou, N., Papatheodorou, L., Ioannou, M., et al. (2007). Differential expression of leptin and leptin's receptor isoform (Ob-Rb) mRNA between advanced and minimally affected osteoarthritic cartilage; effect on cartilage metabolism. ***Osteoarthritis and Cartilage, 15,*** 872-883.

Swagerty, D. L. Jr., & Hellinger, D. (2001). Radiographic assessment of osteoarthritis. ***American Family Physician,*** 64, 279-86.

Swallow, C. J., Grinstein, S., Sudsbury, R. A., & Rotstein, O. D. (1991). Cytoplasmic pH regulation in monocytes and macrophages: Mechanisms and functional implications. ***Clinical and Investigative Medicine, 14,*** 367-378.

Symmons, D., Mathers, C., & Plfeger, B. (2006). Global Burden of Osteoarthritis in the Year 2000. Retrieved April 13, 2008 from http://www.who.int/healthinfo/ statistics /bod_osteoarthritis.pdf.

Takahashi, T., Kondoh, T., Fukuda, M. Yamazaki, Y., Toyosaki, T., & Suzuki, R. (1998). Proinflammatory cytokines detectable in synovial fluids from patients with temporomandibular disorders. *Oral Surgery, Oral Medicine, Oral Pathology, Oral Radiology, and Endodontics, 85,* 135-41.

Tang, C. H., Chiu, Y. C., Tan, T. W., Yang, R. S., & Fu, W. M. (2007). Adiponectin enhances IL-6 production in human synovial fibroblast via an AdipoR1 receptor, AMPK, p38, and NFκB pathway. *The Journal of Immunology, 179,* 5483-5492.

Tchetina, E. V., Squires, G., & Poole, A. R. (2005). Increased type II collagen degradation and very early focal cartilage degeneration is associated with upregulation of chondrocyte differentiation related genes in early human articular cartilage lesions. *Journal of Rheumatology, 32*, 876-86.

Thumboo, J., & O'Duffy, J. D. (1998). Prospective study of the safety of joint and soft tissue aspirations and injections in patients taking warfarin sodium. *Arthritis and Rheumatism, 41,* 736-9.

Toda, Y., & Tsukimura, N. (2006). A 2-year follow-up study to compare the efficacy of lateral wedged insoles with subtalar strapping and in-shoe lateral wedged insoles in patients with varus deformity osteoarthritis of the knee. *Osteoarthritis and Cartilage*, *14,* 231-7.

Trock, D. H., Bollet, A. J., Dyer, R. H., Fielding, L. P., Miner, W. K., & Markoll, R. (1993). A double-blind trial of the clinical effects of pulsed electromagnetic fields in osteoarthritis. *The Journal of Rheumatology, 20,* 456-460.

Trock, D. H., Bollet, A. J., & Markoll, R. (1994). The effect of pulsed electromagnetic fields in the treatment of osteoarthritis of the knee and cervical spine. Report of randomized, double blind, placebo controlled trials. *Journal of Rheumatology, 21,* 1903-1911.

United States Census Bureau. International Data Base. Retrieved April 13, 2008 from http://www.census.gov/ipc/www/idb/worldpopinfo.html.

United Nations. Department of Public Health. World Population Will Increase by 2.5 Billion by 2050; People Over 60 to Increase by More Than 1 Billion. United Nations Press Release. Retrieved April 13, 2008 from http://www.un.org/News/Press/docs//2007/pop952.doc.htm.

Ushiyama, T., Chano, T., Inoue, K., & Matsusue, Y. (2003). Cytokine production in the infrapatellar fat pad: Another source of cytokines in knee synovial fluids. ***Annals of the Rheumatic Diseases, 62,*** 108-112.

van der Sluijs, J. A., Geesink, R. G. T., van der Linden, A. J., Bulstra, S. K., Kuyer, R., & Drukker, J. (1992). The reliability of the Mankin score for osteoarthritis. ***Journal of Orthopaedic Research, 10,*** 58-61.

Vilalta, C., Nunez, M., Segur, J.M., Domingo, A., Carbonell, J. A., & Macule, F. (2004). Knee osteoarthritis: Interpretation variability of radiological signs. ***Clinical Rheumatology, 23,*** 501-504.

Wakita, T., Mogi, M., Kurita, K., Kuzushima, M., & Togari, A. (2006). Increase in RANKL:OPG ratio in synovia of patients with temporomandibular joint disorder. ***Journal of Dental Research, 85,*** 627-632.

Walker, J. S., Nguyen, T. V., & Day, R. O. (1994). Clinical response to non-steroidal anti-inflammatory drugs in urate-crystal induced inflammation: A simultaneous study of intersubject and intrasubject variability. ***British Journal of Clinical Pharmacology, 38,*** 341-347.

Wang, J., Verdonk, P., Elewaut, D., Veys, E. M., & Verbruggen, G. (2003). Homeostasis of the extracellular matrix of normal and osteoarthritic human articular cartilage chondrocytes in vitro. ***Osteoarthritis and Cartilage, 11,*** 801-809.

Wang, W., Wang, Z., Zhang, G., Clark, C. C., & Brighton, C. T. (2004). Up-regulation of chondrocyte matrix genes and products by electric fields. ***Clinical Orthopaedics and Related Research, 427S,*** S163-S173.

Ward, T. T., & Steigbigel, R. T. (1978). Acidosis of synovial fluid correlates with synovial fluid leukocytes. ***The American Journal of Medicine, 64,*** 933-936.

Weiss, D. S., Kirsner, R., & Eaglstein, W. H. (1990). Electrical stimulation of wound healing. ***Archives of Dermatology, 126,*** 222-225.

World Health Organization Scientific Group (1996). Research on the menopause in the 1990s: A report of the WHO Scientific Group. ***World Health Organization Technical Report Series, 866,*** 1-107

Yamamoto, K., Shishido, T., Masaoka, T., & Imakiire, A. (2005). Morphological studies on the ageing and osteoarthritis of the articular cartilage in C57 black mice. ***Journal of Orthopaedic Surgery, 13,*** 8-18.

Zakzanis, K. K. (2001). Statistics to tell the truth, the whole truth, and nothing but the truth: Formulae, illustrative numerical examples, and heuristic interpretation of effect size analyses for neuropsychological researchers. ***Archives of Clinical Neurophysiology, 16,*** 653-667.

Zhang, W., Moskowitz, R. W., Nuki, G., Abramson, S., Altman, R. D., Arden, N., et al. (2008). OARSI recommendations for the management of hip and knee osteoarthritis, Part II: OARSI evidence-based, expert consensus guidelines. ***Osteoarthritis and Cartilage, 16,*** 137-162.

Zizic, T. M., Hoffman, K. C., Holt, P. A., Hungerford, D. S., O'Dell, J. R., Jacobs, M. A., et al. (1995). The treatment of osteoarthritis of the knee with pulsed electrical stimulation. ***The Journal of Rheumatology, 22,*** 1757-1761.

APPENDIX A
PROGRESSION OF OSTEOARTHRITIS MODEL

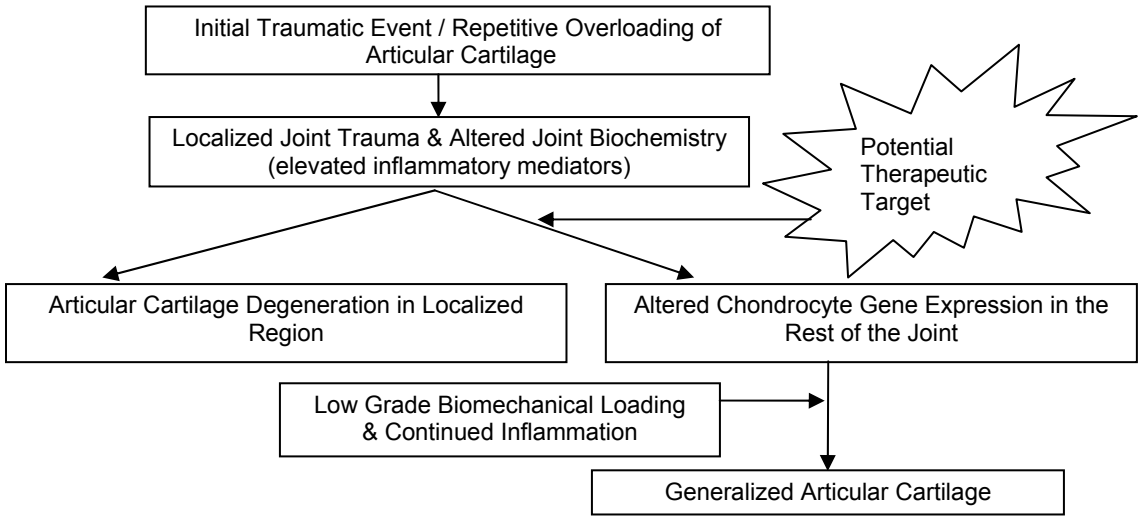

Figure A-1. Progression of Osteoarthritis Model.

APPENDIX B
CONCEPTUAL MODEL FOR BIOELECTRICAL CHANGES

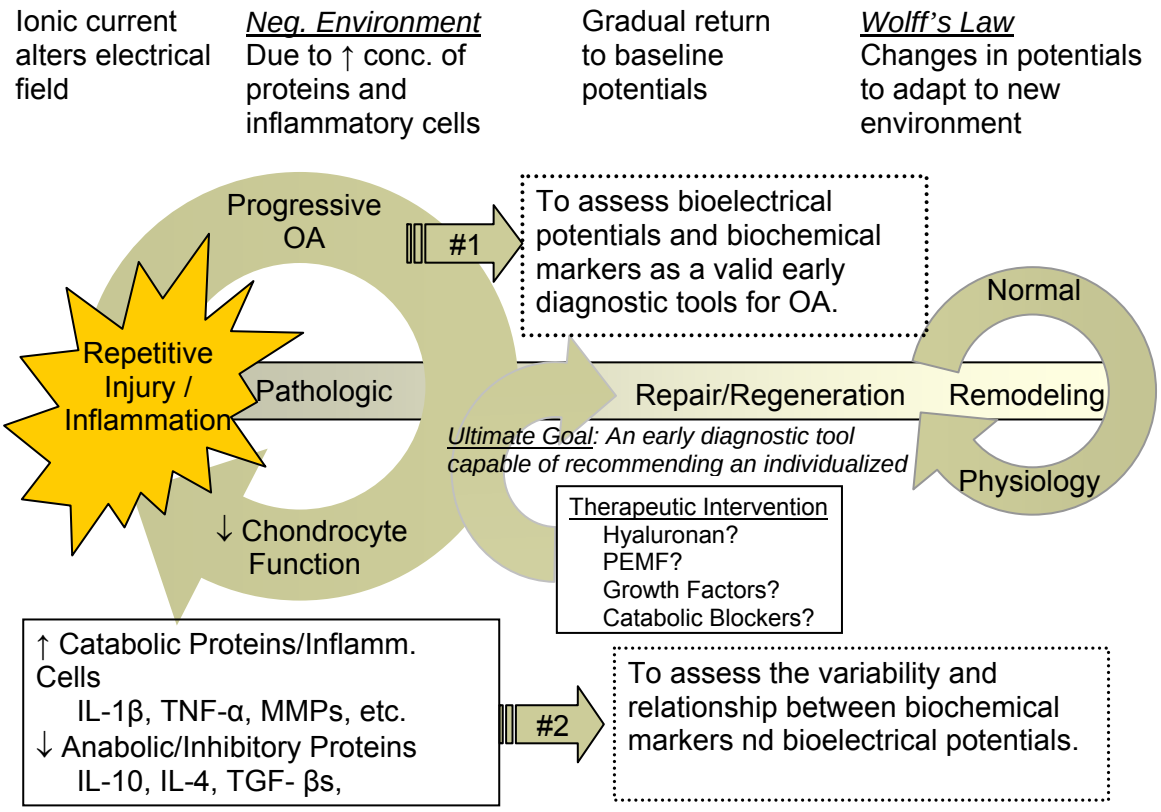

Figure B-1. Conceptual Model for Biolectrical Changes.
Osteoarthritis involves a repetitive cycle of inflammation and repetitive loading. The degenerative progression is associated with elevated concentrations of proteins, producing a net negative charge within the joint. One long-term goal is to determine whether bioelectrical potentials and/or biochemical markers can be utilized as an early diagnostic test for osteoarthritis (#1). A second long-term goal is to assess the variability among biochemical markers and bioelectrical potentials to improve the understanding of the pathophysiology of osteoarthritis and potential subsets of osteoarthritis (#2). The ultimate goal in osteoarthritis research is to develop an early diagnostic tool capable guiding clinicians to select a disease modifying osteoarthritic therapeutic intervention specific to the individual joint or osteoarthritis subset. Conc. = Concentration, IL = Interleukin, MMPs = Matrix Metalloproteinases, OA = Osteoarthritis, PEMF = Pulsed Electromagnetic Fields, TGF = Transforming Growth Factor, and TNF = Tumor Necrosis Factor.

APPENDIX C
RAT PERFORMING THE REPETITIVE REACHING TASK

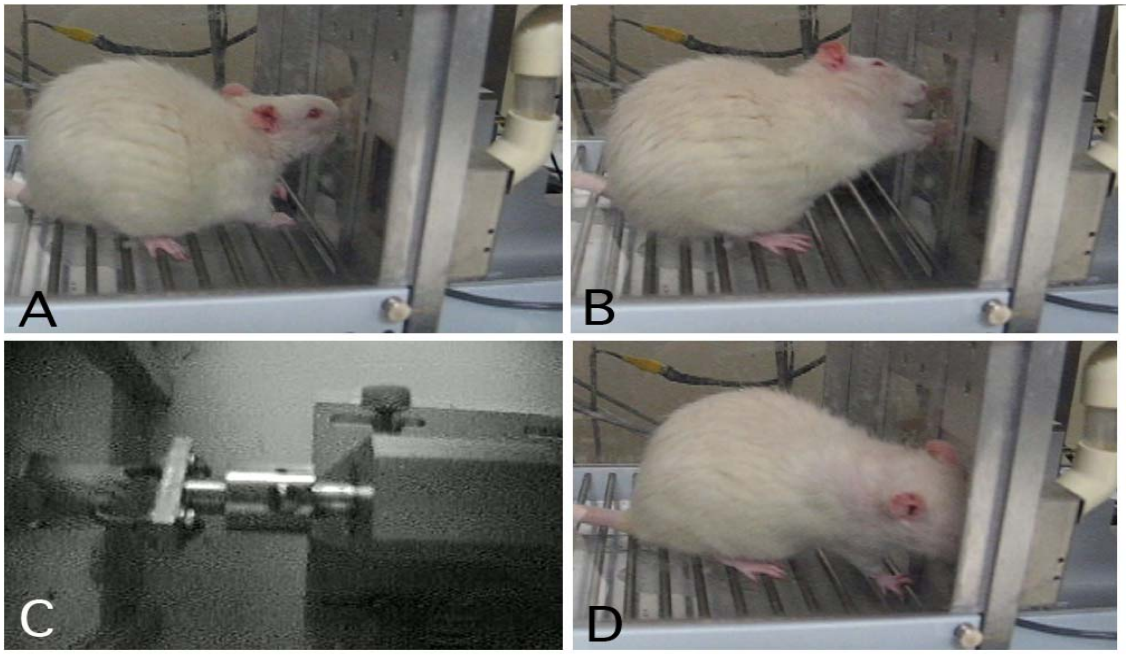

Figure C-1. Rat performing the repetitive reaching task. A) Rat awaits auditory stimulus with snout in portal. B) Rat reaches for force handle with left forepaw. C) Rat grasps and isometrically pulls force handle, which is attached to force transducer, until a predetermined force threshold is reached and held for at least 50 ms. D) Upon successful achievement of reach force and time criteria, rat releases handle and retrieves foot pellet reward by mouth from food trough.

APPENDIX D
MODIFIED MANKIN SCORING SYSTEM

Table D-1. Modified Mankin Scoring System

Criteria	Score
Structure	
Normal	0
Irregular surface, including fissures into the radial layer	1
Pannus	2
Superficial cartilage layers (≥ 6) absent	3
Slight disorganization of radial layer	4
Fissures into calcified cartilage layer	5
Disorganization (chaotic structure, clusters, osteoclast activity)	6
Cellular Abnormalities	
Normal	0
Hypercellularity, including small superficial clusters	1
Clusters	2
Hypocellularity	3
Matrix Staining	
Normal/slight reduction	0
Straining reduced in radial layer	1
Reduced in interterritorial matrix	2
Only present in pericellular matrix	3
Absent	4

APPENDIX E
HISTOPATHOLOGICAL IMAGES

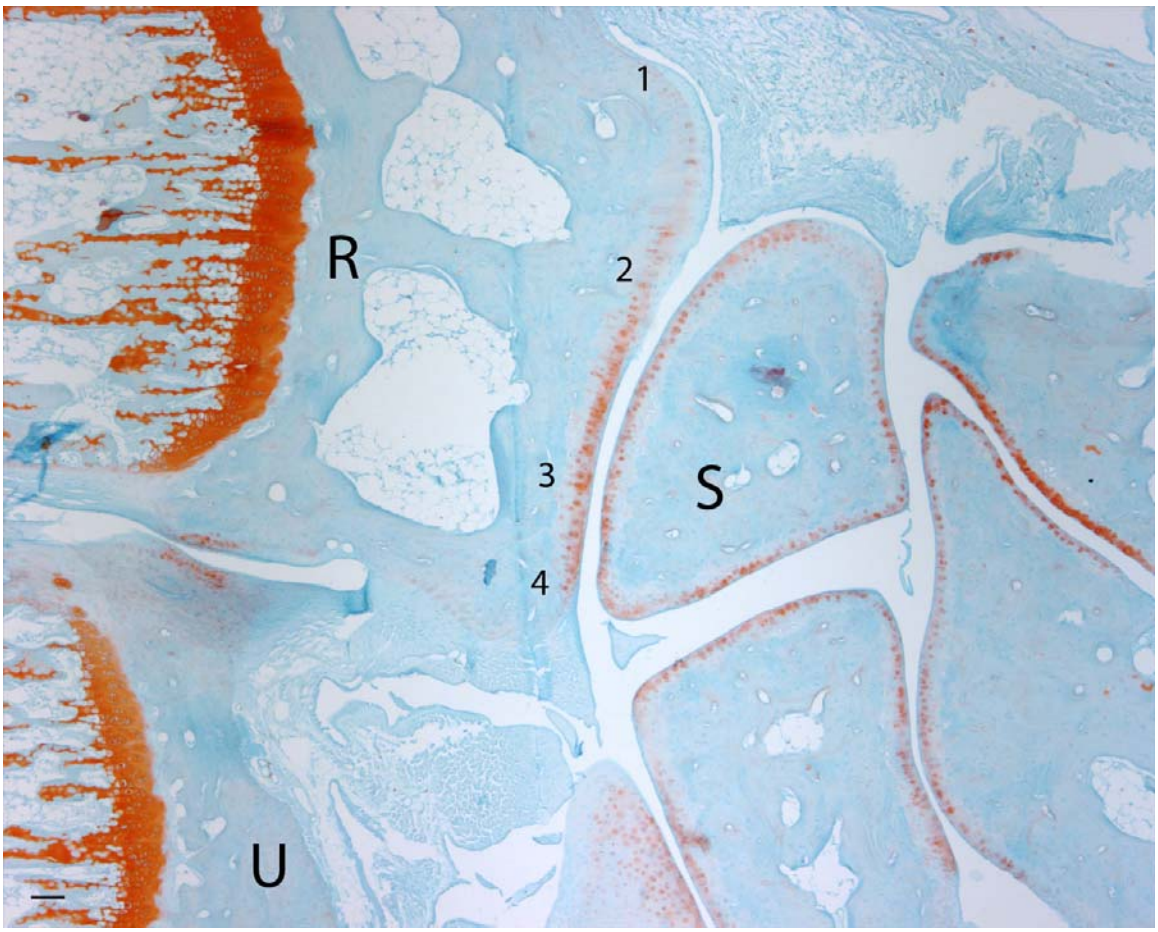

Figure E-1. Rat wrist joint stained with safranin O and fast green. R = radius, S = scaphoid, and U = ulna. 1 to 4 represent scored zones. Scale Bar = 50 µm.

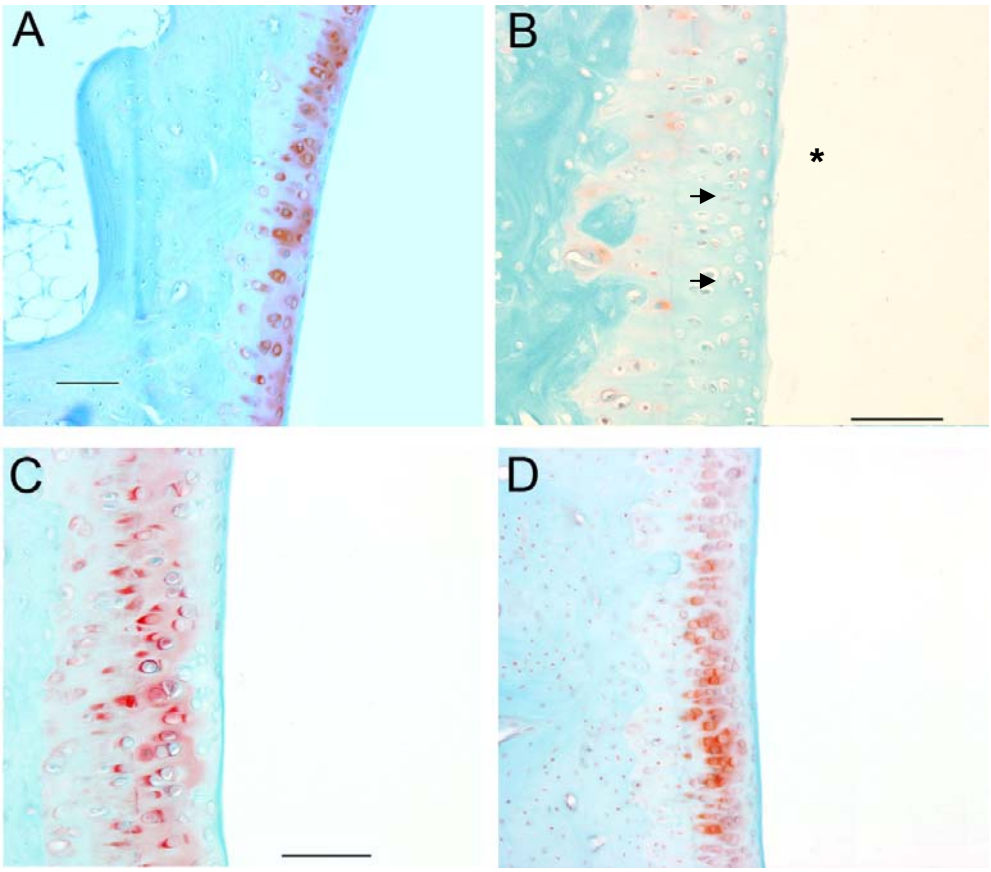

Figure E-2. Distal radius cartilage stained with safranin O and fast green in TR CON+IBU (A), HRHF (B), TR CON (C), and HRHF+IBU (D). HRHF had histopathological scores greater than TR CON+IBU, TR CON, and HRHF+IBU. Frame B demonstrates a HRHF animal with structural changes (* = pannus), cellular changes (arrow = superficial clustering), and reduced proteoglycan staining (red staining). Scale bars = 50 µm.

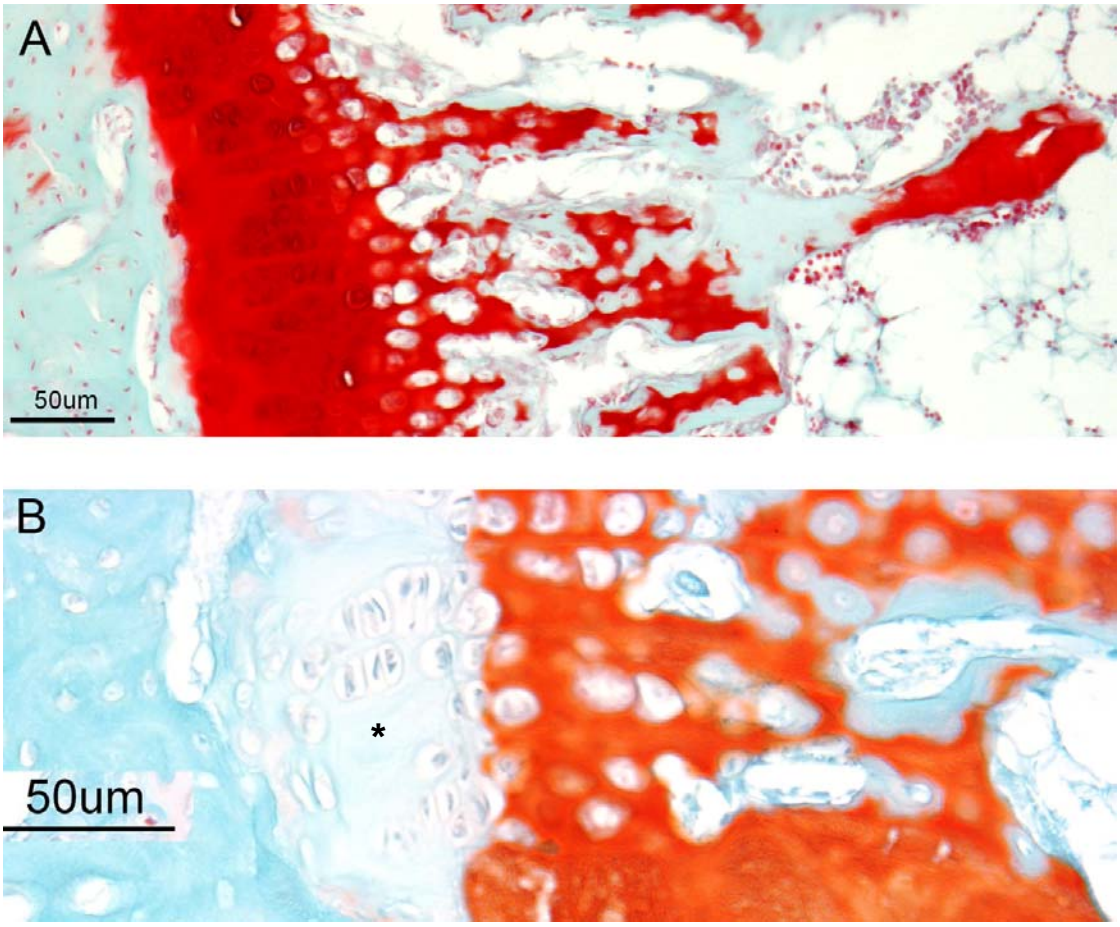

Figure E-3. Distal radius epiphyseal plate staining with safranin O and fast green. Proteoglycan staining (red staining) in TR CON+IBU (A) and HRHF+IBU was significantly greater than HRHF animals (B). Almost half of the epiphyseal plate width in the HRHF image has no proteoglycan staining (area marked with *). Scale bars = 50 µm.

APPENDIX F
ANIMAL RAW DATA

Table F-1. Average Ibuprofen Intake Across Weeks

Animal	Group	Average Actual Dose (mg/kg BW)
0404	TR CON+IBU	33.76
0414	TR CON+IBU	44.64
0416	TR CON+IBU	39.71
0418	TR CON+IBU	39.30
0433	TR CON+IBU	44.72
0439	TR CON+IBU	36.09
0441	TR CON+IBU	39.65
0442	TR CON+IBU	34.73
0443	TR CON+IBU	36.85
0444	TR CON+IBU	37.06
0501	HRHF12+IBU	41.93
0502	HRHF12+IBU	38.61
0503	HRHF12+IBU	41.66
0504	HRHF12+IBU	42.32
0505	HRHF12+IBU	36.28
0506	HRHF12+IBU	47.23
0521	HRHF12+IBU	50.26
0522	HRHF12+IBU	48.74
0523	HRHF12+IBU	50.22
0524	HRHF12+IBU	51.43
0525	HRHF12+IBU	55.78
0526	HRHF12+IBU	53.72
0773	HRHF12+IBU	57.92
0774	HRHF12+IBU	54.55
0775	HRHF12+IBU	46.94
0779	HRHF12+IBU	54.53
0782	HRHF12+IBU	54.74
0783	HRHF12+IBU	51.00

Table F-1. (continued)

Animal	Group	Average Actual Dose (mg/kg BW)
0642	HRHF6+IBU	56.85
0646	HRHF6+IBU	55.73
0654	HRHF6+IBU	39.96
0687	HRHF6+IBU	38.90
0692	HRHF6+IBU	38.10
0693	HRHF6+IBU	37.35
0696	HRHF6+IBU	33.08
0705	HRHF6+IBU	56.41
0707	HRHF6+IBU	52.66
0710	HRHF6+IBU	50.64
0711	HRHF6+IBU	57.33
0716	HRHF6+IBU	59.89

Note. TR CON+IBU = trained controls with ibuprofen, HRHF6+IBU = 6 weeks of high-repetition and high-force task plus ibuprofen, and HRHF12+IBU = 12 weeks of high-repetition and high-force task plus ibuprofen.

Table F-2. Histopathological Scores of the Radiocarpal Joint in Zone 1

Animal	Limb	Structure	Cellular	Stain	Score
0226	NORMAL	---	---	---	---
	NORMAL	---	---	---	---
0227	NORMAL	0	0	1	1
	NORMAL	---	---	---	---
0230	HRHF12S	3	2	4	9
	HRHF12R	1	2	4	7
0231	HRHF12R	3	3	4	10
	HRHF12S	0	3	3	6
0232	HRHF12S	0	2	3	5
	HRHF12R	3	3	3	9
0236	HRHF12R	3	3	4	10
	HRHF12S	---	---	---	---
0238	HRHF12S	1	2	3	6
	HRHF12R	0	1	4	5
0239	HRHF12R	1	2	4	7
	HRHF12S	---	---	---	---
0240	HRHF12R	0	2	3	5
	HRHF12S	---	---	---	---
0241	HRHF12S	3	2	4	9
	HRHF12R	1	2	4	7
0242	HRHF12S	1	1	3	5
	HRHF12R	---	---	---	---
0321	NORMAL	1	3	4	8
	NORMAL	1	3	1	5
0322	NORMAL	---	---	---	---
	NORMAL	1	1	3	5
0323	NORMAL	---	---	---	---
	NORMAL	0	2	3	6
0324	NORMAL	4	2	1	7
	NORMAL	0	2	1	3
0404	TR CON+IBU	0	2	2	4
	TR CON+IBU	1	2	1	4
0414	TR CON+IBU	3	2	1	6
	TR CON+IBU	1	2	1	4
0416	TR CON+IBU	1	2	0	3
	TR CON+IBU	---	---	---	---

Table F-2. (continued)

Animal	Limb	Structure	Cellular	Stain	Score
0418	TR CON+IBU	1	2	2	5
	TR CON+IBU	---	---	---	---
0428	NORMAL	---	---	---	---
	NORMAL	---	---	---	---
0429	NORMAL	---	---	---	---
	NORMAL	0	3	2	5
0439	TR CON+IBU	---	---	---	---
	TR CON+IBU	---	---	---	---
0504	HRHF12+IBUR	1	2	1	4
	HRHF12+IBUS	3	1	3	7
0505	HRHF12+IBUS	---	---	---	---
	HRHF12+IBUR	1	1	2	4
0506	HRHF12+IBUS	2	2	1	5
	HRHF12+IBUR	1	2	2	5
0521	HRHF12+IBUS	---	---	---	---
	HRHF12+IBUR	3	2	2	7
0522	HRHF12+IBUS	3	3	3	9
	HRHF12+IBUR	3	2	3	8
0523	HRHF12+IBUS	---	---	---	---
	HRHF12+IBUR	---	---	---	---
0648	TR CON	3	2	4	9
	TR CON	1	2	1	4

Note. --- = articular cartilage could not be scored. HRHF12R = 12 weeks of high-repetition and high-force task reach limb, HRHF12S = 12 weeks of high-repetition and high-force task support limb, HRHF12+IBUR = 12 weeks of high-repetition and high-force task plus ibuprofen reach limb, and HRHF12+IBUS = 12 weeks of high-repetition and high-force task plus ibuprofen support limb, TR CON = trained controls, and TR CON+IBU = trained controls plus ibuprofen.

Table F-3. Histopathological Scores of the Radiocarpal Joint in Zone 2

Animal	Limb	Structure	Cellular	Stain	Score
0226	NORMAL	---	---	---	---
	NORMAL	---	---	---	---
0227	NORMAL	0.0	0.0	1.0	1.0
	NORMAL	0.0	0.0	1.5	1.5
0230	HRHF12S	1.5	2.0	3.0	6.5
	HRHF12R	1.0	3.0	3.0	7.0
0231	HRHF12R	2.0	2.0	3.0	7.0
	HRHF12S	1.0	2.0	2.0	5.0
0232	HRHF12S	1.0	2.0	3.0	6.0
	HRHF12R	0.5	2.5	1.5	4.5
0236	HRHF12R	1.0	3.0	3.5	7.5
	HRHF12S	---	---	---	---
0238	HRHF12S	1.0	1.5	1.0	3.5
	HRHF12R	1.0	1.5	4.0	6.5
0239	HRHF12R	0.0	1.0	2.0	3.0
	HRHF12S	---	---	---	---
0240	HRHF12R	2.0	1.0	2.0	5.0
	HRHF12S	---	---	---	---
0241	HRHF12S	1.5	2.0	2.0	5.5
	HRHF12R	1.5	2.0	2.0	5.5
0242	HRHF12S	1.0	2.5	2.5	6.0
	HRHF12R	---	---	---	---
0321	NORMAL	0.0	1.0	1.0	2.0
	NORMAL	0.0	1.0	0.0	1.0
0322	NORMAL	---	---	---	---
	NORMAL	2.0	1.0	2.0	5.0
0323	NORMAL	1.0	1.5	1.0	3.5
	NORMAL	0.0	1.0	2.0	3.0
0324	NORMAL	2.0	2.0	1.0	5.0
	NORMAL	1.0	1.5	1.0	3.5
0404	TR CON+IBU	1.0	2.5	2.5	6.0
	TR CON+IBU	1.0	1.0	0.0	2.0
0414	TR CON+IBU	0.0	0.0	1.0	1.0
	TR CON+IBU	3.0	3.0	1.5	7.5
0416	TR CON+IBU	0.0	2.0	0.0	2.0
	TR CON+IBU	---	---	---	---

Table F-3. (continued)

Animal	Limb	Structure	Cellular	Stain	Score
0418	TR CON+IBU	1.0	1.0	1.0	3.0
	TR CON+IBU	---	---	---	---
0428	NORMAL	---	---	---	---
	NORMAL	---	---	---	---
0429	NORMAL	---	---	---	---
	NORMAL	1.0	1.0	3.0	5.0
0439	TR CON+IBU	---	---	---	---
	TR CON+IBU	---	---	---	---
0504	HRHF12+IBUR	0.0	1.0	1.0	2.0
	HRHF12+IBUS	1.0	1.0	0.0	2.0
0505	HRHF12+IBUS	---	---	---	---
	HRHF12+IBUR	1.5	1.0	2.0	4.5
0506	HRHF12+IBUS	1.0	1.5	1.5	4.0
	HRHF12+IBUR	0.0	1.0	1.0	2.0
0521	HRHF12+IBUS	1.0	1.0	3.0	5.0
	HRHF12+IBUR	1.0	1.0	1.0	3.0
0522	HRHF12+IBUS	1.0	1.0	1.0	3.0
	HRHF12+IBUR	1.0	1.0	1.5	3.5
0523	HRHF12+IBUS	1.0	2.5	3.0	6.5
	HRHF12+IBUR	---	---	---	---
0648	TR CON	1.0	1.0	3.0	5.0
	TR CON	---	---	---	---

Note. --- = articular cartilage could not be scored. HRHF12R = 12 weeks of high-repetition and high-force task reach limb, HRHF12S = 12 weeks of high-repetition and high-force task support limb, HRHF12+IBUR = 12 weeks of high-repetition and high-force task plus ibuprofen reach limb, and HRHF12+IBUS = 12 weeks of high-repetition and high-force task plus ibuprofen support limb, TR CON = trained controls, and TR CON+IBU = trained controls plus ibuprofen.

Table F-4. Histopathological Scores of the Radiocarpal Joint in Zone 3

Animal	Limb	Structure	Cellular	Stain	Score
0226	NORMAL	---	---	---	---
	NORMAL	---	---	---	---
0227	NORMAL	0.0	0.0	1.0	1.0
	NORMAL	---	---	---	---
0230	HRHF12S	1.0	2.5	3.0	6.5
	HRHF12R	1.0	2.5	1.5	5.0
0231	HRHF12R	1.0	2.0	3.0	6.0
	HRHF12S	1.0	2.5	3.0	6.5
0232	HRHF12S	1.0	2 .0	3.0	6.0
	HRHF12R	0.5	1.5	2.0	4.0
0236	HRHF12R	1.0	2.5	2.5	6.0
	HRHF12S	---	---	---	---
0238	HRHF12S	1.0	2.0	3.5	6.5
	HRHF12R	1.0	1.5	4.0	6.5
0239	HRHF12R	0.0	0.0	1.0	1.0
	HRHF12S	---	---	---	---
0240	HRHF12R	1.0	1.5	2.5	5.0
	HRHF12S	---	---	---	---
0241	HRHF12S	1.0	0.5	1.0	2.5
	HRHF12R	2.0	2.0	2.5	6.5
0242	HRHF12S	0.0	1.5	2.0	3.5
	HRHF12R	---	---	---	---
0321	NORMAL	0.0	1.0	1.0	2.0
	NORMAL	0.0	1.0	0.0	1.0
0322	NORMAL	---	---	---	---
	NORMAL	1.0	1.0	1.0	3.0
0323	NORMAL	1.0	2.0	2.0	5.0
	NORMAL	0.0	1.0	2.0	3.0
0324	NORMAL	0.0	2.0	1.0	3.0
	NORMAL	1.0	1.5	1.0	3.5
0404	TR CON+IBU	1.0	2.0	0.0	3.0
	TR CON+IBU	0.0	0.0	0.0	0.0
0414	TR CON+IBU	0.0	1.0	0.5	1.5
	TR CON+IBU	1.0	1.0	1.0	3.0
0416	TR CON+IBU	0.0	2.0	0.0	2.0
	TR CON+IBU	---	---	---	---

Table F-4. (continued)

Animal	Limb	Structure	Cellular	Stain	Score
0418	TR CON+IBU	---	---	---	---
	TR CON+IBU	1.0	0 .0	1.0	2.0
0428	NORMAL	---	---	---	---
	NORMAL	---	---	---	---
0429	NORMAL	---	---	---	---
	NORMAL	1.0	1.0	1.0	3.0
0439	TR CON+IBU	---	---	---	---
	TR CON+IBU	---	---	---	---
0504	HRHF12+IBUR	0.0	1.0	1.0	2.0
	HRHF12+IBUS	1.0	1.0	0.0	2.0
0505	HRHF12+IBUS	---	---	---	---
	HRHF12+IBUR	1.5	1.0	3.0	5.5
0506	HRHF12+IBUS	0.0	2.0	0.0	2.0
	HRHF12+IBUR	1.0	1.0	1.0	3.0
0521	HRHF12+IBUS	1.0	1.0	3.0	5.0
	HRHF12+IBUR	0.0	1.0	0.0	1.0
0522	HRHF12+IBUS	1.0	1.0	1.0	3.0
	HRHF12+IBUR	1.0	1.5	1.5	4.0
0523	HRHF12+IBUS	1.0	2.0	1.5	4.5
	HRHF12+IBUR	---	---	---	---
0648	TR CON	1.0	1.5	3.0	5.5
	TR CON	1.5	1.0	1.0	3.5

Note. --- = articular cartilage could not be scored. HRHF12R = 12 weeks of high-repetition and high-force task reach limb, HRHF12S = 12 weeks of high-repetition and high-force task support limb, HRHF12+IBUR = 12 weeks of high-repetition and high-force task plus ibuprofen reach limb, and HRHF12+IBUS = 12 weeks of high-repetition and high-force task plus ibuprofen support limb, TR CON = trained controls, and TR CON+IBU = trained controls plus ibuprofen.

Table F-5. Histopathological Scores of the Radiocarpal Joint in Zone 4

Animal	Limb	Structure	Cellular	Stain	Score
0226	NORMAL	---	---	---	---
	NORMAL	---	---	---	---
0227	NORMAL	0	0	1	1
	NORMAL	---	---	---	---
0230	HRHF12S	1	2	4	7
	HRHF12R	1	2	4	7
0231	HRHF12R	3	2	4	9
	HRHF12S	0	3	3	6
0232	HRHF12S	1	3	3	7
	HRHF12R	1	2	1	4
0236	HRHF12R	3	3	4	10
	HRHF12S	---	---	---	---
0238	HRHF12S	1	0	3	4
	HRHF12R	1	2	4	7
0239	HRHF12R	2	2	2	6
	HRHF12S	---	---	---	---
0240	HRHF12R	0	1	2	3
	HRHF12S	---	---	---	---
0241	HRHF12S	3	3	4	10
	HRHF12R	4	2	4	10
0242	HRHF12S	0	3	4	7
	HRHF12R	---	---	---	---
0321	NORMAL	1	2	2	5
	NORMAL	0	3	3	6
0322	NORMAL	---	---	---	---
	NORMAL	0	1	2	3
0323	NORMAL	0	2	3	5
	NORMAL	0	1	3	4
0324	NORMAL	3	2	2	7
	NORMAL	0	2	1	3
0404	TR CON+IBU	1	3	2	6
	TR CON+IBU	0	3	1	4
0414	TR CON+IBU	1	3	4	8
	TR CON+IBU	0	3	4	7
0416	TR CON+IBU	3	3	4	10
	TR CON+IBU	---	---	---	---

Table F-5. (continued)

Animal	Limb	Structure	Cellular	Stain	Score
0418	TR CON+IBU	---	---	---	---
	TR CON+IBU	3	3	4	10
0428	NORMAL	---	---	---	---
	NORMAL	---	---	---	---
0429	NORMAL	---	---	---	---
	NORMAL	1	3	1	5
0439	TR CON+IBU	---	---	---	---
	TR CON+IBU	---	---	---	---
0504	HRHF12+IBUR	0	2	1	3
	HRHF12+IBUS	1	2	1	4
0505	HRHF12+IBUS	---	---	---	---
	HRHF12+IBUR	1	1	3	5
0506	HRHF12+IBUS	2	2	2	6
	HRHF12+IBUR	0	2	1	3
0521	HRHF12+IBUS	1	2	3	6
	HRHF12+IBUR	0	1	4	5
0522	HRHF12+IBUS	0	2	2	4
	HRHF12+IBUR	0	2	2	4
0523	HRHF12+IBUS	---	---	---	---
	HRHF12+IBUR	---	---	---	---
0648	TR CON	---	---	---	---
	TR CON	3	2	1	6

Note. --- = articular cartilage could not be scored. HRHF12R = 12 weeks of high-repetition and high-force task reach limb, HRHF12S = 12 weeks of high-repetition and high-force task support limb, HRHF12+IBUR = 12 weeks of high-repetition and high-force task plus ibuprofen reach limb, and HRHF12+IBUS = 12 weeks of high-repetition and high-force task plus ibuprofen support limb, TR CON = trained controls, and TR CON+IBU = trained controls plus ibuprofen.

Table F-6. Interleukin-1α Concentrations in Homogenized Joints

Animal	Group	Region	IL-1α (pg/µg/ml)
0434	HRHF12	Reach Wrist	1.3975
		Support Wrist	2.0971
		Reach Diaphysis	1.5923
		Support Diaphysis	1.2852
0435	HRHF12	Reach Wrist	2.9577
		Support Wrist	1.7169
		Reach Diaphysis	0.2222
		Support Diaphysis	0.6712
0436	HRHF12	Reach Wrist	2.1691
		Support Wrist	1.0570
		Reach Diaphysis	0.3271
		Support Diaphysis	0.2026
0437	HRHF12	Reach Wrist	4.1016
		Support Wrist	0.6547
		Reach Diaphysis	1.6945
		Support Diaphysis	0.1660
0438	HRHF12	Reach Wrist	1.1927
		Support Wrist	1.4825
		Reach Diaphysis	0.5933
		Support Diaphysis	1.2568
0440	HRHF12	Reach Wrist	3.5428
		Support Wrist	1.9921
		Reach Diaphysis	0.7397
		Support Diaphysis	0.9127
0004	NORMAL	Reach Wrist	0.0586
		Support Wrist	0.0401
		Reach Diaphysis	0.2030
		Support Diaphysis	0.0317
0005	NORMAL	Reach Wrist	---
		Support Wrist	0.1575
		Reach Diaphysis	---
		Support Diaphysis	0.1575
		Support Diaphysis	0.4602
0016	NORMAL	Reach Wrist	0.5907
		Support Wrist	0.0945
		Reach Diaphysis	0.3268
		Support Diaphysis	0.0945

Table F-6. (continued)

Animal	Group	Region	IL-1α (pg/µg/ml)
0018	NORMAL	Reach Wrist	0.3861
		Support Wrist	1.8260
		Reach Diaphysis	0.1330
		Support Diaphysis	0.7967
9914	NORMAL	Reach Wrist	0.0220
		Support Wrist	0.0966
		Reach Diaphysis	---
		Support Diaphysis	0.0214
0305	NORMAL	Reach Wrist	0.4230
		Support Wrist	0.3314
		Reach Diaphysis	0.2374
		Support Diaphysis	0.3656
0426	NORMAL	Reach Wrist	---
		Support Wrist	---
		Reach Diaphysis	0.4553
		Support Diaphysis	---
0444	NORMAL	Reach Wrist	---
		Support Wrist	---
		Reach Diaphysis	0.0997
0017	NORMAL	Reach Wrist	0.3565
		Support Wrist	0.2323
		Reach Diaphysis	0.3316
		Support Diaphysis	0.4553
0501	HRHF12+IBU	Reach Wrist	0.3767
		Support Wrist	0.3364
		Reach Diaphysis	0.2502
		Support Diaphysis	0.4508
0502	HRHF12+IBU	Reach Wrist	0.9617
		Support Wrist	0.6142
		Reach Diaphysis	0.4257
		Support Diaphysis	0.3037
0503	HRHF12+IBU	Reach Wrist	0.9527
		Support Wrist	0.2944
		Reach Diaphysis	0.2712
		Support Diaphysis	0.2636
0524	HRHF12+IBU	Reach Wrist	0.3832
		Support Wrist	1.1516
		Reach Diaphysis	0.0897
		Support Diaphysis	0.0582

Table F-6. (continued)

Animal	Group	Region	IL-1α (pg/µg/ml)
0525	HRHF12+IBU	Reach Wrist	0.1571
		Support Wrist	0.4854
		Reach Diaphysis	0.1031
		Support Diaphysis	0.0477
0526	HRHF12+IBU	Reach Wrist	0.5609
		Support Wrist	1.0517
		Reach Diaphysis	0.0512
		Support Diaphysis	0.1230
0704	HRHF6	Reach Wrist	0.5868
		Support Wrist	0.5195
		Reach Diaphysis	0.1704
		Support Diaphysis	0.3089
0706	HRHF6	Reach Wrist	0.1982
		Support Wrist	0.1030
		Reach Diaphysis	0.0602
		Support Diaphysis	0.1265
0708	HRHF6	Reach Wrist	0.1495
		Support Wrist	1.0284
		Reach Diaphysis	0.0910
		Support Diaphysis	0.2029
0714	HRHF6	Reach Wrist	0.5290
		Support Wrist	0.6433
		Reach Diaphysis	0.1010
		Support Diaphysis	0.0920
0719	HRHF6	Reach Wrist	0.8138
		Support Wrist	0.7188
		Reach Diaphysis	0.0722
		Support Diaphysis	0.1104
0705	HRHF6+IBU	Reach Wrist	0.2579
		Support Wrist	0.2949
		Reach Diaphysis	0.0577
		Support Diaphysis	0.0425
0707	HRHF6+IBU	Reach Wrist	0.4573
		Support Wrist	1.4375
		Reach Diaphysis	0.1073
		Support Diaphysis	0.0906
0710	HRHF6+IBU	Reach Wrist	0.8072
		Support Wrist	0.8253
		Reach Diaphysis	0.0941
		Support Diaphysis	0.0297

Table F-6. (continued)

Animal	Group	Region	IL-1α (pg/µg/ml)
0711	HRHF6+IBU	Reach Wrist	0.6812
		Support Wrist	0.5173
		Reach Diaphysis	0.4060
		Support Diaphysis	0.1638
0716	HRHF6+IBU	Reach Wrist	0.5581
		Support Wrist	0.4601
		Reach Diaphysis	0.1109
		Support Diaphysis	0.0764

Note. --- = data not available. HRHF12 = 12 weeks high-repetition, high-force task, TR CON = trained controls, HRHF12+IBU = 12 weeks high-repetition, high-force task with ibuprofen, TR CON = trained controls, TR CON+IBU = trained controls plus ibuprofen, HRHF6 = 6 weeks high-repetition, high-force task, and HRHF6+IBU = 6 weeks high-repetition, high-force task with ibuprofen.

Table F-7. Interleukin-1β Concentrations in Homogenized Joints

Animal	Group	Region	IL-1β (pg/µg/ml)
0434	HRHF12	Reach Wrist	1.1505
		Support Wrist	0.7930
		Reach Diaphysis	2.0786
		Support Diaphysis	3.2932
0435	HRHF12	Reach Wrist	0.4526
		Support Wrist	0.7268
		Reach Diaphysis	0.2384
		Support Diaphysis	0.7120
0436	HRHF12	Reach Wrist	1.3080
		Support Wrist	0.7219
		Reach Diaphysis	0.4568
		Support Diaphysis	0.3664
0437	HRHF12	Reach Wrist	0.4781
		Support Wrist	0.4930
		Reach Diaphysis	0.2841
		Support Diaphysis	0.2257
0438	HRHF12	Reach Wrist	0.9523
		Support Wrist	1.2535
		Reach Diaphysis	1.0195
		Support Diaphysis	1.7819
0440	HRHF12	Reach Wrist	2.4258
		Support Wrist	1.3166
		Reach Diaphysis	0.9952
		Support Diaphysis	1.4576
0004	NORMAL	Reach Wrist	0.0401
		Support Wrist	0.1718
		Reach Diaphysis	0.1791
		Support Diaphysis	0.3637
0005	NORMAL	Reach Wrist	---
		Support Wrist	0.7191
		Reach Diaphysis	---
		Support Diaphysis	0.7191
0016	NORMAL	Reach Wrist	0.1987
		Support Wrist	0.0879
		Reach Diaphysis	0.3153
		Support Diaphysis	0.0879

Table F-7. (continued)

Animal	Group	Region	IL-1β (pg/µg/ml)
0017	NORMAL	Reach Wrist	0.9929
		Support Wrist	0.2598
		Reach Diaphysis	0.3156
0018	NORMAL	Reach Wrist	0.3095
		Support Wrist	2.2996
		Reach Diaphysis	0.0715
		Support Diaphysis	0.9920
9914	NORMAL	Reach Wrist	0.0966
		Support Wrist	0.0220
		Reach Diaphysis	---
		Support Diaphysis	0.1890
0305	NORMAL	Reach Wrist	1.3356
		Support Wrist	0.3648
		Reach Diaphysis	0.2461
		Support Diaphysis	1.0748
		Support Diaphysis	0.5301
0426	NORMAL	Reach Wrist	---
		Support Wrist	---
		Reach Diaphysis	0.4580
		Support Diaphysis	---
0444	NORMAL	Reach Wrist	---
		Support Wrist	---
		Reach Diaphysis	0.3250
		Support Diaphysis	0.3880
0501	HRHF12+IBU	Reach Wrist	0.2955
		Support Wrist	0.1553
		Reach Diaphysis	0.5183
		Support Diaphysis	0.6074
0502	HRHF12+IBU	Reach Wrist	0.4719
		Support Wrist	0.8798
		Reach Diaphysis	0.5868
		Support Diaphysis	0.6185
0503	HRHF12+IBU	Reach Wrist	0.2904
		Support Wrist	0.6214
		Reach Diaphysis	0.3150
		Support Diaphysis	0.5678
0524	HRHF12+IBU	Reach Wrist	0.4339
		Support Wrist	0.3081
		Reach Diaphysis	0.1497
		Support Diaphysis	0.1246

Table F-7. (continued)

Animal	Group	Region	IL-1β (pg/µg/ml)
0525	HRHF12+IBU	Reach Wrist	0.2689
		Support Wrist	0.3420
		Reach Diaphysis	0.6942
		Support Diaphysis	0.1473
0526	HRHF12+IBU	Reach Wrist	0.5699
		Support Wrist	0.7051
		Reach Diaphysis	0.2314
		Support Diaphysis	0.3826
0704	HRHF6	Reach Wrist	0.1714
		Support Wrist	0.2827
		Reach Diaphysis	0.3545
		Support Diaphysis	0.3738
0706	HRHF6	Reach Wrist	0.2730
		Support Wrist	0.4358
		Reach Diaphysis	0.3071
		Support Diaphysis	0.2786
0708	HRHF6	Reach Wrist	0.3351
		Support Wrist	0.2863
		Reach Diaphysis	0.2992
		Support Diaphysis	0.3016
0714	HRHF6	Reach Wrist	0.2894
		Support Wrist	0.2270
		Reach Diaphysis	0.3710
		Support Diaphysis	0.3658
0719	HRHF6	Reach Wrist	0.2800
		Support Wrist	0.3710
		Reach Diaphysis	0.2936
		Support Diaphysis	0.3744
0705	HRHF6+IBU	Reach Wrist	0.2443
		Support Wrist	0.2771
		Reach Diaphysis	0.3745
		Support Diaphysis	0.2143
0707	HRHF6+IBU	Reach Wrist	0.1930
		Support Wrist	0.2691
		Reach Diaphysis	0.3775
		Support Diaphysis	0.3986
0710	HRHF6+IBU	Reach Wrist	0.3370
		Support Wrist	0.2051
		Reach Diaphysis	0.3192
		Support Diaphysis	0.3837

Table F-7. (continued)

Animal	Group	Region	IL-1β (pg/µg/ml)
0711	HRHF6+IBU	Reach Wrist	0.1829
		Support Wrist	0.2005
		Reach Diaphysis	0.3804
		Support Diaphysis	0.2607
0716	HRHF6+IBU	Reach Wrist	0.2939
		Support Wrist	0.2103
		Reach Diaphysis	0.2067
		Support Diaphysis	0.1951

Note. --- = data not available. HRHF12 = 12 weeks high-repetition, high-force task, TR CON = trained controls, HRHF12+IBU = 12 weeks high-repetition, high-force task with ibuprofen, TR CON = trained controls, TR CON+IBU = trained controls plus ibuprofen, HRHF6 = 6 weeks high-repetition, high-force task, and HRHF6+IBU = 6 weeks high-repetition, high-force task with ibuprofen.

Table F-8. Tumor Necrosis Factor-α Concentrations in Homogenized Joints

Animal	Group	Region	TNF-α (pg/µg/ml)
0434	HRHF12	Reach Wrist	6.0010
		Support Wrist	4.4077
		Reach Diaphysis	12.1787
		Support Diaphysis	9.0663
0435	HRHF12	Reach Wrist	2.3043
		Support Wrist	3.4693
		Reach Diaphysis	0.8886
		Support Diaphysis	4.4966
0436	HRHF12	Reach Wrist	5.6505
		Support Wrist	3.8858
		Reach Diaphysis	1.3839
		Support Diaphysis	1.0587
0437	HRHF12	Reach Wrist	2.6028
		Support Wrist	3.3435
		Reach Diaphysis	1.2685
		Support Diaphysis	0.7684
0438	HRHF12	Reach Wrist	4.0788
		Support Wrist	4.9148
		Reach Diaphysis	3.1393
		Support Diaphysis	5.4363
0440	HRHF12	Reach Wrist	9.8036
		Support Wrist	5.1780
		Reach Diaphysis	3.1669
		Support Diaphysis	4.5423
0004	NORMAL	Reach Wrist	0.2058
		Support Wrist	0.0000
		Reach Diaphysis	0.0767
		Support Diaphysis	0.0000
0005	NORMAL	Reach Wrist	---
		Support Wrist	0.3276
		Reach Diaphysis	---
		Support Diaphysis	0.3276
0016	NORMAL	Reach Wrist	0.1146
		Support Wrist	0.1302
		Reach Diaphysis	0.4257
		Support Diaphysis	0.1302

Table F-8. (continued)

Animal	Group	Region	TNF-α (pg/µg/ml)
0017	NORMAL	Reach Wrist	0.5402
		Support Wrist	0.0000
		Reach Diaphysis	0.2677
		Support Diaphysis	0.4003
0018	NORMAL	Reach Wrist	0.7270
		Support Wrist	5.9844
		Reach Diaphysis	0.1737
		Support Diaphysis	4.2099
0305	NORMAL	Reach Wrist	0.2198
		Support Wrist	0.1325
		Reach Diaphysis	0.0827
		Support Diaphysis	0.1639
0426	NORMAL	Reach Wrist	---
		Support Wrist	---
		Reach Diaphysis	1.2403
		Support Diaphysis	---
0444	NORMAL	Reach Wrist	---
		Support Wrist	---
		Reach Diaphysis	1.6363
		Support Diaphysis	1.8162
9914	NORMAL	Reach Wrist	---
		Support Wrist	0.0908
		Reach Diaphysis	---
		Support Diaphysis	0.0137
0501	HRHF12+IBU	Reach Wrist	0.1078
		Support Wrist	0.0391
		Reach Diaphysis	0.2172
		Support Diaphysis	0.3155
0502	HRHF12+IBU	Reach Wrist	0.1688
		Support Wrist	0.3005
		Reach Diaphysis	0.1995
		Support Diaphysis	0.3066
0503	HRHF12+IBU	Reach Wrist	0.0810
		Support Wrist	0.1513
		Reach Diaphysis	0.0978
		Support Diaphysis	0.1912
0524	HRHF12+IBU	Reach Wrist	0.0870
		Support Wrist	0.0915
		Reach Diaphysis	0.0838
		Support Diaphysis	0.0310

Table F-8. (continued)

Animal	Group	Region	TNF-α (pg/µg/ml)
0525	HRHF12+IBU	Reach Wrist	0.0647
		Support Wrist	0.0957
		Reach Diaphysis	0.1660
		Support Diaphysis	0.0404
0526	HRHF12+IBU	Reach Wrist	0.1590
		Support Wrist	0.2763
		Reach Diaphysis	0.0609
		Support Diaphysis	0.0572
0704	HRHF6	Reach Wrist	0.1304
		Support Wrist	0.1246
		Reach Diaphysis	0.1703
		Support Diaphysis	0.1575
0706	HRHF6	Reach Wrist	0.1307
		Support Wrist	0.2128
		Reach Diaphysis	0.1845
		Support Diaphysis	0.1412
0708	HRHF6	Reach Wrist	0.2748
		Support Wrist	0.1523
		Reach Diaphysis	0.1665
		Support Diaphysis	0.2010
0714	HRHF6	Reach Wrist	0.1414
		Support Wrist	0.1177
		Reach Diaphysis	0.1428
		Support Diaphysis	0.1699
0719	HRHF6	Reach Wrist	0.2117
		Support Wrist	0.2085
		Reach Diaphysis	0.1354
		Support Diaphysis	0.2450
0705	HRHF6+IBU	Reach Wrist	0.0709
		Support Wrist	0.0875
		Reach Diaphysis	0.1088
		Support Diaphysis	0.0783
0707	HRHF6+IBU	Reach Wrist	0.0622
		Support Wrist	0.0961
		Reach Diaphysis	0.1176
		Support Diaphysis	0.1529
0710	HRHF6+IBU	Reach Wrist	0.1421
		Support Wrist	0.0925
		Reach Diaphysis	0.0710
		Support Diaphysis	0.0999

Table F-8. (continued)

Animal	Group	Region	TNF-α (pg/µg/ml)
0711	HRHF6+IBU	Reach Wrist	0.0744
		Support Wrist	0.1135
		Reach Diaphysis	0.1342
		Support Diaphysis	0.0995
0716	HRHF6+IBU	Reach Wrist	0.1104
		Support Wrist	0.1255
		Reach Diaphysis	0.0817
		Support Diaphysis	0.0698

Note. --- = data not available. HRHF12 = 12 weeks high-repetition, high-force task, TR CON = trained controls, HRHF12+IBU = 12 weeks high-repetition, high-force task with ibuprofen, TR CON = trained controls, TR CON+IBU = trained controls plus ibuprofen, HRHF6 = 6 weeks high-repetition, high-force task, and HRHF6+IBU = 6 weeks high-repetition, high-force task with ibuprofen.

Table F-9. Interleukin-10 Concentrations in Homogenized Joints

Animal	Group	Region	IL-10 (pg/µg/ml)
0434	HRHF12	Reach Wrist	1.8136
		Support Wrist	1.2853
		Reach Diaphysis	2.9493
		Support Diaphysis	1.9407
0435	HRHF12	Reach Wrist	0.9330
		Support Wrist	1.3376
		Reach Diaphysis	0.5761
		Support Diaphysis	1.6037
0436	HRHF12	Reach Wrist	2.1361
		Support Wrist	1.1972
		Reach Diaphysis	0.7313
		Support Diaphysis	0.7496
0437	HRHF12	Reach Wrist	1.8013
		Support Wrist	1.1061
		Reach Diaphysis	0.5793
		Support Diaphysis	0.4568
0438	HRHF12	Reach Wrist	1.6294
		Support Wrist	2.2485
		Reach Diaphysis	1.8329
		Support Diaphysis	2.7742
0440	HRHF12	Reach Wrist	3.7116
		Support Wrist	2.8742
		Reach Diaphysis	1.9094
		Support Diaphysis	3.6164
0004	NORMAL	Reach Wrist	0.0626
		Support Wrist	---
		Reach Diaphysis	0.1329
		Support Diaphysis	0.0000
0005	NORMAL	Reach Wrist	---
		Support Wrist	1.0189
		Reach Diaphysis	---
		Support Diaphysis	1.0189
0016	NORMAL	Reach Wrist	0.1310
		Support Wrist	0.0302
		Reach Diaphysis	0.0818
		Support Diaphysis	0.0302

Table F-9. (continued)

Animal	Group	Region	IL-10 (pg/µg/ml)
0017	NORMAL	Reach Wrist	0.3519
		Support Wrist	0.1535
		Reach Diaphysis	0.2286
		Support Diaphysis	0.1940
0018	NORMAL	Reach Wrist	0.1778
		Support Wrist	2.1190
		Reach Diaphysis	0.0605
		Support Diaphysis	0.8327
0305	NORMAL	Reach Wrist	0.1220
		Support Wrist	0.0821
		Reach Diaphysis	0.0566
		Support Diaphysis	0.0792
0426	NORMAL	Reach Wrist	---
		Support Wrist	---
		Reach Diaphysis	0.5816
		Support Diaphysis	---
0444	NORMAL	Reach Wrist	---
		Support Wrist	---
		Reach Diaphysis	0.5266
		Support Diaphysis	0.6103
9914	NORMAL	Reach Wrist	---
		Support Wrist	0.0573
		Reach Diaphysis	---
		Support Diaphysis	0.0390
0501	HRHF12+IBU	Reach Wrist	0.8376
		Support Wrist	0.4577
		Reach Diaphysis	1.0558
		Support Diaphysis	1.4178
0502	HRHF12+IBU	Reach Wrist	0.8461
		Support Wrist	2.2710
		Reach Diaphysis	1.4591
		Support Diaphysis	1.2924
0503	HRHF12+IBU	Reach Wrist	0.7130
		Support Wrist	0.7976
		Reach Diaphysis	0.9080
		Support Diaphysis	1.4345
0524	HRHF12+IBU	Reach Wrist	1.2689
		Support Wrist	0.7100
		Reach Diaphysis	0.4282
		Support Diaphysis	0.2782

Table F-9. (continued)

Animal	Group	Region	IL-10 (pg/µg/ml)
0525	HRHF12+IBU	Reach Wrist	0.6446
		Support Wrist	0.8404
		Reach Diaphysis	0.9409
		Support Diaphysis	0.4320
0526	HRHF12+IBU	Reach Wrist	0.7870
		Support Wrist	0.9138
		Reach Diaphysis	0.4772
		Support Diaphysis	0.4853
0704	HRHF6	Reach Wrist	0.7984
		Support Wrist	0.4482
		Reach Diaphysis	0.6109
		Support Diaphysis	0.8170
0706	HRHF6	Reach Wrist	0.6323
		Support Wrist	1.0409
		Reach Diaphysis	0.6080
		Support Diaphysis	0.6518
0708	HRHF6	Reach Wrist	0.6245
		Support Wrist	0.3698
		Reach Diaphysis	0.6393
		Support Diaphysis	0.6219
0714	HRHF6	Reach Wrist	0.4048
		Support Wrist	0.3493
		Reach Diaphysis	0.4907
		Support Diaphysis	0.5794
0719	HRHF6	Reach Wrist	0.5082
		Support Wrist	0.6430
		Reach Diaphysis	0.4220
		Support Diaphysis	0.6316
0705	HRHF6+IBU	Reach Wrist	0.3778
		Support Wrist	0.4645
		Reach Diaphysis	0.6346
		Support Diaphysis	0.3586
0707	HRHF6+IBU	Reach Wrist	0.4866
		Support Wrist	0.4827
		Reach Diaphysis	0.5490
		Support Diaphysis	0.6693
0710	HRHF6+IBU	Reach Wrist	0.6902
		Support Wrist	0.4222
		Reach Diaphysis	0.4838
		Support Diaphysis	0.5838

Table F-9. (continued)

Animal	Group	Region	IL-10 (pg/µg/ml)
0711	HRHF6+IBU	Reach Wrist	0.3039
		Support Wrist	0.3920
		Reach Diaphysis	0.9612
		Support Diaphysis	1.1108
0716	HRHF6+IBU	Reach Wrist	0.5259
		Support Wrist	0.4275
		Reach Diaphysis	0.3630
		Support Diaphysis	0.2808

Note. --- = data not available. HRHF12 = 12 weeks high-repetition, high-force task, TR CON = trained controls, HRHF12+IBU = 12 weeks high-repetition, high-force task with ibuprofen, TR CON = trained controls, TR CON+IBU = trained controls plus ibuprofen, HRHF6 = 6 weeks high-repetition, high-force task, and HRHF6+IBU = 6 weeks high-repetition, high-force task with ibuprofen.

Table F-10. Histopathological Staining Scores of the Distal Radius Epiphyseal Plate

Animal	Limb	Staining Score
0226	NORMAL	2
	NORMAL	2
0227	NORMAL	2
	NORMAL	2
0230	HRHF12S	2
	HRHF12R	2
0231	HRHF12R	2
	HRHF12S	2
0232	HRHF12S	1
	HRHF12R	1
0236	HRHF12R	2
	HRHF12S	2
0238	HRHF12S	3
	HRHF12R	2
0239	HRHF12R	---
	HRHF12S	---
0240	HRHF12R	1
	HRHF12S	---
0241	HRHF12S	2
	HRHF12R	3
0242	HRHF12S	2
	HRHF12R	2
0321	NORMAL	2
	NORMAL	1
0322	NORMAL	---
	NORMAL	---
0323	NORMAL	2
	NORMAL	2
0324	NORMAL	2
	NORMAL	2
0404	TR CON+IBU	2
	TR CON+IBU	1
0414	TR CON+IBU	1
	TR CON+IBU	1
0416	TR CON+IBU	1
	TR CON+IBU	1

Table F-10. (continued)

Animal	Limb	Staining Score
0418	TR CON+IBU	1
	TR CON+IBU	1
0428	NORMAL	1
	NORMAL	1
0429	NORMAL	1
	NORMAL	1
0439	TR CON+IBU	1
	TR CON+IBU	---
0504	HRHF12+IBUR	1
	HRHF12+IBUS	1
0505	HRHF12+IBUS	---
	HRHF12+IBUR	0
0506	HRHF12+IBUS	0
	HRHF12+IBUR	0
0521	HRHF12+IBUS	1
	HRHF12+IBUR	1
0522	HRHF12+IBUS	2
	HRHF12+IBUR	1
0523	HRHF12+IBUS	0
	HRHF12+IBUR	---
0648	TR CON	2
	TR CON	1

Note. --- = epiphyseal plate could not be scored. HRHF12R = high-repetition and high-force task reach limb, HRHF12S = high-repetition and high-force task support limb, HRHF12+IBUR = 12 weeks of high-repetition and high-force task plus ibuprofen reach limb, and HRHF12+IBUS = 12 weeks of high-repetition and high-force task plus ibuprofen support limb, TR CON = trained controls, and TR CON+IBU = trained controls plus ibuprofen.

Table F-11. C1,2C Serum Concentrations

Animal	Group	Time (weeks)	Treated	C1,2C (ng/ml)
0425	NORMAL	0	No Ibuprofen	405.83
0427	NORMAL	0	No Ibuprofen	289.11
0430	NORMAL	0	No Ibuprofen	496.08
0424	NORMAL	0	No Ibuprofen	336.04
0426	NORMAL	0	No Ibuprofen	381.76
0428	NORMAL	0	No Ibuprofen	381.76
0433	TR CON+IBU	0	Ibuprofen	352.71
0439	TR CON+IBU	0	Ibuprofen	524.55
0441	TR CON+IBU	0	Ibuprofen	584.91
0442	TR CON+IBU	0	Ibuprofen	227.60
0443	TR CON+IBU	0	Ibuprofen	357.00
0418	TR CON+IBU	0	Ibuprofen	329.60
0704	HRHF	6	No Ibuprofen	486.68
0706	HRHF	6	No Ibuprofen	372.70
0708	HRHF	6	No Ibuprofen	621.90
0714	HRHF	6	No Ibuprofen	507.40
0719	HRHF	6	No Ibuprofen	363.49
0707	HRHF+IBU	6	Ibuprofen	370.81
0642	HRHF+IBU	6	Ibuprofen	415.52
0646	HRHF+IBU	6	Ibuprofen	412.66
0654	HRHF+IBU	6	Ibuprofen	561.91
0687	HRHF+IBU	6	Ibuprofen	466.42
0692	HRHF+IBU	6	Ibuprofen	267.20
0693	HRHF+IBU	6	Ibuprofen	409.82
0436	HRHF	12	No Ibuprofen	601.01
0435	HRHF	12	No Ibuprofen	546.28
0438	HRHF	12	No Ibuprofen	819.53
0440	HRHF	12	No Ibuprofen	349.48
0434	HRHF	12	No Ibuprofen	338.49
0437	HRHF	12	No Ibuprofen	622.89

Table F-11. (continued)

Animal	Group	Time (weeks)	Treated	C1,2C (ng/ml)
0501	HRHF+IBU	12	Ibuprofen	208.27
0502	HRHF+IBU	12	Ibuprofen	337.97
0503	HRHF+IBU	12	Ibuprofen	144.45
0524	HRHF+IBU	12	Ibuprofen	361.35
0525	HRHF+IBU	12	Ibuprofen	295.59
0526	HRHF+IBU	12	Ibuprofen	344.28

Note. HRHF = high-repetition, high-force task, HRHF+IBU = high-repetition and high-force task plus ibuprofen TR CON = trained controls, and TR CON+IBU = trained controls plus ibuprofen.

APPENDIX G
ANIMAL TEST STATISTICS TABLES

Table G-1. Histopathological Scores for the Radiocarpal Articular Cartilage

Comparison	Primary Zone	Secondary Zone	T-test Statistics	P-values	Effect Size
Zone 1 - Zone 2	6.0 ± 0.3	4.2 ± 0.3	4.839	< .001*	0.88
Zone 1 - Zone 3	6.0 ± 0.3	3.5 ± 0.3	6.616	< .001*	1.25
Zone 1 - Zone 4	5.9 ± 0.3	5.7 ± 0.4	0.321	.750	0.09
Zone 2 - Zone 3	4.2 ± 0.3	3.6 ± 0.3	2.510	.016*	0.32
Zone 2 - Zone 4	4.1 ± 0.3	5.7 ± 0.4	-4.205	< .001*	0.76
Zone 3 - Zone 4	3.6 ± 0.3	5.7 ± 0.4	-5.216	< .001*	1.02

Note. Comparison 1 (***N*** = 37), comparison 2 (***N*** = 38), comparison 3 (***N*** = 37), comparison 4 (***N*** = 40), comparison 5 (***N*** = 38), and comparison 6 (***N*** = 39). All values are reported in means and standard error of the mean. * Significant with Bonferroni correction $p \leq .05/6 = .008$.

Table G-2. Histopathological Total Scores ANOVA Summary for Group, Limb, and Zone

Effect	*SS*	*df*	*MS*	*F*	*P*	*Effect Size*	*Power*
Group	85.669	3	28.556	6.351	.002*	.388	.944
Limb	0.005	1	0.005	0.001	.974	.000	.050
Zone	7.044	1	7.044	5.826	.022*	.163	.647
Group X Zone	3.325	3	1.108	0.917	.445	.084	.226
Limb X Zone	0.145	1	0.145	0.120	.732	.004	.063
Group X Limb	2.721	3	0.907	0.202	.894	.020	.083
Group x Limb X Zone	1.962	3	0.654	0.541	.658	.051	.147

Note. TR CON = trained controls (***N*** = 8); TR CON+IBU = trained controls plus ibuprofen limb (***N*** = 6); HRHF = high-repetition, high-force (***N*** = 14); and HRHF+IBU = high-repetition, high-force plus ibuprofen (***N*** = 10). * = significant at $p \leq .05$.

Table G-3. Follow-up Bonferroni Corrected Independent T-tests for Group Differences in Histopathological Total Scores

Group 1	Group 2	Mean Difference (Group 1 – Group 2)	*P*
HRHF12	TR CON	1.98	.034*
	TR CON+IBU	2.69	.006*
	HRHF12+IBU	1.98	.020*
HRHF12+IBU	TR CON	0.00	1.000
	TR CON+IBU	0.71	1.000
TR CON	TR CON+IBU	0.71	1.000

Note. TR CON = trained controls (***N*** = 8); TR CON+IBU = trained controls plus ibuprofen limb (***N*** = 6); HRHF = high-repetition, high-force (***N*** = 14); and HRHF+IBU = high-repetition, high-force plus ibuprofen (***N*** = 10). * = significant at $p \leq .05$.

Table G-4. Epiphyseal Plate Staining Scores ANOVA Summary for Group and Limb

							Post Hoc Analyses	
Effect	*SS*	*df*	*MS*	*F*	*P*	*Power*	Comparison	*P*
Group	11.099	3	3.700	12.384	< .001	.999	HRHF12 - TR CON	1.000
							HRHF12 - TR CON+IBU	.007*
							HRHF12 - HRHF+IBU	< .001*
							HRHF12+IBU - TR CON	.002*
							HRHF12+IBU - TR CON+IBU	.665
							TR CON - TR CON+IBU	.130
Limb	0.007	1	0.007	0.024	.878	.053		
Group x Limb	1.239	3	0.413	1.382	.265	.334		

Note. TR CON = trained controls (***N*** = 8); TR CON+IBU = trained controls plus ibuprofen limb (***N*** = 9); HRHF = high-repetition, high-force (***N*** = 15); and HRHF+IBU = high-repetition, high-force plus ibuprofen (***N*** = 10). * = significant at $p \leq .05$.

Table G-5. C1,2C Serum Concentrations ANOVA Summary for Time and Treatment

Effect	*SS*	*df*	*MS*	*F*	*P*	*Effect Size*	*Power*
Time	17107.387	2	8553.694	0.626	.541	.040	.145
Treatment	92464.315	1	92464.315	6.772	.014*	.184	.712
Time X Treatment	125897.450	2	62948.725	4.610	.018*	.235	.736

Note. NORM = normal controls (***N*** = 6); TR CON+IBU = trained controls plus ibuprofen limb (***N*** = 6); HRHF6 = high-repetition, high-force task for 6 weeks (***N*** = 5); HRHF6+IBU = high-repetition, high-force for 6 weeks plus ibuprofen (***N*** = 7); HRHF12 = high-repetition, high-force task for 12 weeks (***N*** = 6); and HRHF12+IBU = high-repetition, high-force for 12 weeks plus ibuprofen (***N*** = 6). * = significant at $p \leq .05$.

Table G-6. C1,2C Serum Concentrations Follow-up Bonferroni Corrected Independent T-tests for Time x Treatment Effect

Comparison	Group 1	Group 2	T-test Statistic	*P*-value
NORM – TR CON+IBU	381.762 ± 28.473	396.063 ± 54.275	-0.233	.820
NORM – HRHF6	381.762 ± 28.473	470.433 ± 47.729	-1.662	.131
NORM – HRHF6+IBU	381.762 ± 28.473	414.905 ± 33.827	-0.734	.478
NORM – HRHF12	381.762 ± 28.473	546.281 ± 74.261	-2.069	.065
NORM – HRHF12+IBU	381.762 ± 28.473	281.984 ± 35.520	2.192	.053
HRHF6 – HRHF6+IBU	470.433 ± 47.729	414.905 ± 33.827	0.980	.350
HRHF12 – HRHF12+IBU	546.281 ± 74.261	281.984 ± 35.520	3.211	.009

Note. NORM = normal controls (***N*** = 6); TR CON+IBU = trained controls plus ibuprofen limb (***N*** = 6); HRHF6 = high-repetition, high-force task for 6 weeks (***N*** = 5); HRHF6+IBU = high-repetition, high-force for 6 weeks plus ibuprofen (***N*** = 7); HRHF12 = high-repetition, high-force task for 12 weeks (***N*** = 6); and HRHF12+IBU = high-repetition, and high-force for 12 weeks plus ibuprofen (***N*** = 6). All values are reported in means and standard error of the mean. Significant with Bonferroni correction at $p \leq .05/7 = .007$.

Table G-7. Interleukin-1α Concentrations in Homogenized Joints ANOVA Summary for Group, Region, and Limb

Effect	*SS*	*df*	*MS*	*F*	*P*	*Effect Size*	*Power*
Group	21.608	4	5.402	28.381	< .001*	.542	1.000
Region	7.788	1	7.788	40.916	< .001*	.299	1.000
Limb	0.118	1	0.118	0.619	.433	.006	.122
Group x Region	4.506	4	1.126	5.918	< .001*	.198	.980
Group x Limb	2.034	4	0.509	2.672	.037*	.100	.724
Region x Limb	0.075	1	0.075	0.391	.533	.004	.095
Group x Region X Limb	1.339	4	0.335	1.758	.144	.068	.519

Note. NORM = normal controls (***N*** = 9); HRHF6 = high-repetition, high-force for 6 weeks (***N*** = 5); HRHF12 = high-repetition, high-force for 12 weeks (***N*** = 6); HRHF6+IBU = high-repetition, high-force for 6 weeks plus ibuprofen (***N*** = 5); and HRHF12+IBU = high-repetition, high-force for 12 weeks plus ibuprofen (***N*** = 6). * = significant at $p \leq .05$.

Table G-8. Interleukin-1α Concentrations in Radioulnar Diaphyses Follow-up ANOVA Summary for Group

						Post Hoc Analyses	
Effect	*SS*	*df*	*MS*	*F*	*P*	Comparison	*P*
Group	3.772	4	0.943	11.949	< .001*	HRHF12 – NORM	< .001*
						HRHF12 – HRHF6	< .001*
						HRHF12 – HRHF6+IBU	< .001*
						HRHF12 – HRHF12+IBU	< .001*
						HRHF12+IBU - NORM	1.000
						HRHF12+IBU – HRHF6	1.000
						HRHF12+IBU – HRHF6+IBU	1.000
						HRHF6+IBU - NORM	1.000
						HRHF6+IBU – HRHF6	1.000
						HRHF6 – NORM	1.000

Note. NORM = normal controls (***N*** = 15); HRHF6 = high-repetition, high-force for 6 weeks (***N*** = 10); HRHF12 = high-repetition, high-force for 12 weeks (***N*** = 12); HRHF6+IBU = high-repetition, high-force for 6 weeks plus ibuprofen (***N*** = 10); and HRHF12+IBU = high-repetition, high-force for 12 weeks plus ibuprofen (***N*** = 12). * = significant at $p \leq .05$.

Table G-9. Interleukin-1α Concentrations in Wrist Joints Follow-up ANOVA Summary for Group

						Post Hoc Analyses	
Effect	*SS*	*df*	*MS*	*F*	*P*	Comparison	*P*
Group	22.096	4	5.524	16.305	< .001*	HRHF12 – NORM	< .001*
						HRHF12 – HRHF6	< .001*
						HRHF12 – HRHF6+IBU	< .001*
						HRHF12 – HRHF12+IBU	< .001*
						HRHF12+IBU - NORM	1.000
						HRHF12+IBU – HRHF6	1.000
						HRHF12+IBU – HRHF6+IBU	1.000
						HRHF6+IBU - NORM	1.000
						HRHF6+IBU – HRHF6	1.000
						HRHF6 – NORM	1.000

Note. NORM = normal controls (*N* = 13); HRHF6 = high-repetition, high-force for 6 weeks (*N* = 10); HRHF12 = high-repetition, high-force for 12 weeks (*N* = 12); HRHF6+IBU = high-repetition, high-force for 6 weeks plus ibuprofen (*N* = 10); and HRHF12+IBU = high-repetition, high-force for 12 weeks plus ibuprofen (*N* = 12). * = significant at $p \leq .05$.

Table G-10. Interleukin-1α Concentrations in Reach Limbs Follow-up ANOVA Summary for Group

						Post Hoc Analyses	
Effect	*SS*	*df*	*MS*	*F*	*P*	Comparison	*P*
Group	18.356	4	4.589	52.256	< .001*	HRHF12 – NORM	< .001*
						HRHF12 – HRHF6	< .001*
						HRHF12 – HRHF6+IBU	< .001*
						HRHF12 – HRHF12+IBU	< .001*
						HRHF12+IBU - NORM	1.000
						HRHF12+IBU – HRHF6	1.000
						HRHF12+IBU – HRHF6+IBU	1.000
						HRHF6+IBU - NORM	1.000
						HRHF6+IBU – HRHF6	1.000
						HRHF6 – NORM	1.000

Note. NORM = normal controls (***N*** = 13); HRHF6 = high-repetition, high-force for 6 weeks (***N*** = 10); HRHF12 = high-repetition, high-force for 12 weeks (***N*** = 12); HRHF6+IBU = high-repetition, high-force for 6 weeks plus ibuprofen (***N*** = 10); and HRHF12+IBU = high-repetition, high-force for 12 weeks plus ibuprofen (***N*** = 12). * = significant at $p \leq .05$.

Table G-11. Interleukin-1α Concentrations in Support Limbs Follow-up ANOVA Summary for Group

						Post Hoc Analyses	
Effect	*SS*	*df*	*MS*	*F*	*P*	Comparison	*P*
Group	5.269	4	1.317	6.126	< .001*	HRHF12 – NORM	.001*
						HRHF12 – HRHF6	.005*
						HRHF12 – HRHF6+IBU	.005*
						HRHF12 – HRHF12+IBU	.006*
						HRHF12+IBU - NORM	1.000
						HRHF12+IBU – HRHF6	1.000
						HRHF12+IBU – HRHF6+IBU	1.000
						HRHF6+IBU - NORM	1.000
						HRHF6+IBU – HRHF6	1.000
						HRHF6 – NORM	1.000

Note. NORM = normal controls (***N*** = 13); HRHF6 = high-repetition, high-force for 6 weeks (***N*** = 10); HRHF12 = high-repetition, high-force for 12 weeks (***N*** = 12); HRHF6+IBU = high-repetition, high-force for 6 weeks plus ibuprofen (***N*** = 10); and HRHF12+IBU = high-repetition, high-force for 12 weeks plus ibuprofen (***N*** = 12). * = significant at $p \leq .05$.

Table G-12. Interleukin-1β Concentrations ANOVA Summary for Group, Region, and Limb

Effect	*SS*	*df*	*MS*	*F*	*P*	*Effect Size*	*Power*
Group	8.827	4	2.207	10.845	< .001*	.311	1.000
Region	0.001	1	0.001	0.003	.956	.000	.050
Limb	0.126	1	0.126	0.617	.434	.006	.122
Group x Region	0.167	4	0.042	0.205	.935	.008	.092
Group x Limb	0.133	4	0.033	0.163	.957	.007	.083
Region x Limb	0.151	1	0.151	0.743	.391	.008	.137
Group x Region X Limb	0.657	4	0.164	0.807	.524	.033	.250

Note. NORM = normal controls (***N*** = 9); HRHF6 = high-repetition, high-force for 6 weeks (***N*** = 5); HRHF12 = high-repetition, high-force for 12 weeks (***N*** = 6); HRHF6+IBU = high-repetition, high-force for 6 weeks plus ibuprofen (***N*** = 5); and HRHF12+IBU = high-repetition, high-force for 12 weeks plus ibuprofen (***N*** = 6). * = significant at $p \leq .05$.

Table G-13. Interleukin-1β Concentrations Follow-up Bonferroni Corrected Independent T-tests for Group Differences

Group 1	Group 2	Mean Difference (Group 1 – Group 2)	*P*
HRHF12	NORM	0.573	< .001*
	HRHF6	0.727	< .001*
	HRHF6+IBU	0.765	< .001*
	HRHF12+IBU	0.612	< .001*
HRHF12+IBU	NORM	-0.039	1.000
	HRHF6	0.115	1.000
	HRHF6+IBU	0.152	1.000
HRHF6	NORM	-0.154	1.000
	HRHF6+IBU	0.038	1.000
HRHF6+IBU	NORM	-0.192	1.000

Note. NORM = normal controls (*N* = 9); HRHF6 = high-repetition, high-force for 6 weeks (*N* = 5); HRHF12 = high-repetition, high-force for 12 weeks (*N* = 6); HRHF6+IBU = high-repetition, high-force for 6 weeks plus ibuprofen (*N* = 5); and HRHF12+IBU = high-repetition, high-force for 12 weeks plus ibuprofen (*N* = 6). * = significant at $p \leq .05$.

Table G-14. Tumor Necrosis Factor-α Concentrations ANOVA Summary for Group, Region, and Limb

Effect	*SS*	*df*	*MS*	*F*	*P*	*Effect Size*	*Power*
Group	308.327	4	77.082	32.193	< .001*	.575	1.000
Region	0.416	1	0.416	0.174	.678	.002	.070
Limb	0.132	1	0.132	0.055	.815	.001	.056
Group x Region	2.403	4	0.601	0.251	.908	.010	.103
Group x Limb	1.347	4	0.337	0.141	.967	.006	.078
Region x Limb	0.380	1	0.380	0.159	.691	.002	.068
Group x Region X Limb	2.785	4	0.696	0.291	.883	.012	.112

Note. NORM = normal controls (***N*** = 9); HRHF6 = high-repetition, high-force for 6 weeks (***N*** = 5); HRHF12 = high-repetition, high-force for 12 weeks (***N*** = 6); HRHF6+IBU = high-repetition, high-force for 6 weeks plus ibuprofen (***N*** = 5); and HRHF12+IBU = high-repetition, high-force for 12 weeks plus ibuprofen (***N*** = 6). * = significant at $p \leq .05$.

Table G-15. Tumor Necrosis Factor-α Concentrations Follow-up Bonferroni Corrected Independent T-tests for Group Differences

Group 1	Group 2	Mean Difference (Group 1 – Group 2)	*P*
HRHF12	NORM	3.605	< .001*
	HRHF6	4.122	< .001*
	HRHF6+IBU	4.194	< .001*
	HRHF12+IBU	4.152	< .001*
HRHF12+IBU	NORM	-0.547	1.000
	HRHF6	-0.030	1.000
	HRHF6+IBU	0.042	1.000
HRHF6	NORM	-0.518	1.000
	HRHF6+IBU	0.072	1.000
HRHF6+IBU	NORM	-0.589	1.000

Note. NORM = normal controls (*N* = 9); HRHF6 = high-repetition, high-force for 6 weeks (*N* = 5); HRHF12 = high-repetition, high-force for 12 weeks (*N* = 6); HRHF6+IBU = high-repetition, high-force for 6 weeks plus ibuprofen (*N* = 5); and HRHF12+IBU = high-repetition, high-force for 12 weeks plus ibuprofen (*N* = 6). * = significant at $p \leq .05$.

Table G-16. Interleukin-10 Concentrations ANOVA Summary for Effects of Group, Region, and Limb

Effect	*SS*	*df*	*MS*	*F*	*P*	*Effect Size*	*Power*
Group	29.204	4	7.301	23.232	< .001*	.497	1.000
Region	0.024	1	0.024	0.077	.782	.001	.059
Limb	0.191	1	0.191	0.606	.438	.006	.120
Group x Region	0.343	4	0.086	0.273	.985	.011	.108
Group x Limb	0.263	4	0.066	0.209	.933	.009	.093
Region x Limb	0.069	1	0.069	0.218	.641	.002	.075
Group x Region X Limb	0.983	4	0.246	0.782	.540	.032	.242

Note. NORM = normal controls (***N*** = 9); HRHF6 = high-repetition, high-force for 6 weeks (***N*** = 5); HRHF12 = high-repetition, high-force for 12 weeks (***N*** = 6); HRHF6+IBU = high-repetition, high-force for 6 weeks plus ibuprofen (***N*** = 5); and HRHF12+IBU = high-repetition, high-force for 12 weeks plus ibuprofen (***N*** = 6). * = significant at $p \leq .05$.

Table G-17. Interleukin-10 Concentrations Follow-up Bonferroni Corrected Independent T-tests for Group Differences

Group 1	Group 2	Mean Difference (Group 1 – Group 2)	*P*
HRHF12	NORM	1.408	< .001*
	HRHF6	1.147	< .001*
	HRHF6+IBU	1.213	< .001*
	HRHF12+IBU	0.837	< .001*
HRHF12+IBU	NORM	0.570	.006*
	HRHF6	0.309	.715
	HRHF6+IBU	0.376	.293
HRHF6	NORM	0.261	1.000
	HRHF6+IBU	0.066	1.000
HRHF6+IBU	NORM	0.195	1.000

Note. NORM = normal controls (***N*** = 9); HRHF6 = high-repetition, high-force for 6 weeks (***N*** = 5); HRHF12 = high-repetition, high-force for 12 weeks (***N*** = 6); HRHF6+IBU = high-repetition, high-force for 6 weeks plus ibuprofen (***N*** = 5); and HRHF12+IBU = high-repetition, high-force for 12 weeks plus ibuprofen (***N*** = 6). * = significant at $p \leq .05$.

APPENDIX H
INFLAMMATORY PROTEIN CONCENTRATION FIGURES

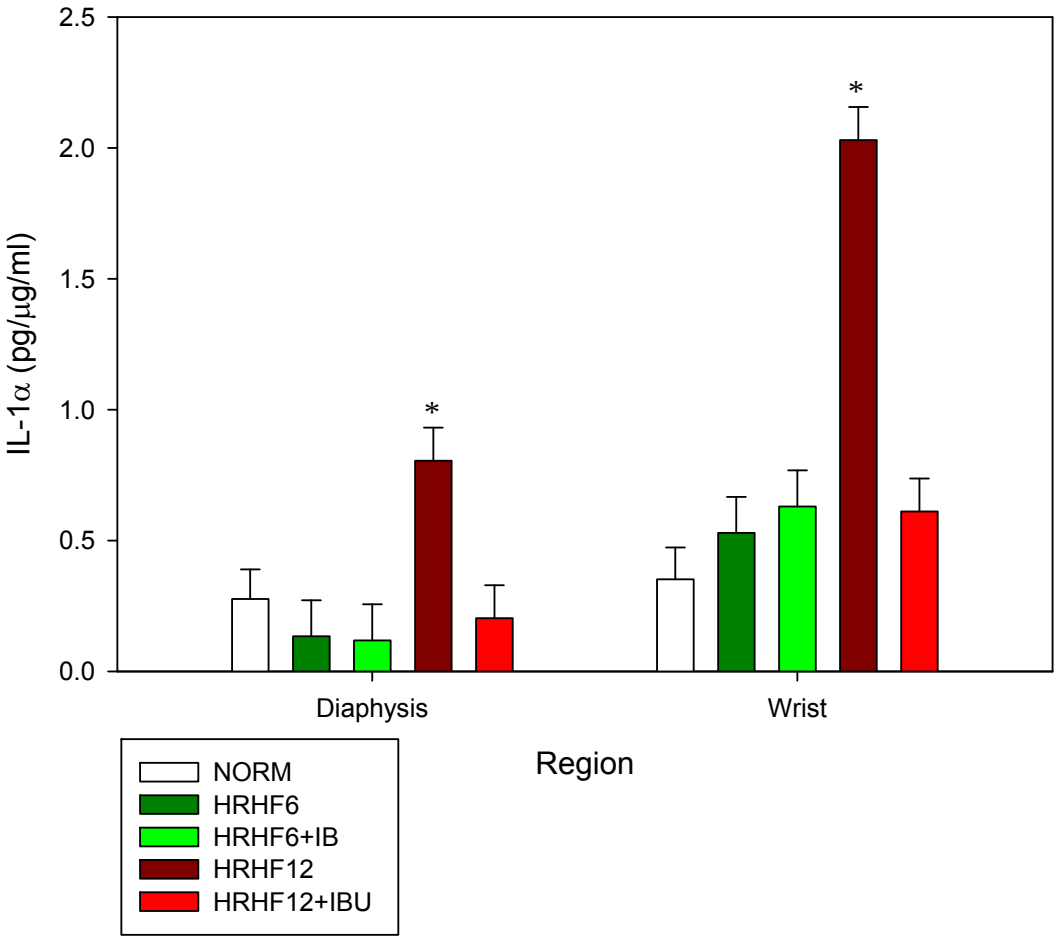

Figure H-1. IL-1α concentrations in wrist joints and radioulnar diaphyses among groups. NORM = normal controls (*N* = 9); HRHF6 = high-repetition, high-force for 6 weeks (*N* = 5); HRHF12 = high-repetition, high-force for 12 weeks (*N* = 6); HRHF6+IBU = high-repetition, high-force for 6 weeks plus ibuprofen (*N* = 5); and HRHF12+IBU = high-repetition, high-force for 12 weeks plus ibuprofen (*N* = 6).
* Significantly different from all other groups within the region: $p \leq .05$.

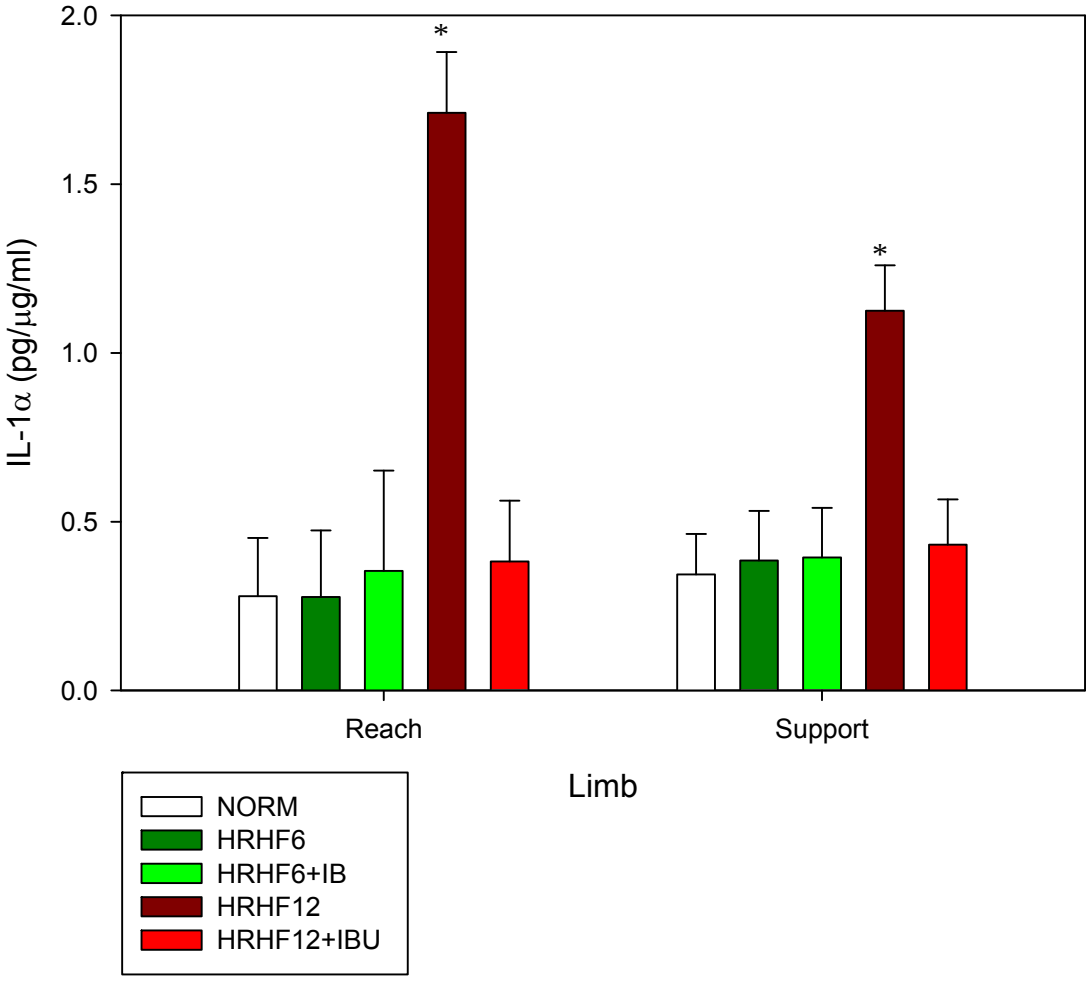

Figure H-2. IL-1α concentrations in reach and support limbs among groups. NORM = normal controls (*N* = 9); HRHF6 = high-repetition, high-force for 6 weeks (*N* = 5); HRHF12 = high-repetition, high-force for 12 weeks (*N* = 6); HRHF6+IBU = high-repetition, high-force for 6 weeks plus ibuprofen (*N* = 5); and HRHF12+IBU = high-repetition, high-force for 12 weeks plus ibuprofen (*N* = 6).
* Significantly different from all other groups within the limb: $p \leq .05$.

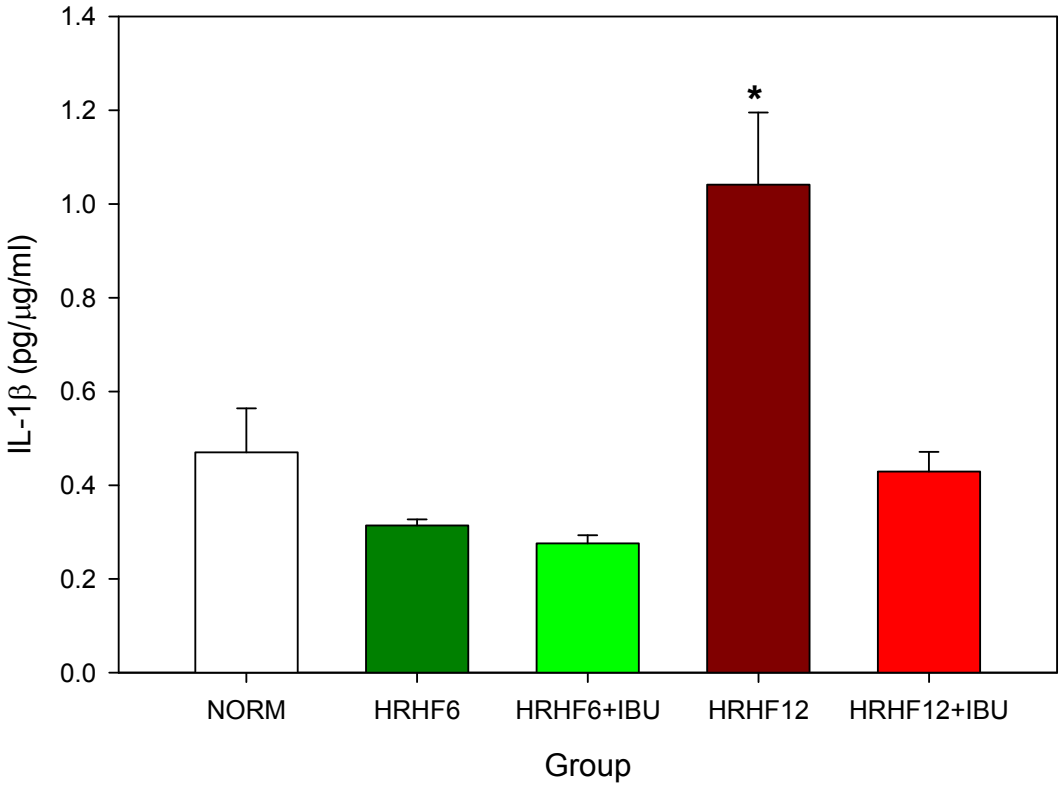

Figure H-3. IL-1β concentrations among groups. NORM = normal controls (*N* = 9); HRHF6 = high-repetition, high-force for 6 weeks (*N* = 5); HRHF12 = high-repetition, high-force for 12 weeks (*N* = 6); HRHF6+IBU = high-repetition, high-force for 6 weeks plus ibuprofen (*N* = 5); and HRHF12+IBU = high-repetition, high-force for 12 weeks plus ibuprofen (*N* = 6).
* Significantly different from all other groups: $p \leq .05$.

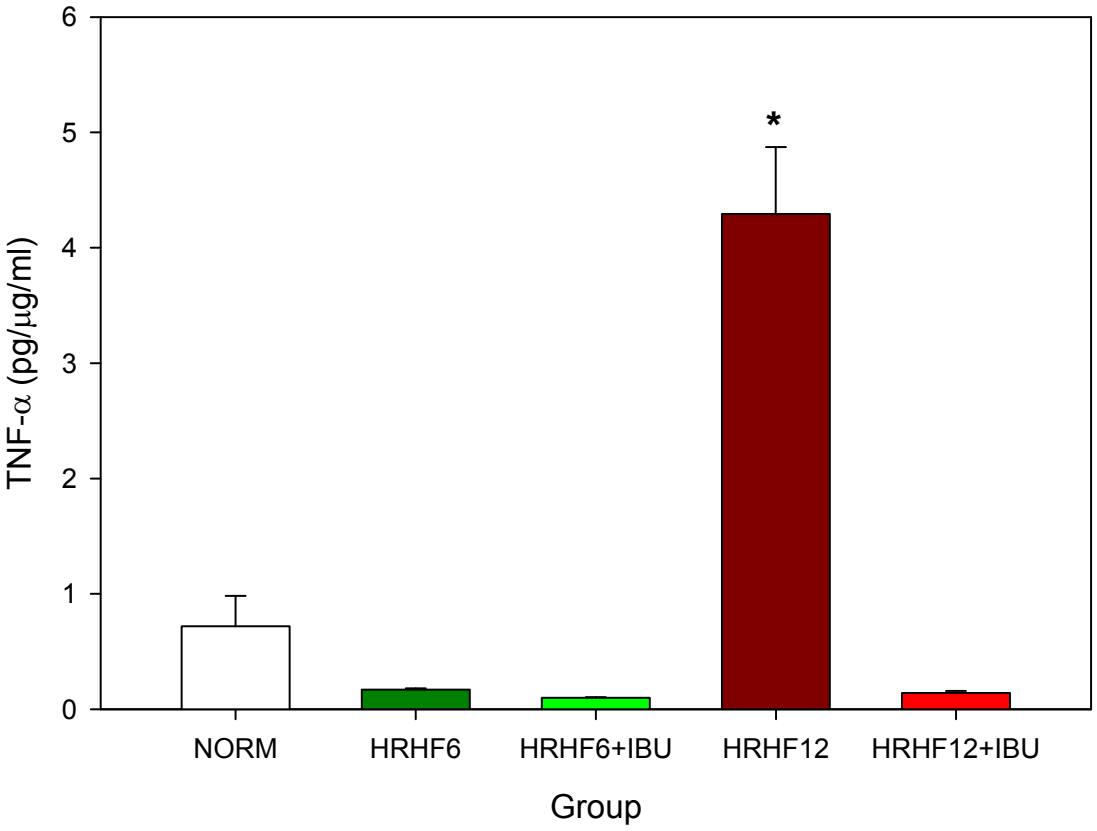

Figure H-4. TNF-α concentrations among groups. NORM = normal controls (*N* = 9); HRHF6 = high-repetition, high-force for 6 weeks (*N* = 5); HRHF12 = high-repetition, high-force for 12 weeks (*N* = 6); HRHF6+IBU = high-repetition, high-force for 6 weeks plus ibuprofen (*N* = 5); and HRHF12+IBU = high-repetition, high-force for 12 weeks plus ibuprofen (*N* = 6).
* Significantly different from all other groups: $p \leq .05$.

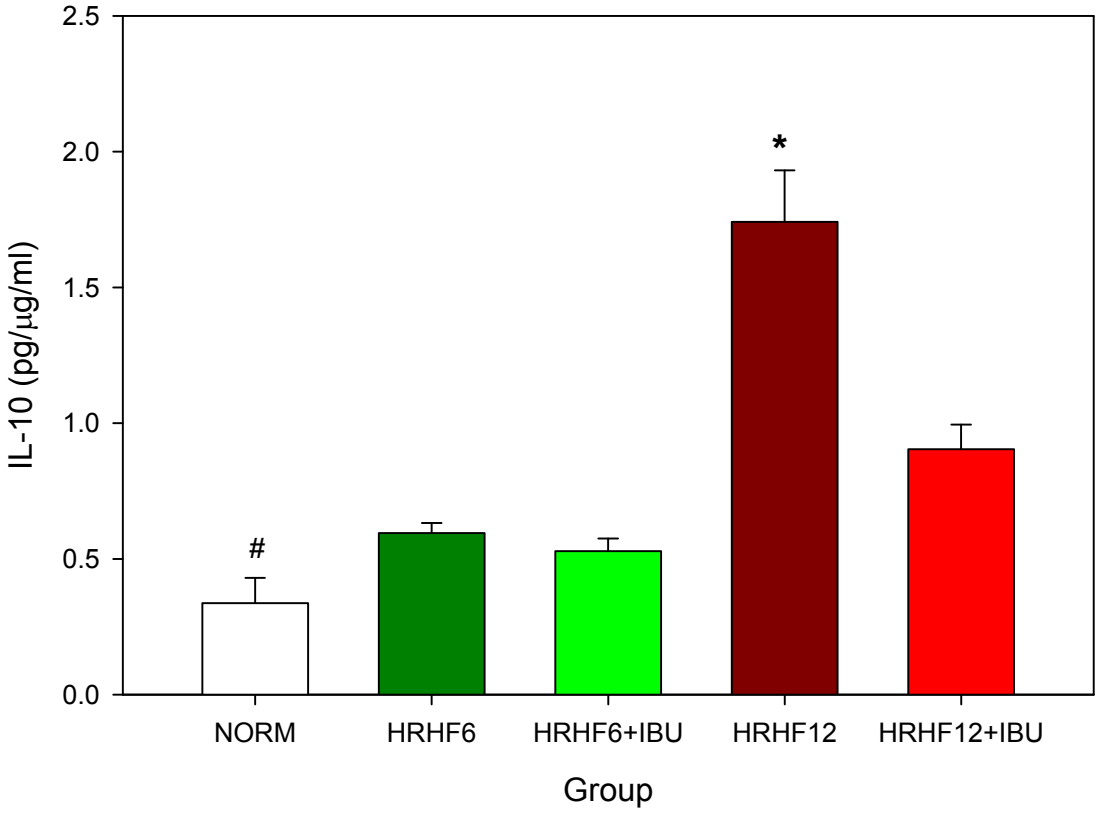

Figure H-5. IL-10 concentrations among groups. NORM = normal controls (*N* = 9); HRHF6 = high-repetition, high-force for 6 weeks (*N* = 5); HRHF12 = high-repetition, high-force for 12 weeks (*N* = 6); HRHF6+IBU = high-repetition, high-force for 6 weeks plus ibuprofen (*N* = 5); and HRHF12+IBU = high-repetition, high-force for 12 weeks plus ibuprofen (*N* = 6).
* Significantly different from all other groups: $p \leq .05$.
# Significantly different from HRHF12+IBU: $p \leq .05$.

APPENDIX I
HISTOPATHOLOGICAL SCORE FIGURES

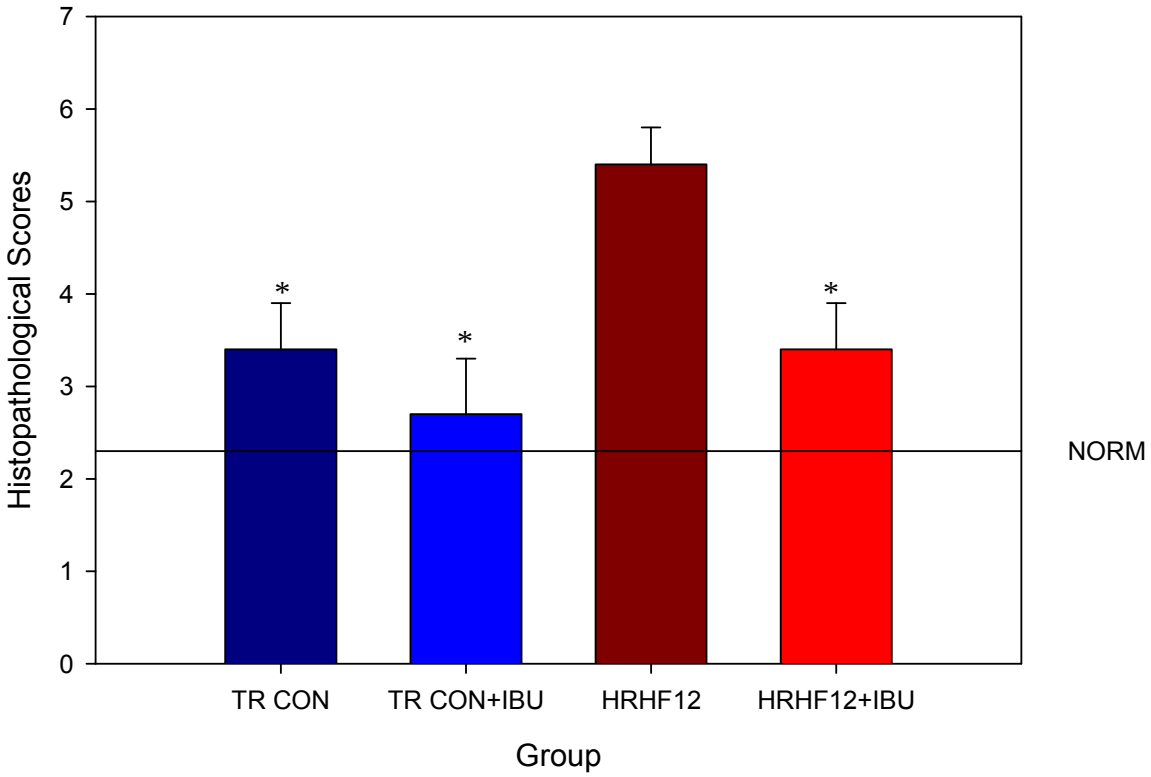

Figure I-1. Histopathological scores (means ± standard error of the mean) for radiocarpal articular cartilage between groups. TR CON = trained controls (*N* = 8); TR CON+IBU = trained controls plus ibuprofen limb (*N* = 6); HRHF12 = high-repetition, high-force for 12 weeks(*N* = 14); HRHF12+IBU = high-repetition, high-force plus ibuprofen for 12 weeks (*N* = 10); and NORM = normal controls (*N* = 5). * Significantly different from HRHF12: $p \leq .05$.

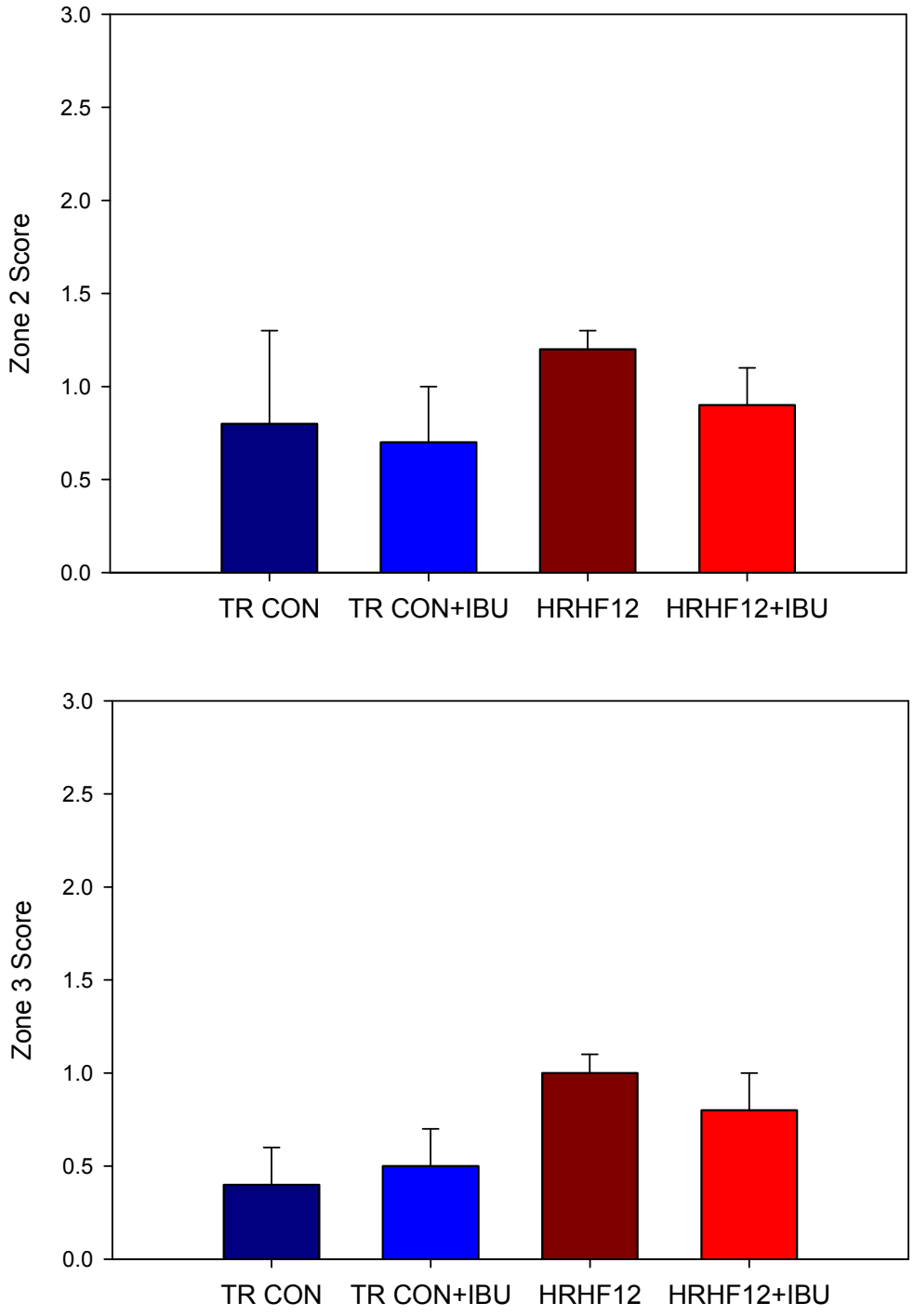

Figure I-2. Structure subscores (means ± standard error of the mean) for radiocarpal articular cartilage among groups. TR CON = trained controls; TR CON+IBU = trained controls plus ibuprofen; HRHF12 = high-repetition, high-force for 12 weeks; and HRHF12+IBU = high-repetition, high-force plus ibuprofen for 12 weeks.

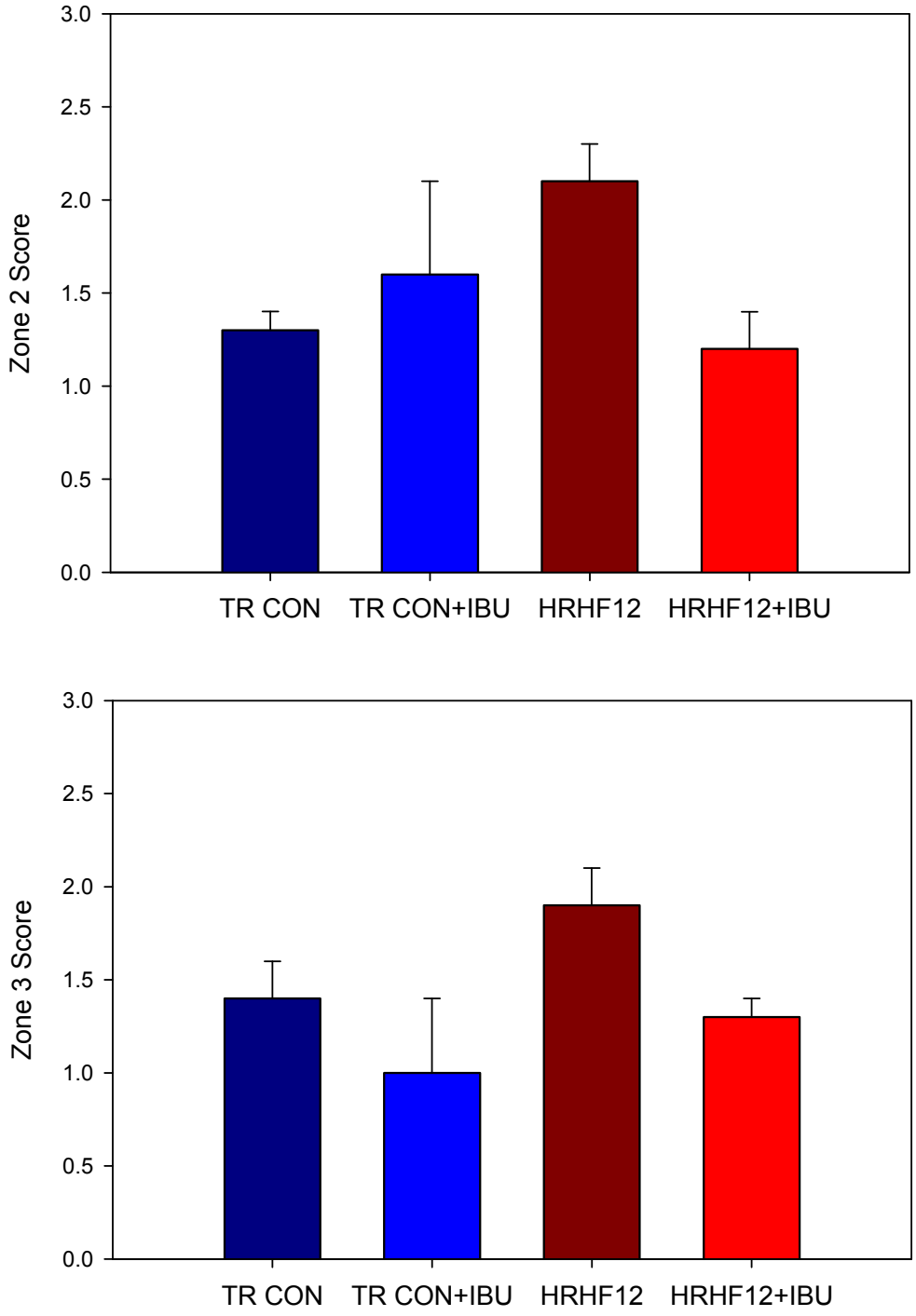

Figure I-3. Cellular subscores (means ± standard error of the mean) for radiocarpal articular cartilage among groups. TR CON = trained controls; TR CON+IBU = trained controls plus ibuprofen; HRHF12 = high-repetition, high-force for 12 weeks; and HRHF12+IBU = high-repetition, high-force plus ibuprofen for 12 weeks.

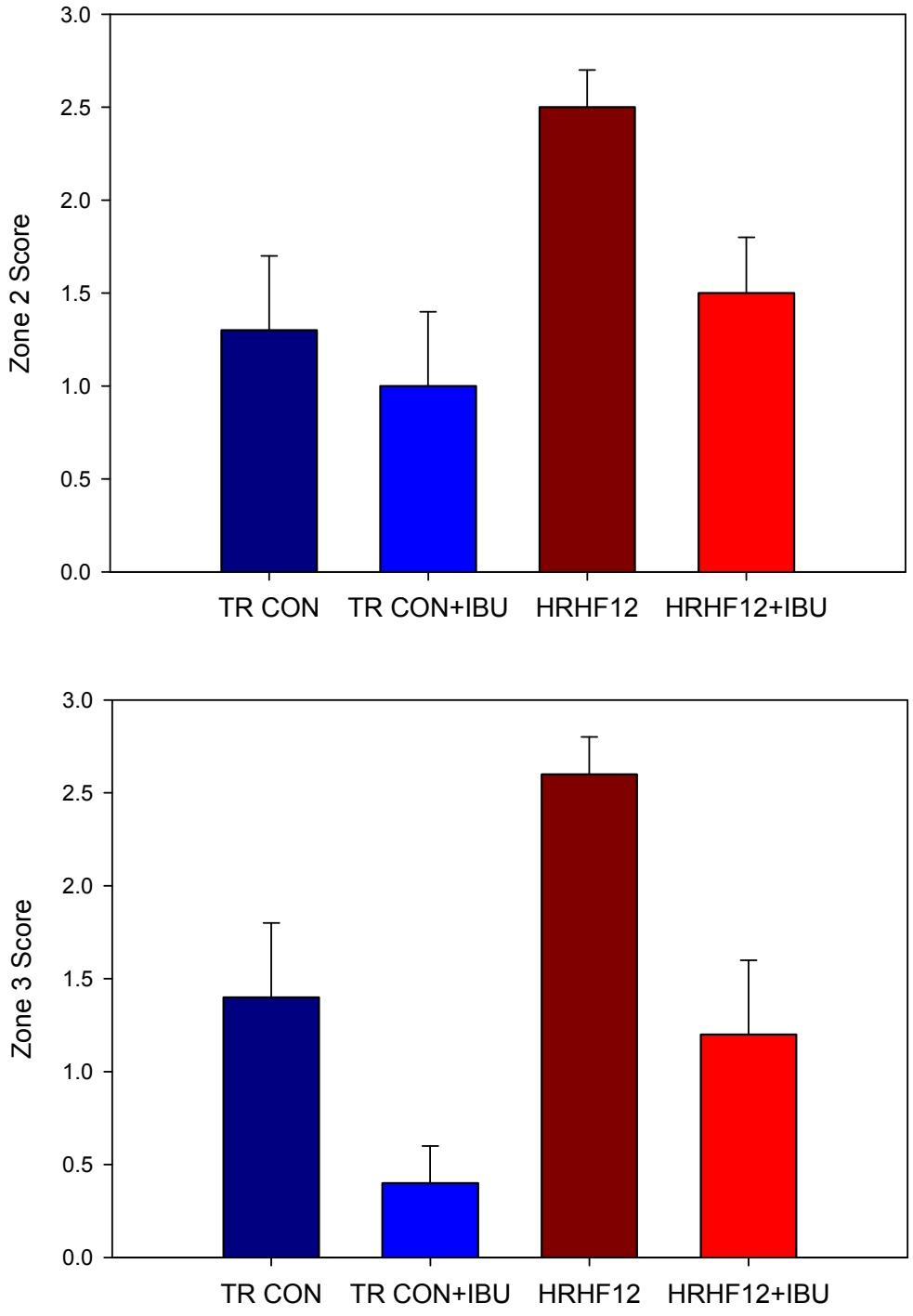

Figure I-4. Staining subscores (means ± standard error of the mean) for radiocarpal articular cartilage among groups. TR CON = trained controls; TR CON+IBU = trained controls plus ibuprofen; HRHF12 = high-repetition, high-force for 12 weeks; and HRHF12+IBU = high-repetition, high-force plus ibuprofen for 12 weeks.

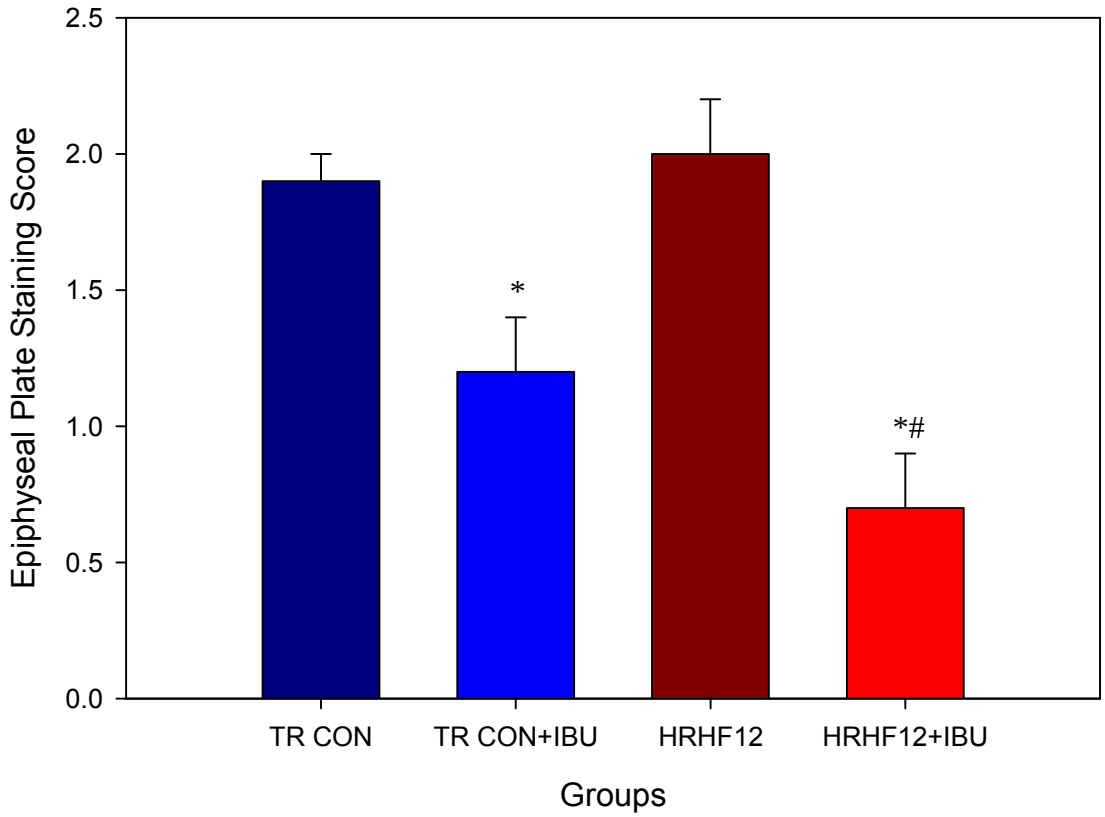

Figure I-5. Distal radius epiphyseal plate staining score (means ± standard error of the mean) among groups. TR CON = trained controls (*N* = 8); TR CON+IBU = trained controls plus ibuprofen (*N* = 9); HRHF12 = high-repetition, high-force for 12 weeks (*N* = 15); and HRHF12+IBU = high-repetition, high-force plus ibuprofen for 12 weeks (*N* = 10).
* Significantly different from HRHF: $p \leq .05$.
# Significantly different from TR CON: $p \leq .05$.

APPENDIX J
IMMUNOHISTOCHEMICAL IMAGES

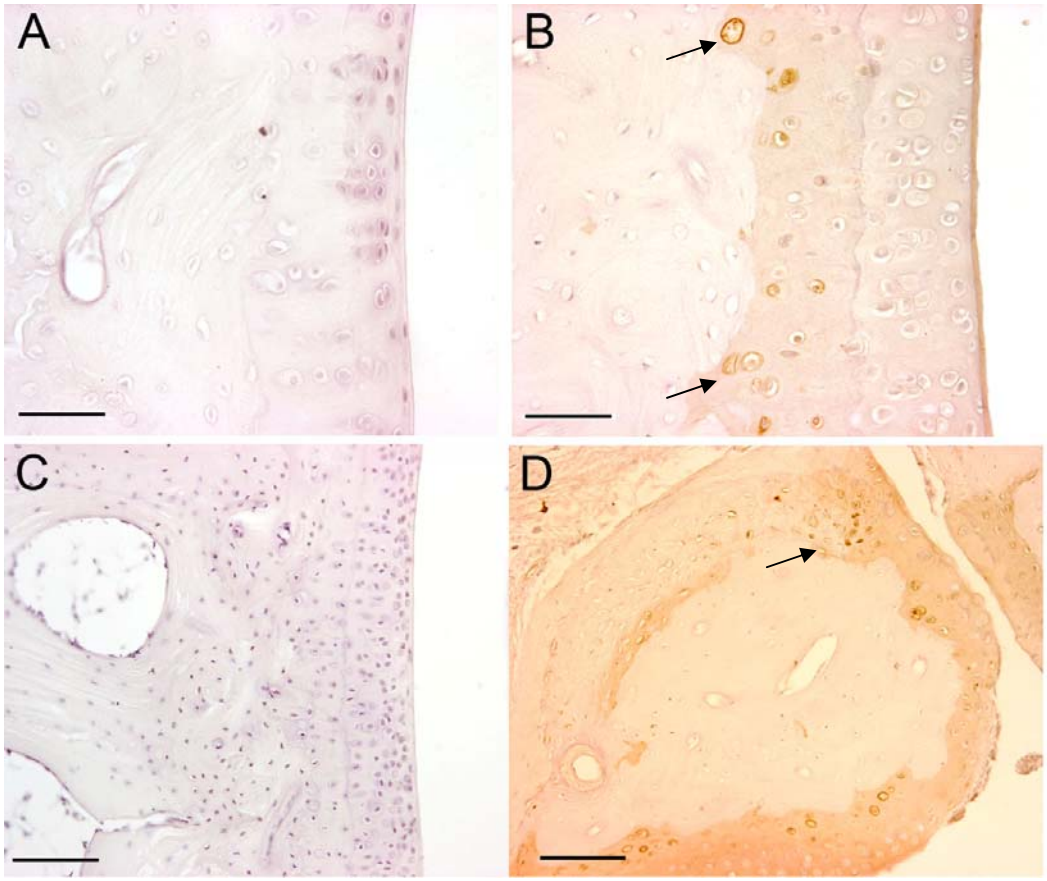

Figure J-1. Immunohistological staining for ED1 in HRHF wrist articular cartilage. ED1 is a marker for a lyosomal glycoprotein associated with osteoclasts, phagocytic macrophages, or their progenitors. Cross sections were counter stained with light hematoxylin. ED1+ cells were absent in NORM (A) and HRHF+IBU (C). Mononucleated ED1+ cells (osteoclast progenitor cells) were identified in the subchondral bone adjacent to the articular cartilage in HRHF distal radii (arrows = ED1+ cells; B). Similar cells were present in HRHF carpal bones (arrows = ED1+ cells; D). Scale bars = 50 µm.

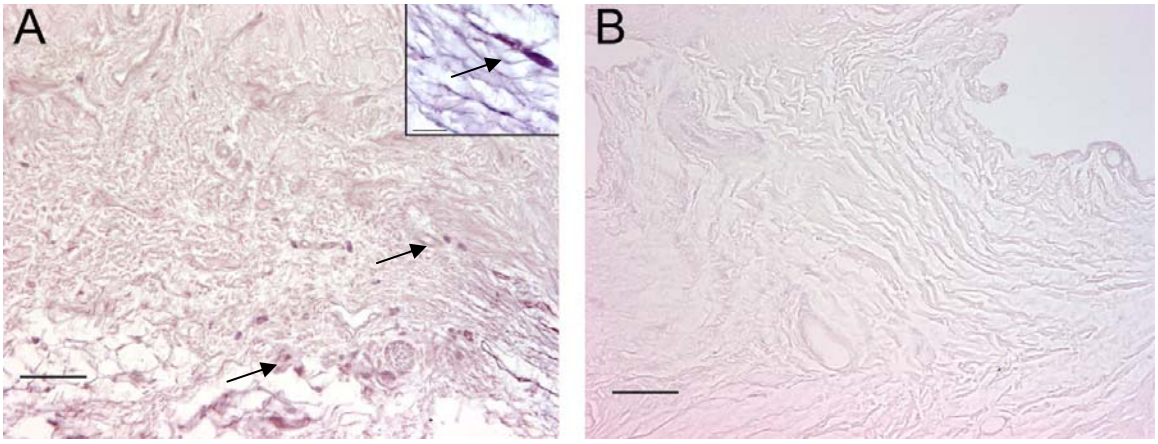

Figure J-2. Immunohistological staining for ED1 in HRHF wrist synoviums. ED1 is a marker for a lyosomal glycoprotein associated with osteoclasts, phagocytic macrophages, or their progenitors. Cross sections were counter stained with light hematoxylin. ED1+ cells, macrophages, were found in the outer synovium of HRHF wrist joints (arrows = ED1+ cells; A). The insert in Frame A shows the ED1+ cells in the outer synovium (arrow = ED1+ cell). No ED1+ cells were identified in TR CON (B). Scale bars = 50 µm, except the A insert = 10 µm.

APPENDIX K
INFORMED CONSENT FORM

TITLE: An Analysis of the Electrochemical Environment of Osteoarthritic Knees

PROTOCOL NO.: 4694

PARTICIPANT: _____ **Number:** _____

INVESTIGATOR: Jeffrey B. Driban, MEd, ATC, CSCS
Doctoral Student
Department of Kinesiology
Temple University
002 Pearson Hall
N. Broad Street
Philadelphia, PA 19122
United States

SITE(S): Department of Orthopaedics; Northeastern Hospital
Department of Orthopaedics; Northeast Philadelphia Office
Department of Orthopaedics; Temple University Hospital

STUDY-RELATED PHONE NUMBER(S):
Jeffrey B. Driban, MEd, ATC, CSCS: 215-204-1963 (office)
Jeffrey B. Driban, MEd, ATC, CSCS: 215-264-2962 (24hr)

Temple University is not receiving monetary compensation for performing this study.

This consent form may contain words that you do not understand. Please ask the study doctor or the study staff to explain any words or information that you do not clearly understand. You may take home an unsigned copy of this consent form to think about or discuss with family or friends before making your decision.

PURPOSE OF THE STUDY

The aim of this research study is to see if there is a link between electrical potentials and the markers of swelling (if present) in your knee. A second aim is to see whether people with arthritis can be divided into smaller groups which may help doctors better treat this disease. You are being asked to be involved because you either have arthritis in your knee(s) or neither of them. The goal of this study is to help improve a treatment which may be able to decrease the pain or slow the progress of arthritis.

PROCEDURES

As a part of this study you will be one of thirty volunteers looked at during an outpatient orthopaedic exam. This study includes two groups of volunteers. The first is made up of patients with moderate to severe arthritis in the knee(s). The other group consists of volunteers with no arthritis in either knee and is physically similar to a volunteer in the first group. Both groups will have the same evaluation. When you see the doctor he will examine your knees and will look at your x-rays. Your x-rays will be looked at to determine the amount of wear in your knees. If you have a lot of wear in your knee(s) you will be in one group. If both of your knees have only a little or no wear you will be placed in the other group.

While you wait for the physician, one of the researchers will help you complete a health history questionnaire and three surveys. They will ask you a series of questions and write your responses on the forms. These surveys will take about 20 minutes to complete. During this time, you will also be asked to have your height and weight recorded. Once you finish your forms and have had your x-rays examined, one of the researchers will shave small areas on your knee if hair is there. They will then clean your skin with alcohol to ensure your skin is clean. Then you will be asked to either lie down or sit in a chair; which ever is more comfortable for you. Next, four sticky electrodes will be placed on your skin to measure the electrical potentials on your skin. Three electrical resistance measurements will then be made by touching the electrodes for five seconds with a small meter. Once the three sets of 90 second measurements is finished the electrodes not on your shin will be removed. Your skin will then be cleaned with alcohol again. If you are one of the first ten

volunteers these steps will be repeated to help check the consistency of the measurements. The doctor will then put on some gloves and have a sterile sheet placed in front of him with a needle resting on it. A needle will then be placed into your knee by the doctor. This will be the same way the doctor always injects knees. A thin electrode will be slid into the needle which will be attached to a unit. This unit can measure the electrical potentials inside your knee. Once that measure is made (less than two minutes) the electrode will be removed. If you are one of the first ten volunteers a second thin needle will be inserted for less than two minutes to help check the consistency of the measurements. The needle will still be in your knee. Next, the doctor will attach a syringe to remove the joint fluid. Less than 1 teaspoon will be removed for examining. If your knee is very swollen the doctor will remove the extra fluid in order to make your knee more comfortable. Your fluid will then be sent to a lab for more measurements. You will be informed of your results at the end of this study. If you are called the results can only be told to you. The needle will go into your knee only once. If you have two arthritic knees you will be asked if both of your knees can be tested to measure its fluids. You may choose to include both knees, only one knee or not participate in this study. The fluid taken from your knee will be examined to see how inflamed your knee is and how much wear your knee has experienced. Once the needle is removed you will be given a band-aid and an ice bag for ten minutes to ease any pain you might have.

RISKS AND DISCOMFORTS

Performing x-rays and placing a needle in the knee does have some risks. There is a risk of an infection any time you get a needle. This will be minimized by providing a sterile environment for the injection and thoroughly cleaning the skin. Your skin will be checked before the needle is inserted to keep sure that your skin is healthy and does not have any marks or cuts which might increase your risk of infection. In a healthy patient the risk of getting infected is 1 in 10,000 knees. Pain and minor bleeding is also common with any injection. No sprays or anesthetics will be used to decrease your pain. These materials may decrease the pain of the injection but may increase the risk of infection and therefore they will not be used. After the needle is removed direct pressure will be placed on your skin to slow the bleeding. Once the

bleeding has stopped you will be given a band-aid and an ice bag. The ice bag will also decrease your pain. If you get sore later in the day, you can apply another ice bag to reduce your pain. If at any point you have concerns or a lot of pain you can call the doctor's office and speak to the doctor, another researcher, or the doctor's staff of certified athletic trainers and/or residents.

If at any point you feel light headed, dizzy or nauseaus please let the doctor, researcher or one of the staff members know immediately. Some patients may feel these symptoms when they get a needle.

For this study your knee will be x-rayed once while you are standing up. If you are visiting the doctor for knee pain or arthritis he may ask for additional films to fully examine your knee. The whole body radiation dose that you will receive from this study is significantly less than what someone living in the United States receives from the total average natural background radiation in a year.

PREGNANCY STATEMENT:

Since there may be some risks to pregnant women and their unborn child, if you are pregnant or planning to become pregnant, you will not be allowed to participate in this study. To protect any pregnant women you will be asked to take an over the counter pregnancy test to keep sure you are not currently pregnant. You will also be asked whether you are currently trying have a baby.

NEW FINDINGS

You will be told about new information that might change your decision to be in this study. You will also be told about new information that may have an affect on your future medical care. You may be asked to sign a revised informed consent form that contains the new information.

BENEFITS

There are no personal benefits for being in this study.

COSTS

The study's physician's fees and tests required by the study will be billed to you in the usual manner. However, any fees not covered by your insurance company will be provided at no cost to you.

COMPENSATION

You will receive no compensation for this study.

ALTERNATIVE TREATMENT

If at any point you do not want to be in this study you can ask to be removed. If you are in the group with no arthritis in either knee you may leave at any time. If you are in the group with an arthritic knee you can choose to leave at anytime or continue with the regular treatment of a swollen knee. This would include having the knee drained/injected, trying medicine or trying nothing.

CONFIDENTIALITY

All documents and information pertaining to this research study will be kept confidential in accordance with all applicable federal, state, and local laws and regulations. I understand that medical records and data generated by the study may be reviewed by Temple University's Institutional Review Board and the Office for Human Research Protections (OHRP), to assure proper conduct of the study and compliance with federal regulations. I understand that the results of this study may be published. If any data is published, I will not be identified by name.

COMPENSATION FOR INJURY

If you sustain an injury as a result of your participation in this study, care and treatment of your injury that is not covered by your medical and hospital coverage or other third party coverage will be provided at Temple University Hospital at no cost to you. Other financial compensation (such as lost wages or pain and suffering) for such injuries is not routinely available. By signing this consent form you are not waiving any of the legal rights that you otherwise would have as a participant in a research study.

VOLUNTARY PARTICIPATION AND WITHDRAWAL

Your participation in this study is entirely voluntary, and refusal to participate will involve no penalty or loss of benefits to you. You may discontinue your participation at any time without penalty or loss of benefits. Your participation in this study may be stopped at any time by the study doctor or the sponsor without your consent.

REASONS FOR REMOVAL FROM THE STUDY

During the study the researcher/doctor may remove you from testing. There may be several reasons: If your medical history form indicates you have health issues (e.g. bleeding disorder, gout, rheumatoid arthritis, etc) that may interfere with the test results or increase your risk you may be excused. The presence of a skin rash at your injection point will also mean you will not be tested for this study. If your joint fluid appears cloudy or an irregular color, it may not be used in the study but will still undergo an evaluation to see why it is not a normal color. Finally, you will not be allowed to participate if you are pregnant or currently trying to become pregnant.

QUESTIONS

If I have any questions about my rights as a research subject, I may contact the Institutional Review Board Coordinator, Richard Throm at (215) 707-8757.

If I have any research-related questions, I may contact Jeffrey B. Driban, MEd, ATC, CSCS:
215-204-1963 (office)
215-264-2962 (24 hour)

If I have any medical/injury -related questions, I may contact E. Balasubramanian, MD:

215-291-3777(office)

Do not sign this consent form unless you have had a chance to ask questions and have received satisfactory answers to all of your questions.

If you agree to participate in this study, you will receive a signed and dated copy of this consent form for your records.

CONSENT

I have read this consent form and the study has been explained to me. All my questions about the study and my participation in it have been answered. I freely consent to participate in this research study.

By signing this consent form I have not waived any of the legal rights that I otherwise would have as a subject in a research study.

An Analysis of the Electrochemical Environment of Osteoarthritic Knees

_____
Subject Name

_____ _____
Signature of Subject Date

_____ _____
Signature of Person Conducting Informed Consent Discussion Date

_____ _____
Signature of Principal Investigator Date

APPENDIX L
HEALTH HISTORY QUESTIONNAIRE

Health History Questionnaire

Participant Number: _____ Date: _____

Date of Birth: _____

Gender (Circle One): Male Female

Height: _____ Weight: _____

Occupation: _____

Please answer the following conditions to the best of your ability.

Have you ever played sports?

____ NO

____ YES (If yes, what sport(s): _____)

What was your level of participation (Check one)?

____ High School
____ Collegiate Intra-murals
____ Recreation League
____ Collegiate Club
____ Collegiate Varsity
____ Professional
____ Other: _____

Number Years of Participation: _____

Do you currently participate in some form of physical activity regularly?

____ NO

____ YES If yes, please explain –

What activity(s):_____

How many days per week? _____

How hours per day? _____

Please list any jobs you have previously or currently are employed in (please include the number of years per job):

Have you injured either knee in the last 6 months?

____ NO

____ YES If yes, what knee: ____ Right

____ Left

Do you have a previous history of knee surgery?

____ NO

____ YES If yes, what knee: ____ Right

____ Left

Does your right knee swell?

____ NO

____ YES (If yes, how often? _____)

Does your left knee swell?

____ NO

____ YES (If yes, how often? _____)

Have you taken an anti-inflammatory for more than a week within the past 6 months? (anti-inflammatory drugs include aspirin, ibuprofen, naprosyn)

____ NO

____ YES (If yes, please answer the next 3 questions)

1) What type of anti-inflammatory?

_____

2) How long were you taking the anti-inflammatory?

_____

3) Are you still taking the anti-inflammatory? If yes, what dose and how often?

_____

Have you taken an antibiotic within the past 3 months?

____ NO

____ YES

Are you currently taking any anticoagulants (e.g., warfarin or coumadin)?

____ NO

____ YES (If yes, what is your current dose? _____)

Please list any other medications you are currently taking on a regular basis. Please include the medication dose and number of times per day you take the medicine.

_____

_____

Are you able to walk without aid (i.e., cane, crutch, walker)?

____ NO (If no, what aid are you using? _____)

____ YES

Are you able to go up and down stairs without difficulty?

____ NO

____ YES

Do you walk with a limp?

____ NO

____ YES

Do you have any predisposing muscle or skeletal disorders that the researchers should be aware of?

____ NO

____ YES (If yes, please explain): _____

Have you ever been diagnosed:	*Please Circle*	
High blood pressure?	NO	YES
Heart disease?	NO	YES
Angina or chest pain?	NO	YES
Heart attack?	NO	YES
Heart surgery?	NO	YES
Heart palpitations/racing heart?	NO	YES
An abnormal electrocardiogram (ECG, EKG, heart tracing)?	NO	YES
High cholesterol?	NO	YES
Heart murmur or defect?	NO	YES
Blood clots or phlebitis?	NO	YES
Frequent pain or cramping in your legs?	NO	YES
Anemia (iron deficiency) or other blood disorders?	NO	YES
Shortness of breath on exertion?	NO	YES
Asthma?	NO	YES
Allergies?	NO	YES
Pneumonia or bronchitis?	NO	YES
Emphysema or other breathing disorder (shortness of breath at rest)?	NO	YES
Stroke?	NO	YES
Seizures?	NO	YES
Dizziness or fainting spells?	NO	YES
Severe muscle weakness?	NO	YES
Glaucoma?	NO	YES
Significant vision or hearing disorder?	NO	YES
Thyroid disorder?	NO	YES
Diabetes or high blood sugar?	NO	YES
Cancer or leukemia?	NO	YES
Rheumatoid arthritis?	NO	YES
Other auto-immune diseases (HIV, AIDS, Lupus)?	NO	YES
Gout or Pseudo-Gout?	NO	YES
Skin rash on your legs?	NO	YES
Osteoarthritis or other bone joint disease?	NO	YES
Do you smoke?	NO	YES

If yes, how much do you smoke?

_____ cigarettes/day _____ packs/week

(Please note: If you have responded yes to any of the above questions, you may be asked to provide further details.)

Please indicate below any medical and/or health concerns you may have which have not been addressed by the previous items on this form.

If there are any questions, please feel free to contact one of the investigators at the following numbers and addresses:

Jeffrey Driban, MEd, ATC, CSCS
(215) 204-1963
002 Pearson Hall, 048-00
Temple University
Philadelphia, PA 19122

Mary F. Barbe, PhD
215-707-4896
3307 N. Broad St
Temple University
Philadelphia, PA 19140

Michael Sitler, EdD, ATC
(215) 204-1950
114 Pearson Hall, 048-00
Temple University
Philadelphia, PA 19122

Dr. E. Balasubramanian, M.D.
(215) 969-9100
9331 Old Bustleton Ave.
Department of Orthopaedics
Temple University Hospital
Philadelphia, PA 19115

APPENDIX M
KELLGREN-LAWRENCE OSTEOARTHRITIS GRADING SYSTEM

Table M-1. Kellgren-Lawrence Osteoarthritis Grading System

Grade	Radiographic Characteristics
0	No features
1	Doubtful: minute osteophytes, doubtful significance
2	Minimal: definite osteophyte, unimpaired joint space
3	Moderate: moderate diminution of joint space
4	Severe: joint space greatly impaired, with sclerosis of subchondral bone

APPENDIX N
MODIFIED HISTORICAL LEISURE ACTIVITY QUESTIONNAIRE

Lifetime Physical Activity Questionnaire

STEP 1: Please place a **check mark** in the first column next to each activity that you have **ever participated in more than 10 times** during your lifetime.

STEP 2: For those activities you have checked, **proceed to the right** answering the questions in the columns above.

Have you ever participated in any of the following? Check if yes ↓	During the Past Year		During ages 51-65 years (a 15-year span) *If younger than 51, skip to next column*			During ages 35-50 years (a 15-year span)			During ages 22-34 years (a 12-year span)			Between age of onset of menstruation to 21 years		
	Number of months	Typical number of hours per week	Number of years (15 max)	Typical number of months per year	Typical number of hours per week	Number of years (15 max)	Typical number of months per year	Typical number of hours per week	Number of years (12 max)	Typical number of months per year	Typical number of hours per week	Number of years (10 max)	Typical number of months per year	Typical number of hours per week
Leisure Time Activities														
Walking for exercise (outdoor, indoor at mall, treadmill)														
Hiking														
Stair-climbing machine														
Jogging (outdoor/treadmill)														
Bicycling (stationery/outdoor)														
Horseback riding														
Dancing (social/ ballet/tap)														
Gymnastics														
Calisthenics/toning exercises														
Yoga														
Aerobics/Jazzercise														
Lifting weights														
Swimming for exercise (i.e. laps)														
Rowing/canoeing/ kayaking/rowing machine														
Water skiing														

Skiing/downhill																
X-country skiing/ski machine																
Skating (ice, roller, in-line)																
Tennis																
Other racquet sports																
Softball/baseball																
Golf (use golf cart)																
Golf (walking)																
Volleyball																
Basketball																
Bowling																
Other :_____																
Household Activities																
Gardening/yard work																
Grooming and feeding children																
Playing with children (walk/run with them)																
Light housecleaning (sweep/dust)																
Heavy housecleaning (scrub floors/vacuum)																

APPENDIX O
HUMAN RAW DATA

Table O-1. Descriptive Characteristics of Participants

Participant	Gender	Age (years)	Weight (kg)	Height (m)	BMI (kg/m^2)	LT PA (MET x Hr)	SF-PCS	SF-MCS
KneeOA1	Female	59.5	107.73	1.62	41.05	2505.6	30.14	46.52
KneeOA2	Male	68.1	102.72	1.74	33.93	221.7	33.32	48.40
KneeOA3	Male	60.4	106.82	1.85	31.21	939.4	30.46	61.77
KneeOA4	Female	71.1	71.82	1.63	27.03	1680.0	NR	NR
Normal1	Male	64.3	84.09	1.73	28.10	4194.8	47.31	54.08
Normal2	Male	54.2	95.91	1.74	31.68	4152.3	57.85	57.40
Normal3	Female	39.5	63.50	1.65	23.32	4029.6	56.20	52.74
Normal4	Male	56.2	67.27	1.69	23.55	78.0	39.07	43.12

Note. KneeOA# = Osteoarthritic knee group participant, Normal# = nonosteoarthritic normal knee group participant, BMI = body mass index, MOSPA = Monica Optional Study of Physical Activity, LT PA = Life Time Physical Activity Score, SF-PCS = Acute Form of the Short Form-36v2™ Health Survey Physical Component Summary measure, SF-MCS = Acute Form of the Short Form-36v2™ Health Survey Mental Component Summary measure, and NR = not recorded due to multiple skipped questions.

Table O-2. Environmental Conditions During Testing

Participant	Air Pressure (mmHg)	Temperature (deg C)	Relative Humidity (%)
KneeOA1	764.29	23.44	35.0
KneeOA2	760.98	22.22	49.5
KneeOA3	760.73	20.11	44.6
KneeOA4	759.46	22.56	29.4
Normal1	762.25	17.28	61.5
Normal2	766.32	20.39	23.0
Normal3	761.49	21.77	47.9
Normal4	761.49	22.72	45.0

Note. KneeOA# = Osteoarthritic knee group participant. Normal# = nonosteoarthritic normal knee group participant.

Table O-3. Electrical Resistance Measurements

Participant	Limb	Resistance Lat-G (MΩ)	Resistance Med-G (MΩ)	Resistance Con-G (MΩ)
KneeOA1	Right	5.5	4.2	9.1
	Left	8.9	9.4	7.7
KneeOA2	Right	0.4	0.4	0.4
	Left	0.3	0.3	0.3
KneeOA3	Right	0.4	0.8	0.6
	Left	2.6	1.2	4.8
KneeOA4	Left	13.6	32.3	13.6
Normal1	Right	0.6	0.3	1.2
Normal2	Left	0.0	0.0	0.0
Normal3	Right	0.4	1.0	0.9
Normal4	Left	0.7	1.1	0.7

Note. KneeOA# = Osteoarthritic knee group participant, Normal# = nonosteoarthritic normal knee group participant, Resistance Lat-G = resistance between lateral and ground electrodes, Resistance Med-G = resistance between medial and ground electrodes, and Resistance Con-M = resistance between control and ground electrodes.

Table O-4. Skin Potentials Measurements

Participant	Limb	Lateral (mV)	Medial (mV)	Control (mV)	Lat-Con (mV)	Med-Con (mV)	Intra-articular (mV)
KneeOA1	Right	-2.37	-17.70	5.96	-8.33	-23.66	NR
	Left	-2.30	14.50	-27.37	25.07	41.87	NR
KneeOA2	Right	-17.87	-13.45	-16.08	-1.79	2.63	113.30
	Left	-9.37	4.83	-9.28	-0.09	14.11	111.05
KneeOA3	Right	0.33	3.79	3.83	-3.80	-0.04	18.46
	Left	-0.36	4.89	-11.60	11.24	16.49	73.49
KneeOA4	Left	-1.73	2.56	-1.04	-0.69	3.60	NR
Normal1	Right	24.44	3.97	-1.81	26.25	5.78	-71.70
Normal2	Left	6.93	5.00	3.34	3.59	1.66	-17.50
Normal3	Right	1.91	10.71	25.46	-23.55	-14.75	79.60
Normal4	Left	-8.82	36.75	-6.48	-2.34	43.23	-45.38

Note. KneeOA# = Osteoarthritic knee group participant, Normal# = nonosteoarthritic normal knee group participant, Lat-Con = difference in skin potentials between lateral and control electrodes, and Med-Con = difference in skin potentials between medial and control electrodes. NR = no recorded data due to calibration error.

Table O-5. Time to Measure Skin Potentials

Participant	Limb	Time to Lateral (min)	Time to Medial (min)	Time to Control (min)
KneeOA1	Right	4.5	7.2	9.5
	Left	2.0	4.2	6.0
KneeOA2	Right	2.9	0.8	6.5
	Left	2.8	1.0	4.7
KneeOA3	Right	5.5	3.1	8.5
	Left	4.8	2.3	7.0
KneeOA4	Left	3.7	1.7	5.6
Normal1	Right	4.7	2.7	6.7
Normal2	Left	4.0	1.9	5.9
Normal3	Right	4.5	2.5	6.5
Normal4	Left	1.0	2.8	4.5

Note. KneeOA# = Osteoarthritic knee group participant, Normal# = nonosteoarthritic normal knee group participant, Lat-Con = difference in skin potentials between lateral and control electrodes, and Med-Con = difference in skin potentials between medial and control electrodes. NR = no recorded data due to calibration error.

Table O-6. Anti-inflammatory/Protective Protein Concentrations

Participant	Limb	IL-4 (pg/µg)	IL-10 (pg/µg)	IL-13 (pg/µg)	IL-1ra (pg/µg)	OPG (pg/µg)
KneeOA1	Right	0.00015	0.00028	0.00015	0.04748	0.00048
	Left	0.00019	0.00025	0.00014	0.03099	0.00095
KneeOA2	Right	0.00025	0.00021	0.00014	0.06517	0.00001
	Left	0.00016	0.00018	0.00007	0.02500	0.00015
KneeOA3	Right	0.00021	0.00012	0.00006	0.01257	0.00062
	Left	0.00031	0.00012	0.00008	0.01793	0.00130
KneeOA4	Left	0.00028	0.00023	0.00009	0.02573	0.00085
Normal1	Right	0.00065	0.00050	0.00049	0.06756	0.00483
Normal2	Left	0.00043	0.00052	0.00038	0.07984	0.00203
Normal3	Right	0.00094	0.00101	0.00056	0.04979	0.00725
Normal4	Left	0.00138	0.00139	0.00092	0.55410	0.00567

Note. KneeOA# = Osteoarthritic knee group participant, Normal# = nonosteoarthritic normal knee group participant, IL = interleukin, ra = receptor antagonist, and OPG = osteoprotegerin.

Table O-7. Pro-inflammatory/Catabolic Protein Concentrations

Participant	Limb	IL-1α (pg/µg)	IL-1β (pg/µg)	TNF-α (pg/µg)	RANKL (pg/µg)
KneeOA1	Right	0.00014	0.00015	0.00000	0.00013
	Left	0.00017	0.00012	0.00000	0.00016
KneeOA2	Right	0.00011	0.00020	0.00039	0.00013
	Left	0.00009	0.00009	0.00092	0.00012
KneeOA3	Right	0.00010	0.00017	0.00089	0.00014
	Left	0.00007	0.00017	0.00024	0.00027
KneeOA4	Left	0.00007	0.00022	0.00115	0.00015
Normal1	Right	0.00013	0.00060	0.00816	0.00096
Normal2	Left	0.00025	0.00043	0.00049	0.00022
Normal3	Right	0.00045	0.00053	0.00000	0.00028
Normal4	Left	0.00051	0.00063	0.00080	0.00037

Note. KneeOA# = Osteoarthritic knee group participant, Normal# = nonosteoarthritic normal knee group participant, IL = interleukin, TNF = tumor necrosis factor, and RANKL = receptor activator of nuclear factor-kappaB ligand.

Table O-8. Matrix Metalloproteinases and Inhibitors Concentrations

Participant	Limb	TIMP-1 (pg/µg)	TIMP-2 (pg/µg)	MMP-2 (pg/µg)	MMP-3 (pg/µg)	MMP-13 (pg/µg)
KneeOA1	Right	593.92710	358.95687	882.69609	525.85792	0.03173
	Left	407.24178	53.40070	163.21259	177.78849	0.02493
KneeOA2	Right	72.06595	37.38239	85.56800	71.49397	0.01150
	Left	482.33924	30.70262	88.15087	97.75494	0.01075
KneeOA3	Right	14.60692	26.43239	74.18366	47.37351	0.01026
	Left	26.75477	25.85051	68.52747	16.38767	0.01912
KneeOA4	Left	126.70508	27.97256	83.80666	158.96645	0.02910
Normal1	Right	1.77695	1.38376	6.79618	0.78681	0.01424
Normal2	Left	1.40146	0.78436	5.86029	4.10684	0.03929
Normal3	Right	4.43387	2.18627	3.82631	4.69990	0.03150
Normal4	Left	4.91150	4.52300	9.93560	10.62415	0.05363

Note. KneeOA# = Osteoarthritic knee group participant, Normal# = nonosteoarthritic normal knee group participant, TIMP = tissue inhibitor of metalloproteinase, and MMP = matrix metalloproteinase.

Table O-9. Adipokines Concentrations

Participant	Limb	Leptin (pg/µg)	Adiponectin (pg/µg)
KneeOA1	Right	1.48286	741.88408
	Left	1.03653	207.03977
KneeOA2	Right	0.42958	98.10990
	Left	0.32623	80.79484
KneeOA3	Right	0.21472	35.63713
	Left	0.21806	39.97557
KneeOA4	Left	0.78645	57.30602
Normal1	Right	0.10295	15.76324
Normal2	Left	0.07693	6.42103
Normal3	Right	0.10482	28.46539
Normal4	Left	0.10731	9.47962

Note. KneeOA# = Osteoarthritic knee group participant. Normal# = nonosteoarthritic normal knee group participant.